THE MINISTRY OF SCIENCE AND HIGHER EDUCATION OF THE RUSSIAN FEDERATION

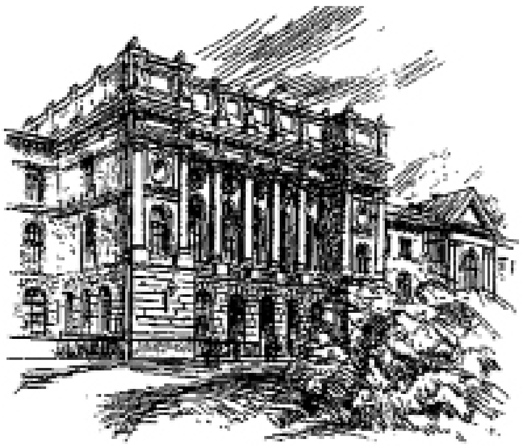

Computing, Telecommunications and Control

Vol. 13, no. 3
2020

Peter the Great St. Petersburg
Polytechnic University
2020

COMPUTING, TELECOMMUNICATIONS AND CONTROL

The journal is included in the List of Leading PeerReviewed Scientific Journals and other editions to publish major findings of PhD theses for the research degrees of Doctor of Sciences and Candidate of Sciences.

The journal is indexed by Ulrich's Periodicals Directory, Google Scholar, EBSCO, ProQuest, Index Copernicus, VINITI RAS Abstract Journal (Referativnyi Zhurnal), VINITI RAS Scientific and Technical Literature Collection, Russian Science Citation Index (RSCI) database © Scientific Electronic Library and Math-Net.ru databases.

The journal is registered with the Federal Service for Supervision in the Sphere of Telecom, Information Technologies and Mass Communications (ROSKOMNADZOR). Certificate ЭЛ No. ФС77-77378 issued 25.12.2019.

The address: 195251 Polytekhnicheskaya Str. 29,
St. Petersburg, Russia.

МИНИСТЕРСТВО НАУКИ И ВЫСШЕГО ОБРАЗОВАНИЯ РОССИЙСКОЙ ФЕДЕРАЦИИ

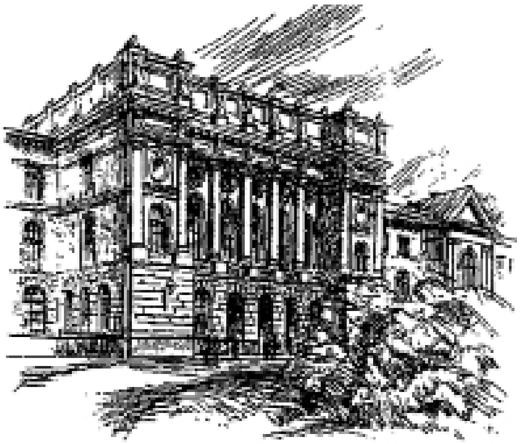

Информатика, телекоммуникации и управление

Том 13, № 3
2020

Санкт-Петербургский политехнический
университет Петра Великого
2020

ИНФОРМАТИКА, ТЕЛЕКОММУНИКАЦИИ И УПРАВЛЕНИЕ

Журнал с 2002 года входит в Перечень ведущих рецензируемых научных журналов и изданий, в которых должны быть опубликованы основные результаты диссертаций на соискание ученой степени доктора и кандидата наук.

Сведения о публикациях представлены в Реферативном журнале ВИНИТИ РАН, в международной справочной системе «Ulrich`s Periodical Directory», в базах данных Российский индекс научного цитирования (РИНЦ), Google Scholar, EBSCO, Math-Net.Ru, ProQuest, Index Copernicus

Журнал зарегистрирован Федеральной службой по надзору в сфере информационных технологий и массовых коммуникаций (Роскомнадзор). Свидетельство о регистрации ЭЛ № ФС77-77378 от 25.12.2019.

При перепечатке материалов ссылка на журнал обязательна.

Точка зрения редакции может не совпадать с мнением авторов статей.

Адрес редакции: Россия, 195251, Санкт-Петербург, ул. Политехническая, д. 29.

Тел. редакции (812) 552-62-16.

Contents

Содержание

DOI: 10.18721/JCSTCS.13301
УДК 721.021.23, 004.942

INFORMATION MODELING FOR CULTURAL PRESERVATION: PORTICO OF THE NEW HERMITAGE AND ATLAS SCULPTURES. PART 1: BASIC APPROACHES AND APPROBATION RESULTS

A.A. Fedotov[1], *T.V. Prazdnikova*[2], *V.L. Badenko*[1], *V.K. Yadykin*[1]

[1] Peter the Great St. Petersburg Polytechnic University,
St. Petersburg, Russian Federation;

[2] The State Hermitage Museum,
St. Petersburg, Russian Federation

This article presents the results of interaction between Peter the Great St. Petersburg Polytechnic University and the State Hermitage in a promising direction of using the latest achievements in the field of information technology in solving the problems of preserving cultural heritage. The authors use information modeling of the portico of the New Hermitage building and Atlas sculptures based on laser scanning data as an example. An overview of modern technologies currently used to preserve historical sites is presented. The main advantages obtained through the use of new technologies and the capabilities of modern software systems focused on working with information models are demonstrated. Digital representations of the building structures calculation results of the portico of the New Hermitage are analyzed. In addition, on the basis of the study of the stress-strain state of the entire structure, the reasons for the formation of cracks on the wrists and ankles of the granite Atlas sculptures were analyzed. The possibility of using the created model for reproducing an object using modern technologies of three-dimensional printing is shown.

Keywords: BIM, HBIM, laser scanning, cultural heritage, Historical Building Information Modeling.

Citation: Fedotov A.A., Prazdnikova T.V., Badenko V.L., Yadykin V.K. Information modeling for cultural preservation: Portico of the New Hermitage and Atlas sculptures. Part 1: Basic approaches and approbation results. Computing, Telecommunications and Control, 2020, Vol. 13, No. 3, Pp. 7–16. DOI: 10.18721/JCSTCS.13301

ИНФОРМАЦИОННОЕ МОДЕЛИРОВАНИЕ ДЛЯ СОХРАНЕНИЯ КУЛЬТУРНОГО НАСЛЕДИЯ: ПОРТИК ЗДАНИЯ НОВОГО ЭРМИТАЖА И СКУЛЬПТУРЫ АТЛАНТОВ. ЧАСТЬ 1: БАЗОВЫЕ ПОДХОДЫ И РЕЗУЛЬТАТЫ АПРОБАЦИИ

А.А. Федотов[1], *Т.В. Праздникова*[2], *В.Л. Баденко*[1], *В.К. Ядыкин*[1]

[1] Санкт-Петербургский политехнический университет Петра Великого,
Санкт-Петербург, Российская Федерация;

[2] Государственный Эрмитаж,
Санкт-Петербург, Российская Федерация

Представлены результаты взаимодействия СПбПУ и Государственного Эрмитажа в перспективном направлении использования последних достижений в области информационных технологий при решении задач сохранения культурного наследия на примере информационного моделирования портика здания Нового Эрмитажа и скульптур атлантов на основе данных лазерного сканирования. Представлен обзор современных технологий, применяемых в настоящее время для сохранения исторических объектов культурного наследия. Продемонстрированы основные преимущества, получаемые за счет применения новых технологий, и возможности современных программных комплексов, ориентированных на работу с информационными моделями. Проанализированы цифровые представления результатов расчетов строительных конструкций портика Нового Эрмитажа. При этом на основе исследования напряженно-деформированного состояния всего сооружения проанализированы причины образования трещин на запястьях и щиколотках гранитных скульптур атлантов. Показана возможность использования созданной модели для воспроизведения объекта при помощи современных технологий трехмерной печати.

Ключевые слова: информационное моделирование, лазерное сканирование, культурное наследие, Эрмитаж, расчетная модель.

Ссылка при цитировании: Федотов А.А., Праздникова Т.В., Баденко В.Л., Ядыкин В.К. Информационное моделирование для сохранения культурного наследия: портик здания Нового Эрмитажа и скульптуры атлантов. Часть 1: Базовые подходы и результаты апробации // Computing, Telecommunications and Control. 2020. Т. 13. № 3. С. 7–16. DOI: 10.18721/JCSTCS.13301

Information modeling technologies for the preservation of cultural heritage

Modern computer technologies are widely used in the modern world and the construction industry is not an exception. More and more projects on the domestic construction market successfully implement the concept of building information modeling (BIM technologies). A BIM building model is a precise three-dimensional geometry filled with all kinds of information about its constituent structures, materials, construction work and more. BIM technologies allow ensuring the integrity of information at all stages of the life cycle of a structure: from concept to reconstruction [1].

For cultural heritage objects, the concept of HBIM (Historical Building Information Modeling) was proposed, which involves the use of BIM-modeling with all its advantages in the preservation and reconstruction of historical buildings [2]. HBIM is a reliable basis for decision-making, restoration, renovation and energy efficiency of a cultural heritage building [3]. Moreover, HBIM allows to create a common environment for the free exchange and competent use of information by specialists of different profiles: art historians, designers, maintenance specialists, etc. [4]. The HBIM model of a historic building is an extensive database in which the geometric model is associated with attributive information of a wide variety of nature, reflecting the individual characteristics of the building [5]. HBIM can be used both as an archive and an information resource, and act as a management tool capable of providing adequate service to the facility [6]. In summary, we can say that HBIM has the following advantages:

1. Storage of historical attributive and graphical information about building components;
2. Providing clear and reliable visual display, including using virtual and augmented reality technologies;
3. The ability to carry out strength, heat engineering and other calculations based on the reflection of a set of structural details in the model;
4. Automation of documentation development;
5. Creation of an environment for adequate maintenance of the cultural heritage object to ensure its safety.

Below is a list of some successful examples of HBIM applications in the UK [7]:

1. Waverly railway station in Edinburgh, Scotland. The project is an example of the organization of joint work during the modeling of complex geometry and unique elements of the ticket hall dome. The

resulting model was further used not only in the maintenance of the building, but also for visual display on the website.

2. Woodsit Hall Mansion, Staffordshire, England. The model of the dilapidated mansion was filled with valuable descriptive and historical information, and was also used to establish automatic generation of construction documents such as blueprints for plans and facades.

3. The building of the former post office in Dundee, Scotland. HBIM as a communication tool became a collaboration solution and enabled modeling and rendering of unique architectural elements, including sculpture. The model contains design information about all the elements and was the basis for the automatic creation of drawings.

This article presents the final results of interaction between SPbPU and the State Hermitage in the promising direction of using the latest achievements in the field of information technology to solve the most important tasks of preserving cultural heritage. The article is focused primarily on cultural workers and allows them to understand the new opportunities that open up before them. Therefore, technical details are omitted, they will be the topic of the next publication in the journal and are partially presented in previous publications of the authors [3, 9, 15]. Thus, the objective of this article is to determine the prospects of information modeling for the preservation of cultural heritage.

Portico of the New Hermitage building

Ten monolithic Atlas figures, carved out of stone, have been decorating the portico of the New Hermitage building for over one hundred and seventy years, being its symbol and at the same time one of the visiting cards of St. Petersburg. The Atlas sculptures were carved from Serdobol granite by Russian stonecutters under the direction of sculptor A.I. Terebenev, and installed at the pylons of the portico of the New Hermitage in 1848.

The sculptures do not carry any load, except their own weight. At the same time, they are rigidly connected with the structure of the portico and their condition directly depends on the condition of the portico. First cracks in the walls of the building and in the Serdobol granite of the figures were recorded at the end of the 19th century. In 1909, the St. Petersburg Palace Administration appointed a special commission, which recommended "... in no case to start permanent sealing without establishing the exact cause of the destruction and not taking measures to eliminate them".

Until the revolutionary events of 1917, inspections were carried out every two years. In the late 1920s and early 1930s, the survey and partial restorations were carried out under the supervision of sculptor-restorer I.V. Krestovsky. He was the first to suggest that, in addition to deformations of the foundations, cracks appear due to the figures not being able to support their own enormous weight. Copper collars were installed on the two corner sculptures with the most open cracks, fixed from the back of the sculptures through hinged anchors to the pylons of the portico.

On December 29, 1941, an artillery shell hit the slab of the portico. Two previously intact Atlas figures displayed cracks on the arms and key plates between the arms.

In 1994, a research was carried out under the guidance of Doctor of Mineralogical Sciences, Professor of the St. Petersburg State Mining Institute R.E. Dashko. There was an engineering and geodetic monitoring carried out, on the basis of which it was concluded that the heterogeneity of the foundation under the building and the influence of unstable soils with an incessant process of microbiological damage are the factors that contribute to uneven precipitation of the New Hermitage building and the appearance of microcracks in the Atlas figures.

The study of the Atlas figures was carried out in late 2009 and early 2010 by scientists of the Scientific and Technical Center of the JSC "Radioavionics", which were tasked with clarifying the structures and the state of preservation of the Atlases' mountings. The study was carried out using the method of ultra-broadband radar sounding.

In the period from 2000 to 2016, protective measures were taken several times to preserve the "living" cracks of the Atlases with plastic compounds that prevent the ingress of moisture and foreign objects.

A set of scientific studies has shown that the opening of cracks is seasonal. The sculptures of the Atlases, the portico and the building of the New Hermitage itself are a single organism, and issues related to the preservation of sculptures must be resolved in a comprehensive manner, in conjunction with the problems of the building.

Despite the large volume of research carried out, the stress-strain state of the portico with the Atlas figures as a discrete element of the New Hermitage building remains completely incomprehensible. The creation of a 3D model as a basis for further monitoring of the of portico's state will become the basis for further research, modeling the stress-strain states of the structures of the monument and developing solutions to stabilize its condition.

The results of modelling the Atlas sculptures and the portico of the New Hermitage building

If we are talking about large objects such as buildings and structures, then the best way to transfer the geometry of the real world to the virtual one is laser scanning. A laser scanner emits hundreds of thousands of beams per second in all directions around it and registers their return after being reflected from hard surfaces. Thus, the result of laser scanning is a massive and dense 3D point cloud containing hundreds of millions of points. Information about coordinates (X, Y, Z) and its color (R, G, B) is stored for each point in the cloud. Thus, such a cloud of points accurately enough (up to 1-2 mm) reproduces the external appearance of the scanned object [8, 9].

When examining the structure and sculptures of the portico of the New Hermitage, the decisive role was played by the accuracy of measurements and the ability to quickly obtain data in conditions of a dense flow of tourists. That is why the Leica BLK360 laser scanner was chosen as the main tool. The closest attention was paid to the granite statues of Atlas, whose height, together with the pedestal, reaches 6.5 m. A portable lift was used to access the upper elements of the sculptures (Fig. 1).

Fig. 1. Laser scanning process

The resulting cloud contains 160 million points. In this case, the points are automatically colored depending on the material of the surface that reflected the ray. For example, in Fig. 2, stone surfaces are red, plaster is yellow, and the green shadows below are people. Information about what material the object is made of is very important for further processing of the obtained data (Fig. 2).

Geometry alone is not enough for BIM. In fact, the information model of an existing building is its digital representation in the virtual world, which is created on the basis of a wide variety of data: geometry, materials, operating conditions, structural features and much more. In mechanical engineering, such objects are commonly referred to as digital twins [10]. All this together makes it possible not only to have a three-dimensional model in order to display it, for example, on a computer screen, but also to perform a complex analysis of the structure [11–13].

In the process of generating the information model of the New Hermitage portico, 12 categories of unique structural elements of a historical object were formed on the basis of the point cloud: windows, columns, pilasters, capitals, pedestals, Atlas statues, etc. All these objects in the information model are logically and structurally related (Fig. 3).

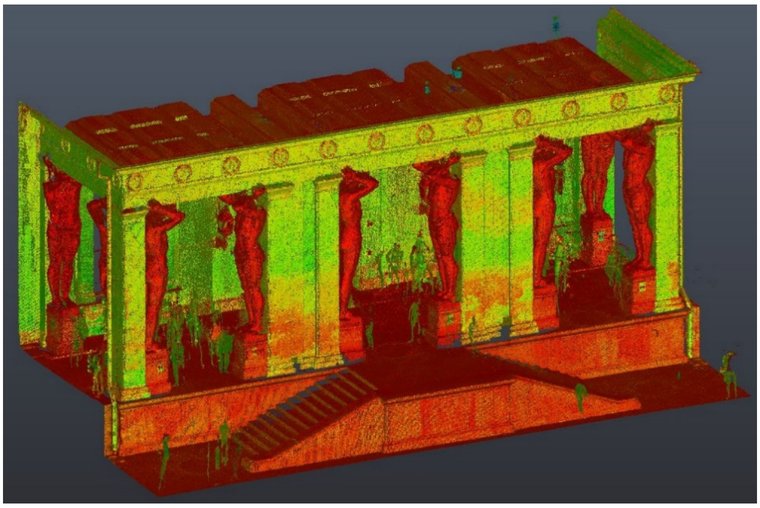

Fig. 2. Point cloud

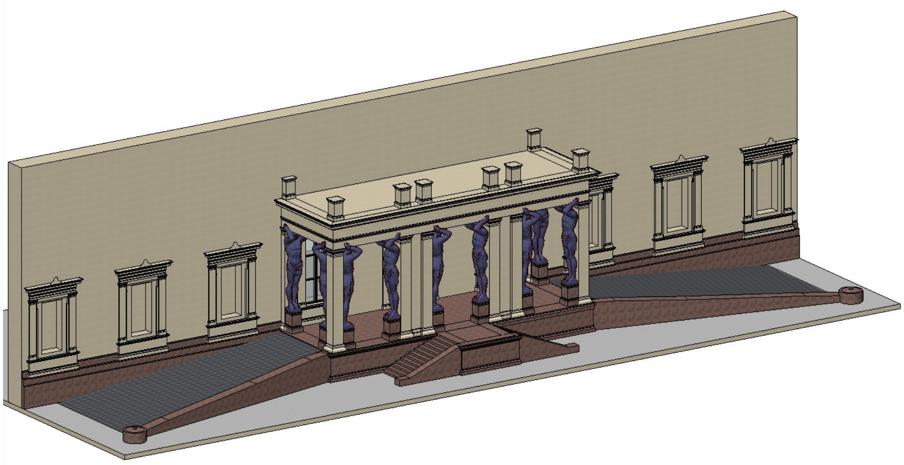

Fig. 3. Information model

Thanks to modern software systems focused on working with information models, we have the opportunity not to build a new mathematical model for calculating a building structure, but to analyze its digital representation directly. This approach makes it possible to predict how a building will behave even in extreme conditions [14–16].

When analyzing the structure of the portico of the New Hermitage, first of all, the reasons for the formation of cracks on the wrists and ankles of the granite sculptures of the Atlas were analyzed. For this, during the study, the strength and deformation characteristics (stress-strain state) of the entire structure were studied (Fig. 4).

The high level of detail of the model allows it to be used not only as an engineering analysis tool, but also as a demonstration model for the general public. Opportunities appear to create a digital asset of a cultural heritage object [17].

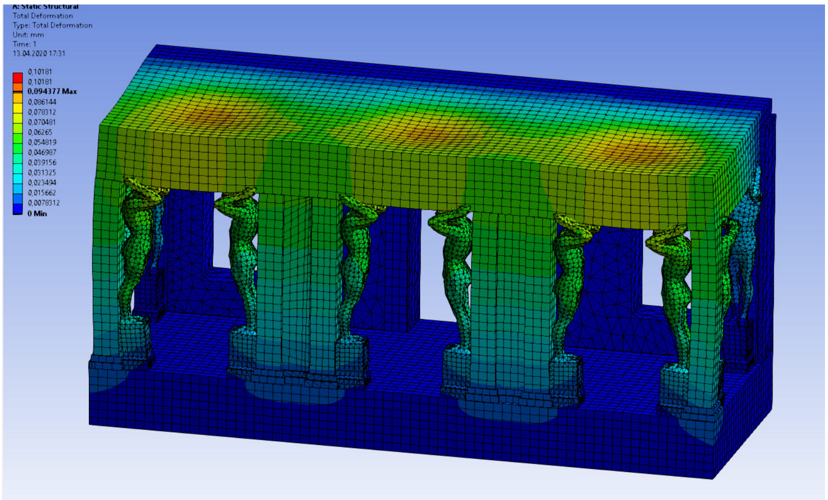

Fig. 4. Analysis result

Fig. 5. A copy of the portico of the New Hermitage, printed on a 3D printer

The very first results of the analysis of the three-dimensional Atlas models showed that the figures are practically identical, the discrepancies in the geometric parameters are no more than 1-2 mm, and occur very rarely. This once again confirms the professionalism of A.I. Terebenev and the Russian stonecutters working under his leadership.

With textures overlaid, the image takes on a photorealistic look. Such three-dimensional models are used in educational, cultural and entertainment spheres, virtual and augmented reality technology used as well [18–20]. Modern 3D editors make it possible for a person to come face to face with the object of their interest and provide all the necessary information in an interactive form, be it a historical reference, strength parameters or a manual for maintenance and support. In particular, within the framework of the described project, a hard copy of the portico of the New Hermitage was printed on a 3D printer (Fig. 5).

Conclusions

Modern methods of obtaining and processing digital information have great potential for application in all fields of science and technology. In particular, when it comes to computer analysis of scenes and obtaining digital 3D models from them [1, 9, 21, 22]. Laser scanning makes it possible to obtain highly adequate 3D point clouds representing real objects of a rather complex shape, for example, objects of cultural and historical heritage. Existing computer technologies, specialized software allows these data to be efficiently processed and used to build information models of the scanned objects. Correct collection and processing of information is the key to accurately predict the behavior of objects over time.

Cultural heritage sites require particularly careful and responsible maintenance throughout their entire service life. The cost of miscalculation or neglect of the structural features of a historic building, even with minor renovations, can be too high. It is in our power and interest to apply the best world practices for the preservation and restoration of cultural heritage. Only in this way will we preserve the history of our country for future generations.

The model of the portico of the New Hermitage building formed in the course of the presented HBIM study allows making conclusions on the geometric characteristics of the object, which is very important from a cultural and historical point of view, as well as on the behavior of the building structures of the object under various conditions that can change over time, for example, hydrogeological conditions associated with climate change. Among the results obtained, of particular interest is the discovered fact that the figures of the Atlas are absolutely identical, which only confirms the professionalism of A. Terebenev and the Russian stonecutters working under his leadership.

In conclusion, it should be noted that now the full potential of the HBIM technology remains unrevealed. Until now, many processes have been performed manually and relied on the experience of the specialists. In the future, technology will not only expand, mastering new functions and areas of application, but also deepen, increasing its own efficiency and the degree of automation.

Acknowledgements

The work on the monument was carried out jointly with the Department of History and Restoration of Architectural Monuments under the auspices of the Chief Architect of the State Hermitage, V.P. Lukin. The authors express their deep gratitude to the Director of the Hermitage Mikhail B. Piotrovsky for supporting the experimental work on laser scanning at such a landmark historical site not only for the Hermitage, but also for St. Petersburg.

REFERENCES

1. **Volk R., Stengel J., Schultmann F.** Building Information Modeling (BIM) for existing buildings – Literature review and future needs. *Automation in construction*, 2014, Vol. 38, Pp. 109–127.

2. **Dore C., Murphy M.** Current state of the art Historic Building Information Modelling. *International Archives of the Photogrammetry, Remote Sensing and Spatial Information Sciences – ISPRS Archives*, 2017, Vol. 42(2W5), Pp. 185–192

3. **Fateeva E., Badenko V., Fedotov A., Kochetkov I.** System analysis of the quality of meshes in HBIM. *MATEC Web of Conferences*. EDP Sciences, 2018, Vol. 170, P. 03033.

4. **Murphy M., McGovern E., Pavia S.** Historic Building Information Modelling – Adding intelligence to laser and image based surveys of European classical architecture. *ISPRS Journal of Photogrammetry and Remote Sensing*, 2013, Vol. 76, Pp. 89–102.

5. **Bruno S., De Fino M., Fatiguso F.** Historic Building Information Modelling: performance assessment for diagnosis-aided information modelling and management. *Automation in Construction*, 2018, Vol. 86, Pp. 256–276.

6. **Pocobelli D.P., Boehm J., Bryan P., Still J., Grau-Bové J.** BIM for heritage science: A review. *Heritage Science*, 2018, Vol. 6, No. 1, P. 30.

7. **Antonopoulou S., Bryan P.** Historic England BIM for heritage: Developing a Historic Building Information Model. *Swindon: Historic England. Retrieved March*, 2017, Vol. 10, P. 2019.

8. **Fryskowska A., Stachelek J.** A no-reference method of geometric content quality analysis of 3D models generated from laser scanning point clouds for HBIM. *Journal of Cultural Heritage*, 2018, Vol. 34, Pp. 95–108.

9. **Badenko V., Fedotov A., Vinogradov K.** Algorithms of laser scanner data processing for ground surface reconstruction. *Lecture Notes in Computer Science*, Vol. 10961, Pp. 397–411.

10. **Borovkov A.I., Ryabov Yu.A.** Definition, development and application of digital twins: The approach of the NTI Competence Center of SPbPU "New production technologies". *Tsifrovaya podstantsiya*, 2019, No. 12, Pp. 20–25. (rus)

11. **Murphy M., McGovern E., Pavia S.** Historic Building Information Modelling – Adding intelligence to laser and image based surveys of European classical architecture. *ISPRS Journal of Photogrammetry and Remote Sensing*, 2013, Vol. 76, Pp. 89–102.

12. **Quattrini R., Pierdicca R., Morbidoni C.** Knowledge-based data enrichment for HBIM: Exploring high-quality models using the semantic-web. *Journal of Cultural Heritage*, 2017, Vol. 28, Pp. 129–139.

13. **Banfi F.** Building Information Modelling – A novel parametric modeling approach based on 3D surveys of historic architecture. *Lecture Notes in Computer Science*, 2016, Vol. 10058, Pp. 116–127.

14. **Brumana R., Oreni D., Barazzetti L., Cuca B., Previtali M., Banfi, F.** Survey and scan to BIM model for the knowledge of built heritage and the management of conservation activities. *Research for Development*, 2020, Pp. 391–400.

15. **Badenko V., Fedotov A., Zotov D., Lytkin S., Volgin D., Garg R.D., Liu M.** Scan-to-BIM methodology adapted for different application. *Int. Arch. Photogramm. Remote Sens. Spatial Inf. Sci*, 2019, Vol. XLII-5/W2, Pp. 1–7.

16. **Oreni D., Brumana R., Della Torre S., Banfi F., Barazzetti L., Previtali M.** Survey turned into HBIM: The restoration and the work involved concerning the Basilica di Collemaggio after the earthquake (L'Aquila). *ISPRS annals of the photogrammetry, remote sensing and spatial information sciences*, 2014, Vol. 2, No. 5, Pp. 267–273.

17. **Badenko V.L., Bolshakov N.S., Fedotov A.A., Yadykin V.K.** Digital twins of complex technical systems in industry 4.0: basic approaches. *St. Petersburg State Polytechnical University Journal. Economics*, 2020, Vol. 13, No. 1, Pp. 20–30. (rus). DOI: 10.18721/JE.13102

18. **Osello A., Lucibello G., Morgagni F.** HBIM and virtual tools: A new chance to preserve architectural heritage. *Buildings*, 2018, Vol. 8, No. 1, P. 12.

19. **Lee J., Kim J., Ahn J., Woo W.** Context-aware risk management for architectural heritage using Historic Building Information Modeling and virtual reality. *Journal of Cultural Heritage*, 2019, Vol. 38, Pp. 242–252.

20. **Bolognesi C.M.** Digital Workflow for virtual and augmented visit of architecture. *Lecture Notes in Computer Science*, 2018, Vol. 11197, Pp. 126–133.

21. **Makarov A.S., Bolsunovskaya M.V.** Comparative analysis of methods for detecting special points in images at different lighting levels. *St. Petersburg State Polytechnical University Journal. Computer Science. Telecommunications and Control Systems*, 2018, Vol. 11, No. 2, Pp. 7–18. (rus). DOI: 10.18721/JCSTCS.11201

22. **Avtyushenko A.L., Ivanov V.M.** Computer technologies for converting two-dimensional objects into a three-dimensional scene. *St. Petersburg State Polytechnical University Journal. Computer Science. Telecommunications and Control Systems*, 2015, No. 5 (229), Pp. 7–17. (rus). DOI: 10.5862/JCSTCS.229.1

Received 26.07.2020.

СПИСОК ЛИТЕРАТУРЫ

1. **Volk R., Stengel J., Schultmann F.** Building Information Modeling (BIM) for existing buildings – Literature review and future needs // Automation in Construction. 2014. Vol. 38. Pp. 109–127.

2. **Dore C., Murphy M.** Current state of the art Historic Building Information Modelling // International Archives of the Photogrammetry, Remote Sensing and Spatial Information Sciences – ISPRS Archives. 2017. Vol. 42(2W5). Pp. 185–192.

3. **Fateeva E., Badenko V., Fedotov A., Kochetkov I.** System analysis of the quality of meshes in HBIM // MATEC Web of Conferences. EDP Sciences, 2018. Vol. 170. P. 03033.

4. **Murphy M., McGovern E., Pavia S.** Historic Building Information Modelling – Adding intelligence to laser and image based surveys of European classical architecture // ISPRS J. of Photogrammetry and Remote Sensing. 2013. Vol. 76. Pp. 89–102.

5. **Bruno S., De Fino M., Fatiguso F.** Historic Building Information Modelling: Performance assessment for diagnosis-aided information modelling and management // Automation in Construction. 2018. Vol. 86. Pp. 256–276.

6. **Pocobelli D.P., Boehm J., Bryan P., Still J., Grau-Bové J.** BIM for heritage science: A review // Heritage Science. 2018. Vol. 6. No. 1. P. 30.

7. **Antonopoulou S., Bryan P.** Historic England BIM for heritage: Developing a Historic Building Information Model // Swindon: Historic England. Retrieved March. 2017. Vol. 10. P. 2019.

8. **Fryskowska A., Stachelek J.** A no-reference method of geometric content quality analysis of 3D models generated from laser scanning point clouds for HBIM // J. of Cultural Heritage. 2018. Vol. 34. Pp. 95–108.

9. **Badenko V., Fedotov A., Vinogradov K.** Algorithms of laser scanner data processing for ground surface reconstruction // Lecture Notes in Computer Science. Vol. 10961. Pp. 397–411.

10. **Боровков А.И., Рябов Ю.А.** Определение, разработка и применение цифровых двойников: подход Центра компетенций НТИ СПбПУ «Новые производственные технологии» // Цифровая подстанция. 2019. № 12. С. 20–25.

11. **Murphy M., McGovern E., Pavia S.** Historic Building Information Modelling – Adding intelligence to laser and image based surveys of European classical architecture // ISPRS Journal of Photogrammetry and Remote Sensing. 2013. Vol. 76. Pp. 89–102.

12. **Quattrini R., Pierdicca R., Morbidoni C.** Knowledge-based data enrichment for HBIM: Exploring high-quality models using the semantic-web // J. of Cultural Heritage. 2017. Vol. 28. Pp. 129–139.

13. **Banfi F.** Building Information Modelling – A novel parametric modeling approach based on 3D surveys of historic architecture // Lecture Notes in Computer Science. 2016. Vol. 10058. Pp. 116–127.

14. **Brumana R., Oreni D., Barazzetti L., Cuca B., Previtali M., Banfi, F.** Survey and scan to BIM model for the knowledge of built heritage and the management of conservation activities // Research for Development. 2020. Pp. 391–400.

15. **Badenko V., Fedotov A., Zotov D., Lytkin S., Volgin D., Garg R.D., Liu M.** Scan-to-BIM methodology adapted for different application // Int. Arch. Photogramm. Remote Sens. Spatial Inf. Sci. 2019. Vol. XLII-5/W2. Pp. 1–7.

16. **Oreni D., Brumana R., Della Torre S., Banfi F., Barazzetti L., Previtali M.** Survey turned into HBIM: The restoration and the work involved concerning the Basilica di Collemaggio after the earthquake (L'Aquila) // ISPRS Annals of the Photogrammetry, Remote Sensing and Spatial Information Sciences. 2014. Vol. 2. No. 5. Pp. 267–273.

17. **Баденко В.Л., Большаков Н.С., Федотов А.А., Ядыкин В.К.** Цифровые двойники сложных технических систем в индустрии 4.0: базовые подходы // Научно-технические ведомости СПбГПУ. Экономические науки. 2020. Т. 13. № 1. С. 20–30. DOI: 10.18721/JE.13102

18. **Osello A., Lucibello G., Morgagni F.** HBIM and virtual tools: A new chance to preserve architectural heritage // Buildings. 2018. Vol. 8. No. 1. P. 12.

19. **Lee J., Kim J., Ahn J., Woo W.** Context-aware risk management for architectural heritage using Historic Building Information Modeling and virtual reality // J. of Cultural Heritage. 2019. Vol. 38. Pp. 242–252.

20. **Bolognesi C.M.** Digital workflow for virtual and augmented visit of architecture // Lecture Notes in Computer Science. 2018. Vol. 11197. Pp. 126–133.

21. **Макаров А.С., Болсуновская М.В.** Сравнительный анализ методов обнаружения особых точек на изображениях при различных уровнях освещения // Научно-технические ведомости СПбГПУ. Информатика. Телекоммуникации. Управление. 2018. Т. 11. № 2. С. 7–18. DOI: 10.18721/ JCSTCS.11201

22. **Автюшенко А.Л., Иванов В.М.** Компьютерные технологии конвертации двухмерных объектов в трехмерную сцену // Научно-технические ведомости СПбГПУ. Информатика. Телекоммуникации. Управление. 2015. № 5 (229). С. 7–17. DOI: 10.5862/JCSTCS.229.1

Статья поступила в редакцию 26.07.2020.

THE AUTHORS / СВЕДЕНИЯ ОБ АВТОРАХ

Fedotov Alexander A.
Федотов Александр Александрович
E-mail: alexandrefedotov@gmail.com

Prazdnikova Tatiana V.
Праздникова Татьяна Владимировна
E-mail: prazdnikova.t@gmail.com

Badenko Vladimir L.
Баденко Владимир Львович
E-mail: vbadenko@gmail.com

Yadykin Vladimir K.
Ядыкин Владимир Константинович
E-mail: v.yadikin@gmail.com

DOI: 10.18721/JCSTCS.13302
УДК 004.946

A FAST ALGORITHM FOR VISUAL MODELING OF RICE LEAF CELLS

W. Yi, Y. Zhao

Jiangxi Agricultural University,
Nanchang, China

In order to rapidly construct a visual model of rice leaf cells, the authors employed modeling tools of computer aided geometric design (CAGD): curve and surface. Rice mesophyll cells are an object of the study. In virtue of the Bernstein basis function properties and convex combination optimization, this work reconstructs the computation graph of the de Casteljau algorithm to model rice leaf cells, and C++ programming language and OpenGL rendering library are used to establish the visual model of cells. The theoretical results indicate that the control variables of curve and surface shape can be increased by revising affine combination coefficient through the polynomial space of the Bernstein basis function expansion. In addition, the results suggest that the convex combination optimization approach reduces the calculated time complexity of cytoskeleton interpolation points from O(n2) to O(n). The experimental results show that the convex combination algorithm has a significant advantage in terms of computation speed over the de Casteljau algorithm for each 200 interpolation points of the cytoskeleton. In view of the characteristics of close arrangement, regular shape, and large quantity of plant cells, the method proposed in this study has the ability to provide a feasible technical route and a rapid expression for visual modeling of plant cells.

Keywords: rice leaf cells, fast algorithm, visualization, CAGD, parameter curve.

Citation: Yi W., Zhao Y. A fast algorithm for visual modeling of rice leaf cells. Computing, Telecommunications and Control, 2020, Vol. 13, No. 3, Pp. 17–30. DOI: 10.18721/JCSTCS.13302

БЫСТРЫЙ АЛГОРИТМ ВИЗУАЛЬНОГО МОДЕЛИРОВАНИЯ КЛЕТОК РИСОВЫХ ЛИСТЬЕВ

В. И, И. Чжао

Jiangxi Agricultural University,
Nanchang, China

Для быстрого построения визуальной модели клеток рисового листа используются инструменты компьютерного геометрического проектирования (Computer Aided Geometric Design, CAGD) – «кривые» и «поверхности». В качестве объекта исследования взяты клетки мезофилла риса. На основании свойств базисной функции Бернштейна и оптимизации выпуклых комбинаций создаётся вычислительный граф алгоритма де Кастельжо для моделирования клеток рисового листа, а для построения визуальной модели клеток используется язык программирования C++ с библиотекой рендеринга OpenGL. Теоретические результаты показывают, что управляющие переменные кривой и формы поверхности могут быть увеличены путем пересмотра коэффициента аффинной комбинации через полиномиальное пространство разложения базисной функции Бернштейна. Кроме того, полученные результаты свидетельствуют о том, что подход оптимизации выпуклой комбинации позволяет уменьшить время сложного расчета точек интерполяции цитоскелета с O(n2) до O(n). Экспериментальные результаты демонстрируют, что алгоритм выпуклой комбинации имеет значительное преимущество с точки зрения скорости вычислений по сравнению с алгоритмом де Кастельжо для каждых 200 точек интерполяции цитоскелета. Учитывая особенности близкого расположения, правильной формы и большого количества растительных клеток, предложенный в данном исследовании метод способен обеспечить технологическую схему и быстрое выражение для визуального моделирования растительных клеток.

Ключевые слова: клетки рисовых листьев, быстрый алгоритм, визуализация, CAGD, кривая параметров.

Ссылка при цитировании: И В., Чжао И. Быстрый алгоритм визуального моделирования клеток рисовых листьев // Computing, Telecommunications and Control. 2020. Vol. 13. No. 3. Pp. 17–30. DOI: 10.18721/JCSTCS.13302

Introduction

The leaves are the main vegetative organs that perform crucial functions, such as photosynthesis and water transpiration, etc. Therefore, exploring the leaf morphology not only provides scientific guidance for improving the leaf's external morphology and increasing the internal functioning efficiency, but also has important research significance for improving the rice yield and quality. The research community has studied the rice leaf morphology by using genetic breeding technique, and discovered the gene that affects the leaf width, angle of inclination, and degree of curling. However, these studies mainly focus on a single gene regulation. Currently, it is still unclear whether all the genes affecting the whole rice leaf morphology formation are discovered and if there are any interactions between gene regulation networks [1]. This forms the basis of obstacles in leaf morphology modeling based on the gene regulation network.

In addition, few studies show that the cell morphology and quantity are the major factors that influence the formation of plant leaves, and the effect of mechanical force on cells is the main cause of the morphology formation [2–6]. On the basis of this theory, in this paper, we attempt to take the cell as the smallest research unit and use visualization technology to perform computer modeling for leaf local cells. This is done to provide computer aided design (CAD) support for rice leaf 3D morphology formation research.

Relevant works

The CAD technology can simulate a biological test which is either expensive or not easy to realize on computer platforms. It is an effective quantitative biological research method [7–12]. The interior of a rice leaf is observed using an optical microscope. It has plenty of cells: epidermis, mesophyll and vascular. The epidermis cells are closely arranged in a long geometrical shape. A mesophyll cell is a regular polygon with a thin wall and large intercell spaces. The vascular cells are in a slender geometrical shape [13]. It is known that the geometrical shapes of plant leaf cells are simple, and rapidly reconstructing the visual model is the research key of the CAD technology.

In computer aided geometric design (CAGD), the main research focus is to use the curve parameter equation to describe the object's skeleton morphological information [14–16], which has two aspects. One is using simple and low-order curve to approximate smooth and graceful curve according to the object's geometrical characteristics. The other is using numerical calculations and algorithm optimization to improve the rendering speed of the geometric model. The relevant studies in the first aspect are as follows. Some researchers adopted the Möbius transform to construct a quartic rational parabolic Pythagorean-Hodograph (PH) curve to satisfy C^2 continuous CAD design [17, 18]. In an attempt to satisfy a flexible design of curve inflection points, Lu et al. proposed indirect PH method to guarantee G^1 continuous Hermite interpolation according to the geometrical characteristics of Bessel control polygon [19]. Khan et al. used the convergent Lupaş Bernstein operators proved by Korovkin theorem to control the free deformation of the curve and the surfaces [20]. Kirmani et al. searched for the parameters that satisfy spline 3rd-order polynomial on the basis of Caputo fractional derivative factors, and thus fits the object's geometrical shape [21]. Asghar and Mustafa proposed a general formula for tensor product surfaces subdivision of one and two variables in order to reconstruct high order continuity and realistic vision of the object's geometrical model [22].

In recent years, the advancement in the applications of visualization technology imposes higher requirements for the calculation efficiency of geometric modeling. For example, Nuntawisuttiwong and Dejdumrong reduced the interpolation computing time by transforming Newton-Lagrange polynomials calculation into a linear algorithm [23]. Beccari and Casciola solved the curve that satisfied C^1 continuity by using the integral recursion method. This algorithm is beneficial for improving the storage efficiency of the vector diagram [24]. As the robustness of the integral recursion method is not clear, in order to break through the calculation dependence, Toshiiwal et al. constructed a space curve crossing the entirety of multiple order splines. This method realizes multiple order basis function splines by using the existing B spline [25]. As for subdivision algorithm, Hussain et al. generated a 5 points approximate subdivision mode through variable parameters, and introduced a shape parameter to construct different geometric graphs [26]. In addition, few scholars executed a binary subdivision algorithm after estimating the depth of curve and surface using a data algorithm. The research presented by Shahzad et al. shows that this method provides a significant improvement [27]. Besides, some studies inherited the advantages of endpoints and convex combination of the Bernstein basis function. Woźny and Chudy presented a recursive algorithm to reduce the time complexity of curve solution to linearity [28]. In this work, the second aspect is regarded as foundation, and geometric modeling of rice mesophyll cells as an example. The authors studied rapid solution algorithm of cell's geometric skeleton to improve the visual expression speed of leaf cells.

Materials and methods

The authors selected hybrid rice seed "Gangyou 6366". First, the seed is soaked in water for 10 min. Secondly, 100 plump seeds are selected and placed evenly on the double absorbent paper in a sprouting box, and water is added until the absorbent paper is fully saturated. Finally, the sprouting box is placed in a manual climatic box (MGC-250Hp, Shanghai Yiheng) to accelerate germination. The environmental parameters are: 25 °C temperature, 50 % humidity, 16 hours of light per day. After five days of the experiment, a rice leaf is randomly selected to be transacted at the middle segment. Since leaf epidermis and mesophyll cells are thin and allow the transmission of light, the contours of cells are not clear. Hence, the leaf segment to be observed is placed into absolute ethyl alcohol and heated to 70 °C for 1 hour. Then, Motic BA210 Digital Microscope (100x objective lens, 3-million-pixel charge coupled device (CCD)) is used to shoot the mesophyll cells of this leaf material. Three mesophyll cells are taken as visual modeling objects, with the shapes as shown in Fig. 1. Each closed full line frame is a mesophyll cytoskeleton, and dotted points are prepared curve control points.

The morphological structural changes are difficult to observe to the naked eye from microcosmic perspective, therefore computer simulation technology is used to express cell evolution and group competition [29]. Rational Bézier curve and surface geometric modeling technology is widely applied in CAGD [30]. However, as compared to rigid body objects, the plant leaf cells are large in quantity. Moreover, the cells are deformed due to biophysical mechanical effects. The rapid reconstruction and correct expression of a geometric shape model for a plant cell are the key points of visual simulation. On this basis, three research steps are presented in this work. As shown in Fig. 2, first, rational Bézier geometric modeling computation graph and designing algorithms of de Casteljau recursion and convex combination optimization are proposed, respectively. Secondly, both classes are compared on the basis of computational efficiency, and the faster algorithm is selected to establish a shape mesh model of a rice mesophyll cell. Finally, C++ and OpenGL graphics rendering library are adopted to establish a cell's

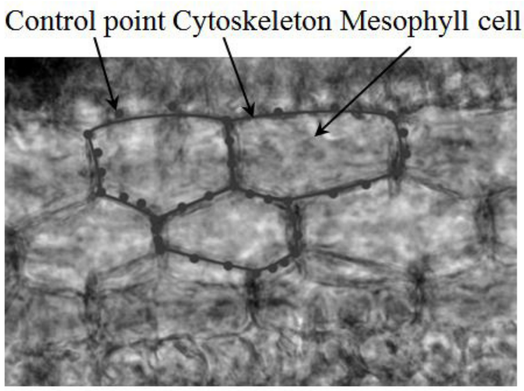

Fig. 1. Geometry of the discolored mesophyll cells

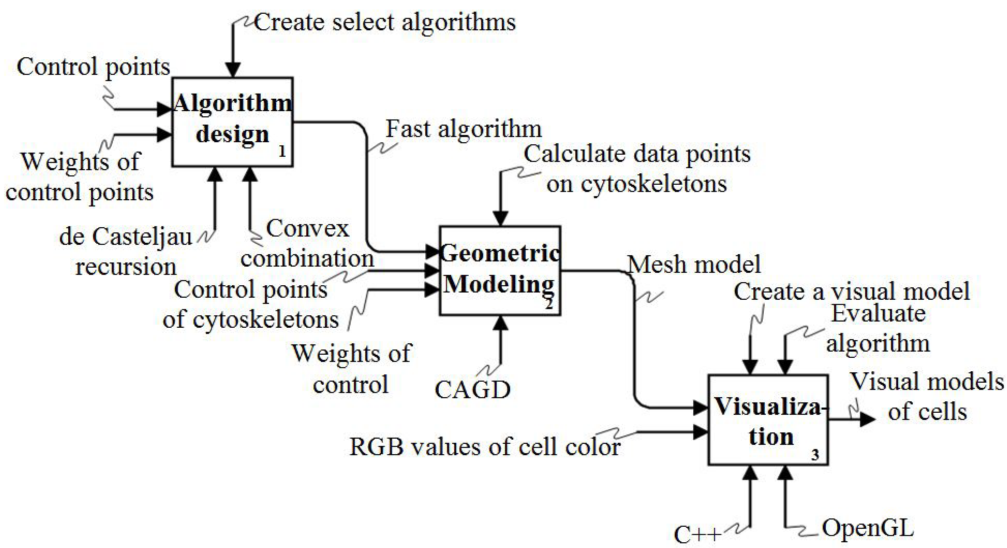

Fig. 2. Main methods and technical roadmap

visual model to estimate the algorithm time complexity. In the aforementioned steps, the rapid geometric modeling algorithm of cells is the main issue to be studied.

The CAGD object modeling is transformed to the evaluation of object geometric data points for control points set $\{ p_i \in \mathbb{R}^3 | i = 0, 1, .., n\}$ and the corresponding weights set $\{\omega_i \in \mathbb{R}^+ | i = 0, 1, ..., n\}$. The rational Bézier curve calculation is presented in (1) and (2):

$$r^n(t) = \sum_{i=0}^{n} p_i \beta_i^n(t) \tag{1}$$

$$\beta_i^n(t) = \frac{\omega_i^n B_i^n(t)}{\sum_{i=0}^{n} \omega_i^n B_i^n(t)}. \tag{2}$$

Where (2) extends to the n^{th} order rational function space $\beta^n = \text{span}\{\beta_i^n(t) \mid i = 0, 1, .., i\}$, and $\beta_i^n(t)$ satisfies the following properties:

(i) Non-negativity: for arbitrary $\omega_i > 0$ and $t \in [0, 1]$, it has: $\beta_i^n(t) \geq 0$;

(ii) Unit decomposability: $\sum_{i=0}^{n} \beta_i^n(t) = 1$; and

(iii) Endpoint property: $\beta_i^n(0) = \delta_{i0}$, $\beta_i^n(1) = \delta_{in}$, in which δ is Kronecker symbol.

Proof: As this space is based on classic Bernstein basis function $\beta_i^n(t)$, according to the non-negativity of Bernstein basis function, when curve control vertex weight $\omega_i > 0$, it is evident that $\beta_i^n(t) \geq 0$.

As the denominator i in (2) is irrelevant to the numerator, when the numerator adds the same sum operation, the cancellation of numerator with denominator is 1.

According to endpoint properties of $\beta_i^n(t)$, it can test that when $t = 0$ and $i = 0$, δ_{i0} =1; and when $t =$ $= 1$ and $i = n$, δ_{in} =1, respectively.

To sum up, the rational basis function $\beta_i^n(t)$ satisfies the properties (i)-(iii).

Assuming that quartic rational Bézier curve's control vertex and weights set $\{ p_i ; \omega_i \mid i = 0, 1, 2, 3\}$ denote the local geometric information of the cytoskeleton, we obtain the curve's polynomial according to (1)-(2):

$$r^3(t) = p_0\beta_0^3 + p_1\beta_1^3 + p_2\beta_2^3 + p_3\beta_3^3 = \frac{(1-t)^3\omega_0}{\omega} p_0 + \frac{3t(1-t)^2\omega_1}{\omega} p_1 + \\ + \frac{3t^2(1-t)\omega_2}{\omega} p_2 + \frac{t^3\omega_3}{\omega} p_3, \tag{3}$$

where $\omega = (1-t)^3\omega_0 + 3t(1-t)^2\omega_1 + 3t^2(1-t)\omega_2 + t^3\omega_3$.

Assuming $\lambda_0 = \dfrac{(1-t)^3\omega_0}{\omega}$, $\lambda_1 = \dfrac{3t(1-t)^2\omega_1}{\omega}$, $\lambda_2 = \dfrac{3t^2(1-t)\omega_2}{\omega}$, and $\lambda_3 = \dfrac{t^3\omega_3}{\omega}$.

The above polynomial coefficient $\lambda_0 + \lambda_1 + \lambda_2 + \lambda_3 = 1$. The aforementioned relation shows that when the given fixed point $t \in (0, 1)$, the data point $r^3(t)$ on the quartic rational Bézier curve is obtained by the affine combination of control points set $\{ p_i \}$. λ is the combination coefficient, and the data point is inside the polygon enclosed by the control points set. When $t = 0$ or 1, β_i^3 satisfies the endpoint property $r^3(0) = p_0$, and $r^3(1) = p_3$.

According to (3), denominator ω expression uses the function of affine combination $L(t) = a^n(1 - t) + b^n t$, that is, $\omega = l_1(t)\, l_2(t) \ldots l_n(t)$, in which a^n and b^n represent the adjacent combinations' coefficients λ_i^n and λ_{i+1}^n, respectively. The aforementioned process can be expressed as the following computation graph, as shown in Fig. 3.

The computation graph displays the data point calculation process of the rational Bézier curve based on de Casteljau recursive algorithm. In a similar way, (3) is generalized to the n^{th} order rational Bézie curve for solution. The recursive calculation is shown below:

$$r_i^k = \begin{cases} r_i^0 = p_i \ , \lambda_i^0 = \omega_i \\ \dfrac{\lambda_i^k(1-t)}{\lambda_i^k(1-t) + \lambda_{i+1}^k t} r_i^{k-1} + \dfrac{\lambda_{i+1}^k t}{\lambda_i^k(1-t) + \lambda_{i+1}^k t} r_{i+1}^{k-1} \end{cases}, \tag{4}$$

where $k = 1, 2, \ldots, n$; $i = 0, 1, \ldots, n-k$. The recursive process of the cytoskeleton data point algorithm is presented in Listing 1.

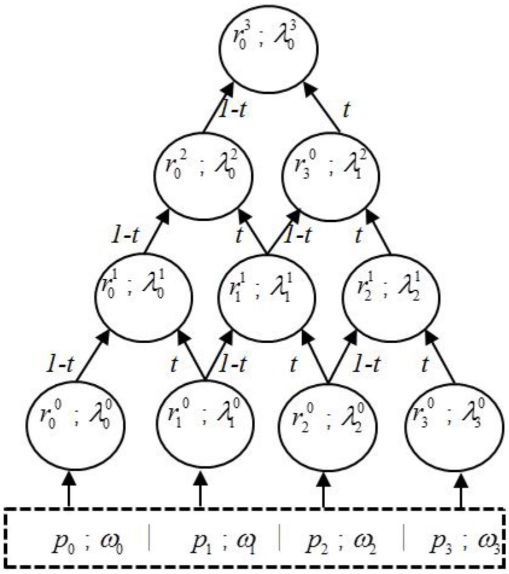

Fig. 3. Computation graph of rational curve modeling based on de Casteljau recursive algorithm

```
Input: int n, float t, vector < Point3 > p, vector < float > ω;
Output: vector < Point3 > cytoskeleton;
Initialize: i = 1, j ← 0, r = p, λ = ω;
While i less than or equal to n
    While j less than or equal to n−i
        u ← (1−t)*λ_j;
        v ← t*λ_{j+1};
        λ_j ← u+v;
        u ← u/λ_j;
        v ← 1−u;
        r_j ← u*r_j + v*r_{j+1};
        cytoskeleton=push_back(r_j);
        j ← j+1;
    i ← i+1;
```

Listing 1. Calculate points of cytoskeleton based on de Casteljau recursive algorithm (Algorithm 1)

According to curve control vertex convex combinations of curves and surfaces, the research idea is rewritten [28]. The de Casteljau recursive computation graph of cytoskeleton evaluation can be rewritten as the optimized convex combination form as shown in Fig. 4.

Thus, the local geometric shape of cytoskeleton can be rewritten as another form s^k, which satisfies the recursive convex combination of (5):

$$s^k = \begin{cases} s^0 = p_0, \ d^0 = 1 \\ \left(1 - d^k\right) s^{k-1} + d^k p_k \end{cases}, \tag{5}$$

where $k \in [0, 1, ..., n]$, $d^k = \dfrac{\lambda^k d^{k-1} t(n-k+1)}{\lambda^{k-1} k(1-t) + \lambda^k d^{k-1} t(n-k+1)}$.

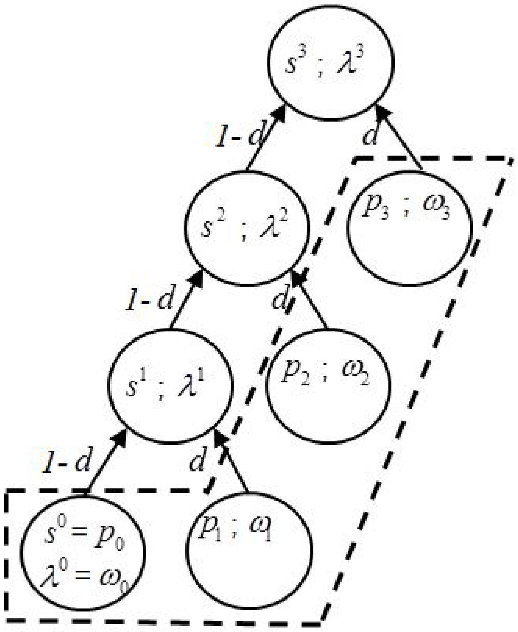

Fig. 4. Computation graph of rational curve modeling based on convex combination optimization

Proof: According to (1), the k-order rational basis function expression can be obtained as follows:

$$d^k = \sum_{i=0}^{k} p_i \frac{\lambda^i B^i(t)}{\sum_{i=0}^{k} \lambda^i B^i(t)}. \tag{6}$$

When $k = 0$, $d^k = 1$.

When $k > 0$, (6) can be written as

$$\sum_{i=0}^{k} p_i \frac{\lambda^i B^i(t)}{\sum_{i=0}^{k} \lambda^i B^i(t)} = \sum_{j=0}^{k-1} p_j \frac{\lambda^j B^j(t)}{\sum_{j=0}^{k} \lambda^j B^j(t)} + p_k \frac{\lambda^k B^k(t)}{\sum_{j=0}^{k} \lambda^j B^j(t)}. \tag{7}$$

According to (1), (2), and basis function property (ii), (7) is substituted into the control vertex and summation formula to obtain: $S^k = S^{k-1}(1-d^k) + p^k d^k$.

$n = k$ and $n = k-1$ are substituted into (2), respectively. (8) and (9) are obtained as

$$d^k(t) = \frac{\lambda^k B^k(t)}{\sum_{k=0}^{k} \lambda^k B^k(t)} = \frac{\lambda^k B^k(t)}{\sum_{k=0}^{k-1} \lambda^{k-1} B^{k-1}(t) + \lambda^k B^k} \tag{8}$$

$$d^{k-1}(t) = \frac{\lambda^{k-1} B^{k-1}(t)}{\sum_{k=0}^{k-1} \lambda^{k-1} B^{k-1}(t)}. \tag{9}$$

(9) is substituted into (8), and (10) is obtained as

$$d_k = \frac{\lambda_k d_{k-1} B_k(t)}{\lambda_{k-1} B_{k-1}(t) + \lambda_k d_{k-1} B_k(t)}. \tag{10}$$

When $0 < k \leq n$, Bernstein basis function is used to expand (10), and we get

$$d^k = \frac{\lambda^k d^{k-1} t(n-k+1)}{\lambda^{k-1} k(1-t) + \lambda^k d^{k-1} t(n-k+1)}. \tag{11}$$

Thus, (5) is proved.

The convex combination algorithm of cytoskeleton data point evaluation is expressed as presented in Listing 2.

Input: int n, **float** n, **vector < Point3 >** p, **vector < float >** ω ;
Output : vector < Point3 > $cytoskeleton$;
Initialize: $d \leftarrow 1.0$, $m \leftarrow 1.0 - t$, $s \leftarrow p_0$, $\lambda \leftarrow \omega$, $cytoskeleton = push\_back(s)$, $k = 1$;
While k **less than or equal to** n
  $d \leftarrow \lambda_k * d * t * (n-k+1)$;
  $d \leftarrow d / (\lambda_{k-1} * k * m + d)$;
  $s \leftarrow (1-d) * s_{k-1} + d * p_k$;
  If k **equal to** $n-1$
    $cytoskeleton = push\_back(s)$;
  $k \leftarrow k+1$;

Listing 2. Calculate points of cytoskeleton based on convex combination optimization (Algorithm 2)

Experimental results

In this work, the configuration parameters of computer hardware include Intel(R) Core(TM)i5-8400 CPU @2.80GHz 2.80GHz, 8G memory, 64-bit Windows 10 Pro, and Intel(R)UHD Graphics 630 NVIDIA GeForce GTX 1050 GPU. The authors used C++ programming design language and OpenGL 2.2 graphics rendering library. The geometric modeling involves processes of CPU and GPU calculations. In view of CPU operations, firstly C++ is adopted to realize the geometric shape mesh point evaluation of Algorithm 1 and Algorithm 2. Then, these values are successively bound to Vertex Buffer Object (VBO), Element Buffer Object (EBO), and Vertex Array Object (VAO), and then imported to the OpenGL graphics rendering library for GPU operations. Finally, after the processing of vertex and fragment shaders, a visual model is displayed on the computer screen. In order to verify the modeling efficiency of Algorithm 1 and Algorithm 2 in CAGD, we perform modeling experiments on the curve and the surface in terms of the two algorithms. As presented in Table 1 and Table 2, the position vector of curve control vertices and the position matrix of surface control vertices are provided.

Table 1

Control points of curve modeling, cm

p_0	p_1	p_2	p_3
[0.0, 3.0, 0.0]	[2.0, 7.0, 0.0]	[4.0, 7.0, 0.0]	[6.0, 3.0, 0.0]

Table 2

Control vertices of surface modeling, cm

p_{ij}	0	1	2	3
0	[0.0, 0.0, 2.0]	[0.0, 1.0, 2.0]	[0.0, 2.0, 2.0]	[0.0, 3.0, 2.0]
1	[2.0, 0.0, 0.0]	[2.0, 1.0, 0.0]	[2.0, 2.0, 0.0]	[2.0, 3.0, 0.0]
2	[4.0, 0.0, 0.0]	[4.0, 1.0, 0.0]	[4.0, 2.0, 0.0]	[4.0, 3.0, 0.0]
3	[6.0, 0.0, 2.0]	[6.0, 1.0, 2.0]	[6.0, 2.0, 2.0]	[6.0, 3.0, 2.0]

Without loss of generality, the value of interpolation points t is 40, and $\omega_i = 1$. The geometric shape visual results of Algorithm 1 and Algorithm 2 are shown in Fig. 5. The control polygon of Algorithm 2 is obtained by the convex combination of Algorithm 1. The curves and surface shapes of the desired values are similar. However, the geometric curvature obtained by Algorithm 2 is larger than the geometric shape of Algorithm 1.

The theoretical time complexities of two aforementioned algorithms are $O(n^2)$ and $O(n)$. As the number of interpolation points in geometric modeling tasks is small, the calculation of the modeling results is completed within 1 ms. In order to further test the calculation efficiencies of two algorithms in rice leaf cells modeling, the three adjacent mesophyll cells marked in Fig. 1 are selected in this study. For each cell,

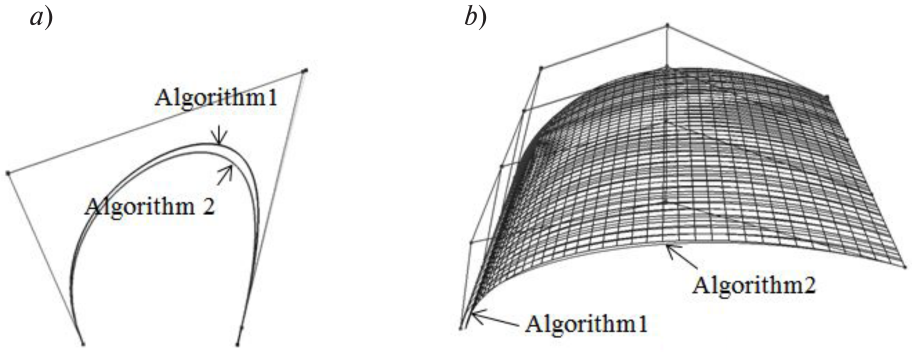

Fig. 5. Geometric modeling of the two algorithms: *a* – curves; *b* – surface

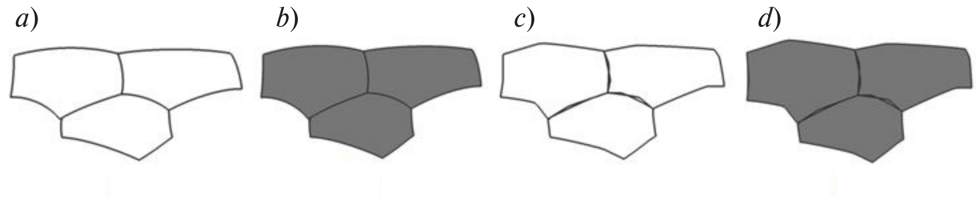

Fig. 6. Simulated results of cells: *a* – cytoskeleton; *b* – Filled color cells;
c – cells deformation on weight changes; *d* – Filled color of cells deformation

we adopt C^0 continuous curve combination. In the process of this experiment, it sets 48,000 rendering points of cell contour. The achieved results are presented in Fig. 6.

Fig. 6 *a*, *b* presents visual images of three cells when all the given control vertexes' weights $\omega_i = 1$. When the control vertexes adjacent to cells are assigned with different weights, the cells deform. The corresponding results are shown in Fig. 6 *c*, *d*. The computational time comparison of two algorithms on the geometric modeling of three adjacent rice mesophyll cells indicates that Algorithm 2 is 8 ms faster than Algorithm 1.

Discussions

The study on cell morphology by quantitative method needs to be supported by high-precision and high-tech devices. The development and application of biological microscopy enable the researchers to collect the geometric information of the microscale objects. A cell is the smallest living system with relatively "short" growth cycle. Traditional biological tests often use biochemistry and genetic methods to study some profiles of the cell living system to obtain the relevant information of cell growth. However, we are challenged with a comprehensive information integration problem, which is to study the operation of cell systems through the integration of multiple systems' profile knowledge. The virtualization and visualization technologies aim at establishing algorithms and models on computer platform to simulate and observe the real-world objects as well as to predict the evolution. In addition, it also helps researchers to build up the cell growth information models at the biochemical, physical and presentation layers. Moreover, it effectively integrates each layer's cell growth information [2, 4].

CAGD usually uses polynomial to approximate the curve and the surface. The space formed by these polynomials is obtained by the affine combination l_n of the Bernstein basis function, i.e., $l_n = a_n(1 - t) + b_n t$. Therefore, in view of Bézier type curve and surface, the improved algorithms are classified into two types. The first type introduces new combination coefficient variables to increase the degree of shape control freedom. For example, the combination coefficient (a_n , b_n) is replaced with $(\lambda_n a_n , \lambda_n b_n)$. The other type uses convex combination properties to change the combination ways of polynomials, thus reducing the computations [28]. The plant cell walls make the cells with the same type connect closely [31]. In this work, the rice mesophyll cells are taken as example, and the studies of two aspects are integrated. In addition, this work also discusses the visualization technology of plant call at presentation layer. Moreover, it studies a set of rapid expression methods in view of plant cell visual modeling. This method designs the affine combination algorithm of rational shape control factor λ, and emphatically analyses the time complexities of these two algorithms. The modeling calculation time of cell parameter curve and surface is shown in Fig. 7.

In the process of cell visualization based on curve modeling, as shown in Fig. 7 a, for every 200 interpolation points, the execution time of Algorithm 1 and that of Algorithm 2 are 6.551724 millisecond and 2.711598746 millisecond, respectively. The execution speed of Algorithm 2 is more significant in terms of statistics than that of Algorithm 1. In addition, the *p*-value of the *t*-test result of the two groups of data is 2.5117e-06 (significantly smaller than 0.01). However, in the process of surface modeling, as shown in Fig. 7 b, for the same interpolation points, the execution speed of Algorithm 2 is faster than that of Al-

a) *b*)

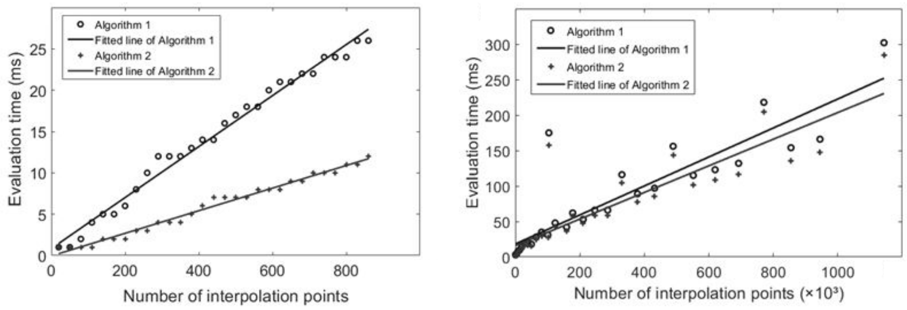

Fig. 7. Time comparison of the two algorithms for cells modeling: *a* – curves; *b* – surfaces

gorithm 1, with *p*-value of 0.6879. Hence, the adoption of Algorithm 2 is an appropriate rapid modeling approach for cytoskeletal curve's visual modeling.

Conclusion

The morphology of rice leaves is directly associated with the number and positional arrangement of cells. The rice cell living system belongs to the scope of micro-modeling. Generally, the modeling is divided into three layers. The bottom layer is a domain layer involving the knowledge field of plant-microbe chemistry. The intermediate layer is a physical mechanism layer that describes biological phenomena. The top layer is a representation layer of changes in cell morphology, which involves computer graphics, informatics, and computing technology, and has important research prospect and application value. This work focuses on the rapid expression method of cell geometric modeling at presentation layer. This work has four major conclusions.

(1) Based on the rational Bernstein basis function extension space, it is easy to obtain new curve and surface shape control variables by changing the affine combination coefficients.

(2) The cytoskeletal curve modeling by the convex combination optimization method (Algorithm 2) proposed in this paper has significant advantage in terms of computation speed over de Casteljau algorithm.

(3) Fixing the control vertex position 3D vectors simulates the deformation of real cell shape by changing the vertex weights (one-dimensional real number), which is beneficial for simplifying the relationship between cell stress and strain.

(4) The visual method in this study has universality in CAGD applications, and is easy to be generalized.

This study was supported by the National Natural Science Foundation of China (Grant No. 61762048; Grant No. 61363041; Grant No. 61562039) and the National Key Research and Development Program of China (Grant No. 2020YFD1100603).

REFERENCES

1. **Xu Jing, Wang Li, Qian Qian, et al.** Research advance in molecule regulation mechanism of leaf morphogenesis in rice (Oryza sativa L.). *ACTA Agronomica Sinica*, 2013, Vol. 39(5), Pp. 767–774. (in Chinese)

2. **Li Qinglin.** *Studies on modeling for the morphological variation of cucumber leaf based on micro-mechanics*. Jiangsu University, 2013. (in Chinese)

3. **Torode T.A., O'Neill R., Marcus S.E., et al.** Branched pectic galactan in phloem-sieve-element cell walls: Implications for cell mechanics. *Plant physiology*, 2018, Vol. 176(2), Pp. 1547–1558.

4. **Yi W., Zhao Y., Wu C., et al.** Algebraic topological method for semantic modelling of plant cell shapes. *2019 XXII International Conference on Soft Computing and Measurements*, St. Petersburg, Russia, 2019, Pp. 176–178, DOI: 10.1109/SCM.2019.8903849

5. **Gao Q., Fang Y., Zhang S., et al.** Dynamic effect of beta-amyloid 42 on cell mechanics. *Journal of Biomechanics*, 2019, No. 86, Pp. 79–88.

6. **Yi W., Zhao Y., Jiang Y., et al.** Computer simulation of plant cell plasmolysis based on physical and mechanical analyses. *2020 IEEE Conference of Russian Young Researchers in Electrical and Electronic Engineering (EIConRus)*, St. Petersburg and Moscow, Russia, 2020, Pp. 560–562. DOI: 10.1109/EIConRus49466.2020.9039139

7. **Marshall W.F.** Introduction to quantitative cell biology. *Colloquium Series on Quantitative Cell Biology*. San Francisco: Morgan & Claypool Life Sciences, 2017, P. 49.

8. **Mogilner A., Allard J., Wollman R.** Cell polarity: Quantitative modeling as a tool in cell biology. *Science*, 2012, Vol. 336(6078), Pp. 175–179.

9. **Avramouli A.** *Validation of modeling and simulation methods in computational biology. GeNeDis*. Springer, Cham, 2020, Pp. 323–330.

10. **Souza N.M., Topham A.T., Bassel G.W.** Quantitative analysis of the 3D cell shape changes driving soybean germination. *Journal of Experimental Botany*, 2017, Vol. 68(7), Pp. 1531–1537.

11. **Earles J.M., Buckley T.N., Brodersen C.R, et al.** Embracing 3D complexity in leaf carbon–water exchange. *Trends in Plant Science*, 2019, Vol. 24(1), Pp. 15–24.

12. **Haas K.T., Wightman R., Meyerowitz E.M., et al.** Pectin homogalacturonan nanofilament expansion drives morphogenesis in plant epidermal cells. *Science*, 2020, Vol. 367(6481), Pp. 1003–1007.

13. **Yang Yan-Hua, Wang Cai-Lin.** Comparative study on the microstructure and ultrastructure for three cultivated varieties of rice. *Bulletin of Botanical Research*, 2010, Vol. 30(2), Pp. 152–156. (in Chinese)

14. **Farin G.** *Curves and surfaces for computer-aided geometric design: A practical guide*. Cambridge: Academic Press, 2014, Pp. 101–288.

15. **Cottrell J.A., Hughes T.J.R., Bazilevs Y.** *Isogeometric analysis: Toward integration of CAD and FEA*. Hoboken: John Wiley & Sons, 2009, Pp. 1–106.

16. **Kobayashi S.** *Differential geometry of curves and surfaces*. Springer, Singapore, 2019.

17. **Farouki R.T., Giannelli C., Sestini A.** New developments in theory, algorithms, and applications for Pythagorean–Hodograph Curves. *Advanced Methods for Geometric Modeling and Numerical Simulation*. Springer, Cham, 2019, Pp. 127–177.

18. **Guo Yu.** *Research on Hermite Interpolation of Quadric Parabolic-PH Curve*. Hefei University of Technology, 2019.

19. **Lu X.J., Zheng J., Cai Y., et al.** Geometric characteristics of a class of cubic curves with rational offsets. *Computer-Aided Design*, 2016, No. 70, Pp. 36–45.

20. **Khan K., Lobiyal D.K.** Bèzier curves based on Lupaş (p, q)-analogue of Bernstein functions in CAGD. *Journal of Computational and Applied Mathematics*, 2017, No. 317, Pp. 458–477.

21. **Kirmani S., Riaz M.B.** Shape preserving fractional order KNR C 1 cubic spline. *The European Physical Journal Plus*, 2019, Vol. 134(7), P. 319.

22. **Asghar M., Mustafa G.** A family of binary approximating subdivision schemes based on binomial distribution. *Mehran University Research Journal of Engineering and Technology*, 2019, Vol. 38(4), Pp. 1087–1100.

23. **Nuntawisuttiwong T., Dejdumrong N.** Fast and efficient algorithms for evaluating uniform and non-uniform Lagrange and Newton curves. *International Journal of Computer and Information Engineering*, 2019, Vol. 13(8), Pp. 448–452.

24. **Beccari C.V., Casciola G.** A Cox-de Boor-type recurrence relation for C1 multi-degree splines. *Computer Aided Geometric Design*, 2019, No. 75, Article 101784.

25. **Toshniwal D., Speleers H., Hiemstra R.R., et al.** Multi-degree B-splines: Algorithmic computation and properties. *Computer Aided Geometric Design*, 2020, No. 76, Article 101792.

26. **Hussain S.M., Rehman A.U., Baleanu D., et al.** Generalized 5-point approximating subdivision scheme of varying arity. *Mathematics*, 2020, Vol. 8(4), P. 474.

27. **Shahzad A., Khan F., Ghaffar A., et al.** A novel numerical algorithm to estimate the subdivision depth of binary subdivision schemes. *Symmetry*, 2020, Vol. 12(1), P. 66.

28. **Woźny P., Chudy F.** Linear-time geometric algorithm for evaluating Bézier curves. *Computer-Aided Design*, 2020, 118: 102760.

29. **Zhao Chun-jiang, Lu Sheng-lian, Guo Xin-yu, et al.** Advances in research of digital plant: 3D Digitization of plant morphological structure. *Scientia Agricultura Sinica*, 2015(17), Pp. 3415–3428. (in Chinese)

30. **Farin G., Josef H., Kim M.-S.** *Handbook of computer aided geometric design*. Elsevier, 2002.

31. **Xiao Bo, Yun Hongxiang, Yang Deyong, et al.** One-dimensional isothermal drying model for parenchyma cell tissue of potato tuber. *Transactions of the Chinese Society of Agricultural Engineering (Transactions of the CSAE)*, 2019, Vol. 35(16), Pp. 309–319. DOI: 10.11975/j.issn.1002-6819.2019.16.034

Received 02.08.2020.

СПИСОК ЛИТЕРАТУРЫ

1. **Xu Jing, Wang Li, Qian Qian, et al.** Research advance in molecule regulation mechanism of leaf morphogenesis in rice (Oryza sativa L.) // ACTA Agronomica Sinica. 2013. Vol. 39(5). Pp. 767–774. (in Chinese)

2. **Li Qinglin.** Studies on modeling for the morphological variation of cucumber leaf based on micro-mechanics. Jiangsu University, 2013. (in Chinese)

3. **Torode T.A., O'Neill R., Marcus S.E., et al.** Branched pectic galactan in phloem-sieve-element cell walls: Implications for cell mechanics // Plant Physiology. 2018. Vol. 176(2). Pp. 1547–1558.

4. **Yi W., Zhao Y., Wu C., et al.** Algebraic topological method for semantic modelling of plant cell shapes // 2019 XXII Internat. Conf. on Soft Computing and Measurements, St. Petersburg, Russia, 2019. Pp. 176–178. DOI: 10.1109/SCM.2019.8903849

5. **Gao Q., Fang Y., Zhang S., et al.** Dynamic effect of beta-amyloid 42 on cell mechanics // J. of Biomechanics. 2019. No. 86. Pp. 79–88.

6. **Yi W., Zhao Y., Jiang Y., et al.** Computer simulation of plant cell plasmolysis based on physical and mechanical analyses // 2020 IEEE Conf. of Russian Young Researchers in Electrical and Electronic Engineering (EIConRus). St. Petersburg and Moscow, Russia, 2020. Pp. 560–562. DOI: 10.1109/EIConRus49466.2020.9039139

7. **Marshall W.F.** Introduction to quantitative cell biology // Colloquium Series on Quantitative Cell Biology. San Francisco: Morgan & Claypool Life Sciences, 2017. P. 49.

8. **Mogilner A., Allard J., Wollman R.** Cell polarity: Quantitative modeling as a tool in cell biology // Science. 2012. Vol. 336(6078). Pp. 175–179.

9. **Avramouli A.** Validation of modeling and simulation methods in computational biology. GeNeDis. Springer, Cham, 2020. Pp. 323–330.

10. **Souza N.M., Topham A.T., Bassel G.W.** Quantitative analysis of the 3D cell shape changes driving soybean germination // J. of Experimental Botany. 2017. Vol. 68(7). Pp. 1531–1537.

11. **Earles J.M., Buckley T.N., Brodersen C.R, et al.** Embracing 3D complexity in leaf carbon–water exchange // Trends in Plant Science. 2019. Vol. 24(1). Pp. 15–24.

12. **Haas K.T., Wightman R., Meyerowitz E.M., et al.** Pectin homogalacturonan nanofilament expansion drives morphogenesis in plant epidermal cells // Science. 2020. Vol. 367(6481). Pp. 1003–1007.

13. **Yang Yan-Hua, Wang Cai-Lin.** Comparative study on the microstructure and ultrastructure for three cultivated varieties of rice // Bulletin of Botanical Research. 2010. Vol. 30(2). Pp. 152–156. (in Chinese)

14. **Farin G.** Curves and surfaces for computer-aided geometric design: A practical guide. Cambridge: Academic Press, 2014. Pp. 101–288.

15. **Cottrell J.A., Hughes T.J.R., Bazilevs Y.** Isogeometric analysis: Toward integration of CAD and FEA. Hoboken: John Wiley & Sons, 2009, Pp. 1–106.

16. **Kobayashi S.** Differential geometry of curves and surfaces. Singapore: Springer, 2019.

17. **Farouki R.T., Giannelli C., Sestini A.** New developments in theory, algorithms, and applications for Pythagorean–Hodograph Curves // Advanced Methods for Geometric Modeling and Numerical Simulation. Springer, Cham, 2019. Pp. 127–177.

18. **Guo Yu.** Research on Hermite Interpolation of Quadric Parabolic-PH Curve. Hefei University of Technology, 2019.

19. **Lu X.J., Zheng J., Cai Y., et al.** Geometric characteristics of a class of cubic curves with rational offsets // Computer-Aided Design. 2016. No. 70. Pp. 36–45.

20. **Khan K., Lobiyal D.K.** Bѐzier curves based on Lupaş (p, q)-analogue of Bernstein functions in CAGD // J. of Computational and Applied Mathematics. 2017. No. 317. Pp. 458–477.

21. **Kirmani S., Riaz M.B.** Shape preserving fractional order KNR C 1 cubic spline // The European Physical Journal Plus. 2019. Vol. 134(7). P. 319.

22. **Asghar M., Mustafa G.** A family of binary approximating subdivision schemes based on binomial distribution // Mehran University Research Journal of Engineering and Technology. 2019. Vol. 38(4). Pp. 1087–1100.

23. **Nuntawisuttiwong T., Dejdumrong N.** Fast and efficient algorithms for evaluating uniform and nonuniform Lagrange and Newton curves // Internat. J. of Computer and Information Engineering. 2019. Vol. 13(8). Pp. 448–452.

24. **Beccari C.V., Casciola G.** A Cox-de Boor-type recurrence relation for C1 multi-degree splines // Computer Aided Geometric Design. 2019. No. 75. Article 101784.

25. **Toshniwal D., Speleers H., Hiemstra R.R., et al.** Multi-degree B-splines: Algorithmic computation and properties // Computer Aided Geometric Design. 2020. No. 76. Article 101792.

26. **Hussain S.M., Rehman A.U., Baleanu D., et al.** Generalized 5-point approximating subdivision scheme of varying arity // Mathematics. 2020. Vol. 8(4). P. 474.

27. **Shahzad A., Khan F., Ghaffar A., et al.** A novel numerical algorithm to estimate the subdivision depth of binary subdivision schemes // Symmetry. 2020. Vol. 12(1). P. 66.

28. **Woźny P., Chudy F.** Linear-time geometric algorithm for evaluating Bézier curves // Computer-Aided Design. 2020. No. 118. Article 102760.

29. **Zhao Chun-jiang, Lu Sheng-lian, Guo Xin-yu, et al.** Advances in research of digital plant: 3D Digitization of plant morphological structure // Scientia Agricultura Sinica. 2015(17). Pp. 3415–3428. (in Chinese)

30. **Farin G., Josef H., Kim M.-S.** Handbook of computer aided geometric design. Elsevier, 2002.

31. **Xiao Bo, Yun Hongxiang, Yang Deyong, et al.** One-dimensional isothermal drying model for parenchyma cell tissue of potato tuber // Transactions of the Chinese Society of Agricultural Engineering (Transactions of the CSAE). 2019. Vol. 35(16). Pp. 309–319. DOI: 10.11975/j.issn.1002-6819.2019.16.034

Статья поступила в редакцию 02.08.2020.

THE AUTHOR / СВЕДЕНИЯ ОБ АВТОРЕ

Yi Wenlong
И Вэньлун
E-mail: yiwenlong@jxau.edu.cn

Zhao Yingding
Чжао Индин
E-mail: zhaoyingding@163.com

DOI: 10.18721/JCSTCS.13303
УДК 004.492.3

TECHNIQUES FOR HYBRIDIZATION OF INTELLIGENT METHODS FOR DETECTING MALICIOUS TRAFFIC

V.E. Chumakov

Don State Technical University,
Rostov-on-Don, Russian Federation

In the modern world of IT technologies, there is a trend of ever-increasing flow of network traffic, network connections and, consequently, a growing number of vulnerabilities of centralized and decentralized systems. The urgency of the research lies in the necessity to modernize and improve existing mechanisms for better malicious traffic detection and enhanced security of the entire network infrastructure. The paper presents a new approach to network traffic research. The advantages of the proposed techniques are given in comparison with modern intrusion detection system based on standard algorithms and intelligent methods. The article indicates the direction in the area of modernization and improvement of algorithms for detection of network anomalies and network intrusions. The main features of the network traffic classification subsystem and the logic of work of each stage are displayed, the results of the system research and testing are presented, recommendations on the application and practical significance of the developed algorithm are described.

Keywords: IDS, IPS, security, network anomalies, intelligent methods.

Citation: Chumakov V.E. Techniques for hybridization of intelligent methods for detecting malicious traffic. Computing, Telecommunications and Control, 2020, Vol. 13, No. 3, Pp. 31–43. DOI: 10.18721/JCSTCS.13303

МЕТОДИКА ГИБРИДИЗАЦИИ ИНТЕЛЛЕКТУАЛЬНЫХ МЕТОДОВ ДЛЯ РАСПОЗНАВАНИЯ ЗЛОВРЕДНОГО ТРАФИКА

В.Е. Чумаков

Донской государственный технический университет,
Ростов-на-Дону, Российская Федерация

В современном мире IT-технологий наблюдается тенденция постоянно растущего потока сетевого трафика, сетевых подключений и соответственно постоянно растущего количества уязвимостей централизованных и децентрализованных систем. Актуальность темы заключается в необходимости модернизации и усовершенствования уже существующих механизмов для более точного распознавания зловредного трафика и повышения уровня защищенности всей сетевой инфраструктуры. Представлен новый подход к исследованию сетевого трафика. Описаны преимущества предлагаемой методики по сравнению с современными системами обнаружения вторжений, основанными на стандартных алгоритмах и интеллектуальных методах. Обозначены направления в области модернизации и усовершенствования алгоритмов по обнаружению сетевых аномалий и сетевых вторжений. Отображены основные моменты работы подсистемы классификации сетевого трафика и логика работы каждого этапа, представлены результаты исследования и тестирования системы, описаны рекомендации по применению и практической значимости разработанного алгоритма.

Ключевые слова: IDS, IPS, безопасность, сетевые аномалии, интеллектуальные методы.

Ссылка при цитировании: Чумаков В.Е. Методика гибридизации интеллектуальных методов для распознавания зловредного трафика // Computing, Telecommunications and Control. 2020. Vol. 13. No. 3. Pp. 31–43. DOI: 10.18721/JCSTCS.13303

Introduction

At present, the quality of commercial information provides the required economic benefits for any line of business of modern company, so it becomes important to find methods to protect mission-critical data from malfeasance. This allows companies to compete successfully in the labor market.

However, the methods applied in modern systems are not sufficiently effective and use outdated algorithms, provided that the exact characteristics of the attacks are known [2–5, 11–15]. Consequently, network attacks are constantly changing, and network traffic has become imperfect information, which includes data that is not completely reliable, inaccurate, or uncertain.

In view of this, it can be concluded that nowadays to provide an adequate level of network security the use of intrusion and anomaly detection systems (IDS/ADS) is a priority in the construction of network infrastructure of any company.

The aim of the developed method is to increase the efficiency of the IDSs through the proposed techniques for hybridization of intelligent methods.

Scientific novelty lies in the developed method of combined attack detection with the help of a two-level algorithm for detecting contention mechanisms when classifying mixed network traffic and the possibility of assigning arbitrary nesting of data about a network connection, thereby making it possible to work with “raw” data rather than using a well-structured signature base structure, which means that hardware attachment disappears when network anomalies are detected.

Existing methods of operation with the IDS/ADS

Modern IDS and ADS are modular architectures and typically consist of three modules, as follows:

1) The information gathering subsystem module, which serves to accumulate primary information on the network infrastructure portion protected and collects information both on the circulating network flow of the enterprise and on the services in operation, and software on protected workstations [1].

2) The module of the analysis subsystem assumes all the functions of detecting intrusion into the network infrastructure by using the existing analyzers which at the system output either confirm the fact of a host being hacked or a penetration into the enterprise network occurring, or disprove the existence of these actions by detecting the response of several types, such as false positive or false negative discoveries. As a rule, such a module works according to the Bayesian statistics rule, using the following common formula:

$$P\left(I \middle| \mathrm{A}_1, \mathrm{A}_2, \ldots, \mathrm{A}_n\right) = P\left(\mathrm{A}_1, \mathrm{A}_2, \ldots, \mathrm{A}_n \middle| I\right) \frac{P(I)}{P\left(\mathrm{A}_1, \mathrm{A}_2, \ldots, \mathrm{A}_n\right)}, \tag{1}$$

where I is responsible for detected intrusions, $\mathrm{A}_1, \ldots, \mathrm{A}_n$ is a recorded sequence of events, while each individual event of Am is a feature accumulation for calculating the estimate of the protected infrastructure, and $P(I \mid \mathrm{A}_1, \mathrm{A}_2, \ldots, \mathrm{A}_n)$ is the empirical probability of the intrusion into the network infrastructure.

3) The event alert subsystem module which is recorded by the IDS/ADS, in some cases with the possibility of access rights differentiation as several information security officers responsible for monitoring the various parts of the network infrastructure often work in the same enterprise.

In addition to the conventional and constantly modernized IDSs, there are also developments similar to the system proposed by the author based on the use of neural networks or fuzzy logic [2–5] used. In the next section, we will present the advantages of the proposed system as compared to the IDS/ADS and the systems being developed based on intelligent methods.

Advantages of the proposed system

After analysis and empirical research, it can be concluded that the existing IDSs have the malfunction module algorithm shown in Fig. 1 and the following drawbacks.

Modern IDS/ADS work on the principle of previously developed antivirus solutions, but to detect intrusions instead of malicious section of the code, the malicious section of the record in the header of the resulting frame is used, which is compared with the available IDS/IPS signature base. Thus, all the above

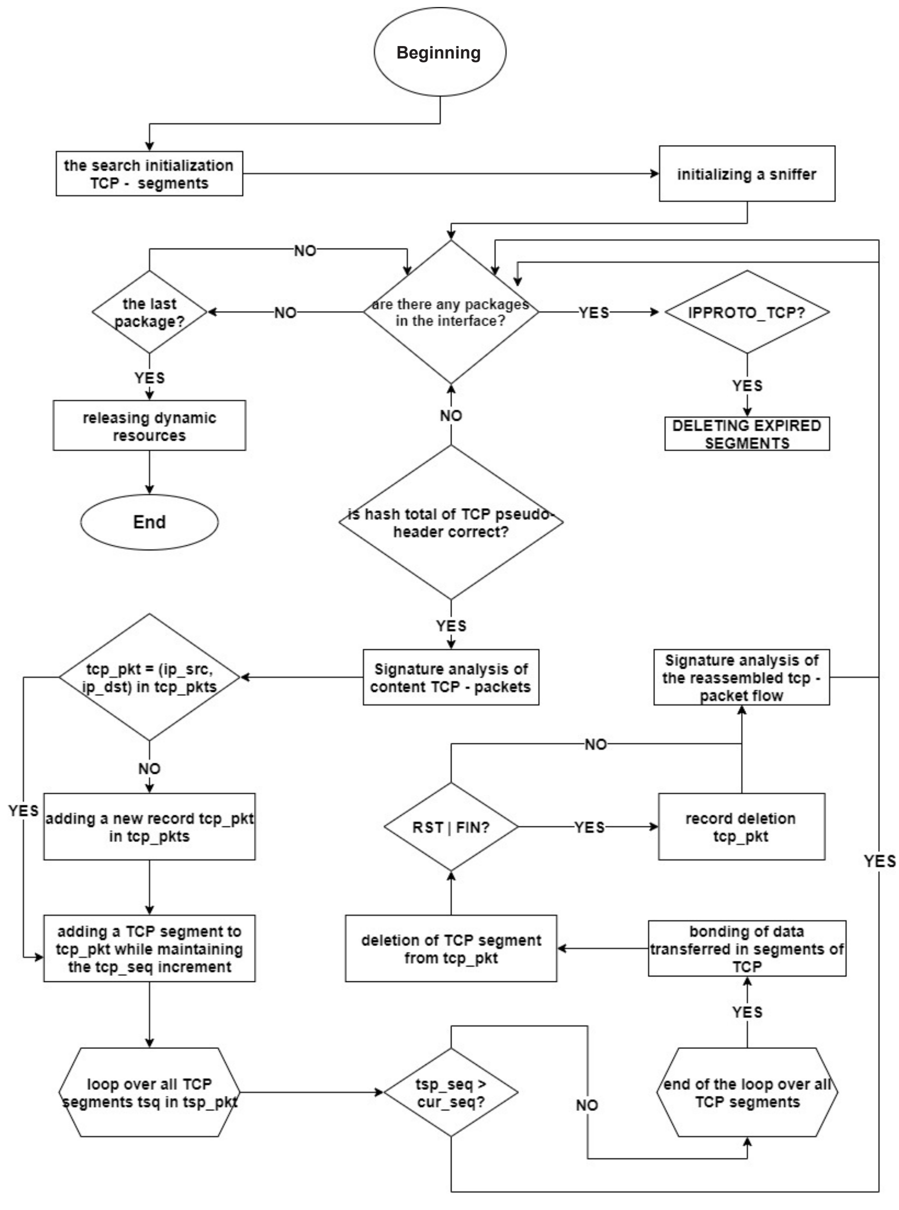

Fig. 1. Standard criteria selection algorithm

mentioned solutions start their activities when a section of the network infrastructure has already become contaminated. The signature base must be constantly updated as well, otherwise the system can miss malicious traffic due to outdated information. Thus, the flow of network traffic is exposed to zero-day attacks.

Existing systems based on the use of intelligent methods have other disadvantages. The systems developed on the basis of neural networks are not used in the branch under consideration due to the prolonged model training and the inflexible structure of work. This causes some difficulties in operation with network traffic, due to the constantly updated protocols, services and service quality elements (QoS) [6]. Systems developed on the basis of fuzzy logic have a very complex business logic of the work of the whole system, due to the constantly upgradable mathematical model of the system operation, which in its turn increases the malicious traffic detection time, and have a rule base too large to trigger the activation function, thereby increasing the number of false-negative responses [7].

The hybridization method proposed by the author is primarily aimed at work with input traffic. The first step of the proposed system is to pre-process raw data through the machine-learning algorithms. This reduces the load on the fuzzy logic module and the number of rules in the rule base by a several-fold factor, thereby reducing the operating time of the accumulative apparatus of the activation function triggering.

Research methodology

Currently, network traffic is standardized under different protocols of the common OSI model, which consists of seven levels and allows different network devices to interact with each other [8]. However, for an intelligent IDS, the input network flow is raw data and a heap about incoming frame, with introductory information such as flags, window sizes, packet length and various headers.

The empirical investigation involved the Friday_DDos array, which contains a classified set of weekly network traffic with a number of attacks of different type [9]. The array used consists of 80 columns indicating criteria and 215000 rows indicating the number of network connections received.

As discussed earlier, the standard criteria selection methods have very complex business logic, consisting of different triggers for a positive response to one of the parameters, such as whether the last packet is used in a session, whether the batch total is correct, which protocol is used. Therefore, all these parameters slow down the system, which in its turn destabilizes the flexibility, modularity and the operating principle of the system in real time.

The method of using machine-learning algorithms proposed by the author makes it possible to correct the deficiencies described above. Thus, machine-learning algorithms to recognize already classified attacks in the Friday_DDos set were compared, the results of comparisons are presented in Table 1.

Table 1

Results of comparison of machine-learning algorithms

	Accuracy, %
Principal Components Analysis (PCA)	76
Logistic regression	99.7
Support vector machine (SVM)	99.2
K-mean method	99.5
Feedforward neural networks (FF)	89
Decision trees	99

Based on the above table, it can be concluded that four algorithms have shown the highest recognition accuracy, but only one algorithm, namely the decision tree algorithm, allows for the informative visualization of distribution of the recognition weights. This algorithm was chosen, because the visualization gives the information security officer a great idea of the stability of the recognition system and the absence of false positive and negative responses.

Because the data set used consists of multiple features, the task of identifying the main attribute that will be located in the root tree is a complex process. To solve this problem, the algorithm uses several additional operations. Consider each of them.

Entropy is used as a definition of the coefficient dimensionality of the information to be analyzed. It is worth noting that the higher the indicator, the more difficult it is to draw conclusions when collecting data. This parameter is defined by the formula:

$$\mathrm{E}(\mathrm{T}, X) = \sum_{c \in X} P(c)\,\mathrm{E}(c), \tag{2}$$

where T shows the state of the object, X describes the selected criterion, c is one of the notations in the term set, and E is the probability of the object belonging to a process.

IG is a process that reduces the value of entropy, which is calculated by the following formula:

$$\mathrm{IG} = Entropy(before) - \sum_{j=1}^{K} Entropy(j,\ after), \tag{3}$$

where (*before*) is a state of the dataset before the partition, (j, *after*) is respectively a state after partition, K is a number of criteria that are generated for the further partition.

Gini is a specialized index that determines the value of each element in which the dataset is divided. It is calculated by the formula:

$$\mathrm{Gini} = 1 - \sum_{i=1}^{c} (p_i)^2, \tag{4}$$

where c is also one of the elements of the state and p is defined by the target variable of success.

GR is defined by a gain factor that helps to solve the problem of data increase during the dataset partition, taking into account the number of branches that will grow as the most significant coefficients are determined. The formula is as follows:

$$\mathrm{GR} = \frac{IG}{SI} = \frac{Entropy(before) - \sum_{j=1}^{k} Entropy(j,\ after)}{\sum_{j=1}^{k} w_j \log_2 w_j}, \tag{5}$$

where (*before*) is a dataset before the partition by criteria, k is a number of the selected parameters for the partition, (j, *after*) is a subset obtained after the partition of the dataset.

As a result of the operation of the selected algorithm of 80 indicators, the input data is reduced to 4, as shown in Fig. 2. Thus, we have 3 levels of immersion and only 4 indicators by which we can classify the traffic as malicious, by means of the following piece of code shown in Listing 1.

After an analytical review of the existing classification methods, it can be concluded that modern solutions have a number of shortcomings, namely:

– The input data of such systems is a crisp set like $\{X, \mu^*A(x)\}$, where $\mu^*A(x)$ is an ownership function, which in its turn forces the systems to standardize their solutions to a certain traffic array, thereby skipping and not identifying zero-day threats.

```
dot_data = StringIO()
dt_feature_names = list(X)
export_graphviz(clf, out_file=dot_data,
filled=True, rounded=True,
special_characters=True,class_names=['Benign','Ddos'],max_depth=3,
feature_names=dt_feature_names)
graph = pydotplus.graph_from_dot_data(dot_data.getvalue())
Image(graph.create_png())
```

Listing 1. Start of the Decision Trees algorithm

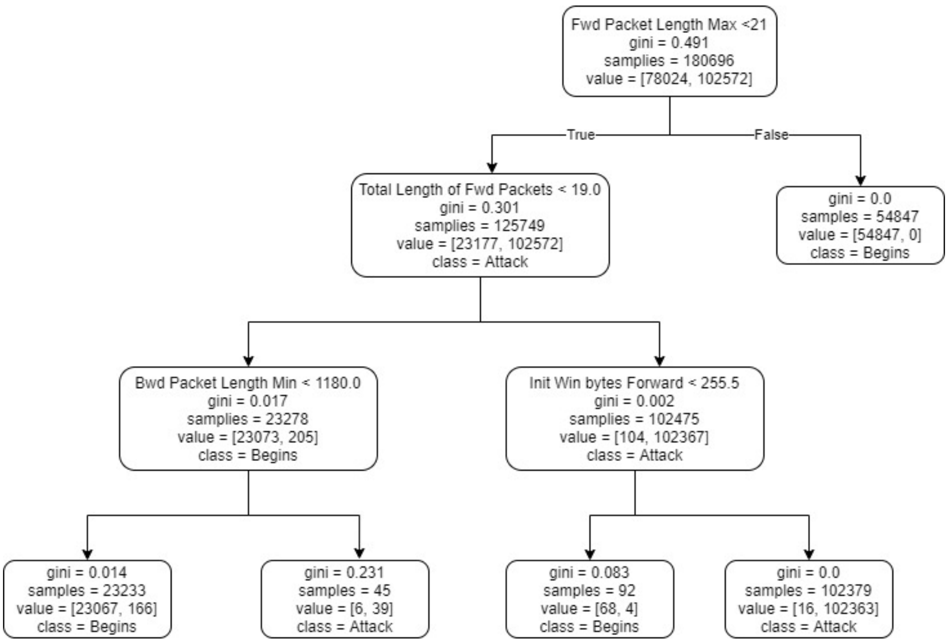

Fig. 2. Result of the algorithm operation

– As an activation function, a condition of compliance with a signature base within the standard solutions and a set of several activation functions with fuzzy logic to partition a strongly expanding rule base are used.

– The size of the rule base is hundreds of thousands of conditions for different protocols, various levels of interaction, and distinct scenarios of potential penetrations into the network infrastructure.

The solution for hybridization of machine-learning algorithms and fuzzy logic proposed by the author makes it possible to eliminate the listed disadvantages. It is proposed to use the Mamdani architecture as a fuzzy logic model, which in our case consists of 4 input functions obtained after the operation of the machine-learning algorithm, the module of calculation and activation of the activation function, and 1 output function, which is responsible for the classification of traffic as legitimized, malicious or mixed. The structure of this model is shown in Fig. 3.

As an activation function, we use a triangular function that has three points (a, b, c), two of which determine the position on the X-axis and one which is the vertex of the triangular function determining

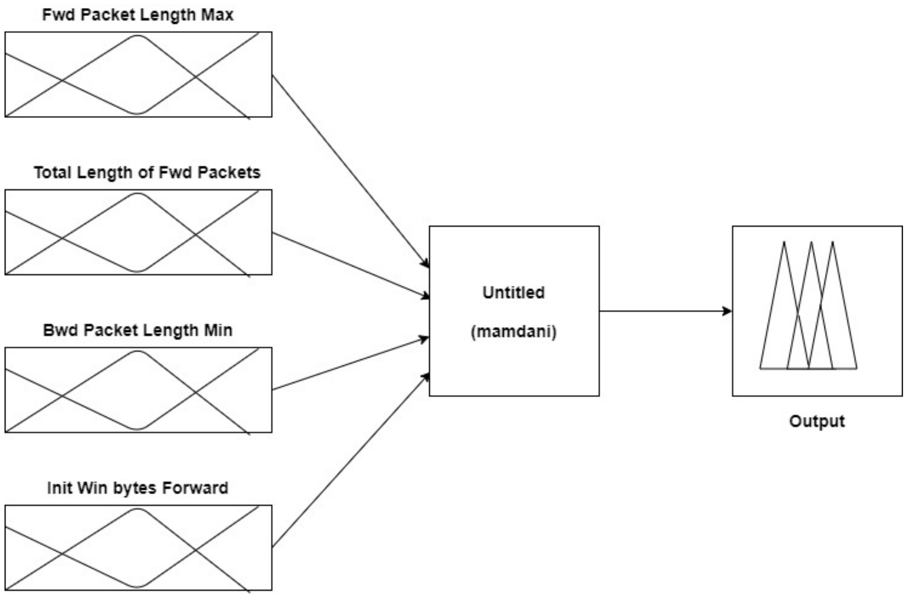

Fig. 3. Mamdani model structure

the position on the Y-axis [10]. According to this function, its value F (x) is calculated by the following formula:

$$F(x) = \begin{cases} 1-\dfrac{b-x}{b-a}, & a \le x \le b, \\ 1-\dfrac{x-b}{c-b}, & b \le x \le c, \\ 0, & x \notin (a;d). \end{cases} \tag{6}$$

After processing raw data as incoming network traffic and identifying markers through machine-learning algorithms, fuzzy logic model identification and activation function construction, direct recognition of incoming network connections is carried out in several steps, namely:

1. The first step is a procedure of fuzzification. At this stage, the degree of ownership of the function for the extremities of each input variable was determined. To do this, the following code fragment, shown in Listing 2, must be executed:

```
Fwd_lo = fuzz.trimf(Fwd_Packet_Length_Max, [0, 0, 21])
Fwd_md = fuzz.trimf(Fwd_Packet_Length_Max, [17, 20, 25])
Fwd_hi = fuzz.trimf(Fwd_Packet_Length_Max, [22, 27, 27])
Total_lo = fuzz.trimf(Total_Length_of_Fwd_Packets, [0, 0, 19])
Total_md = fuzz.trimf(Total_Length_of_Fwd_Packets, [10, 18, 22])
Total_hi = fuzz.trimf(Total_Length_of_Fwd_Packets, [21, 27, 27])
Init_lo=fuzz.trimf(Init_Win_bytes_forward,[0,0,255])
Init_md=fuzz.trimf(Init_Win_bytes_forward,[220,250,300])
Init_hi=fuzz.trimf(Init_Win_bytes_forward,[260,300,300])
Bwd_lo = fuzz.trimf(Bwd_Packet_Length_Min,[0,0,1180])
Bwd_md=fuzz.trimf(Bwd_Packet_Length_Min,[900,1180,1300])
```

```
Bwd_hi=fuzz.trimf(Bwd_Packet_Length_Min,[1190,1300,1300])
tip_lo = fuzz.trimf(x_tip, [0, 0.2, 0.5])
tip_md = fuzz.trimf(x_tip, [0.5, 0.65, 0.79])
tip_hi = fuzz.trimf(x_tip, [0.8, 0.89, 1])
```

Listing 2. Start of the procedure of fuzzification

2. This was followed by a cut off procedure for one part of a separate rule and ownership function. To do this, the following code fragment shown in Listing 3 must be executed:

```
tip_activation_lo = np.fmin(active_rule6, tip_lo)
tip_activation_md = np.fmin(serv_level_md, tip_md)
tip_activation_hi = np.fmin(active_rule7, tip_hi)
```

Listing 3. Start of the cut off procedure

3. Then the truncations of the function obtained at the second stage were accumulated by calculating the maximum value from the presented fuzzy sets. To do this, the following code fragment shown in Listing 4 must be executed:

```
active_rule1 = np.fmax(qual_level_lo, serv_level_lo)
active_rule4=np.fmax(active_rule1,Init_level_lo)
active_rule6=np.fmax(active_rule4,bwd_level_lo)
active_rule3 = np.fmax(qual_level_hi, serv_level_hi)
active_rule5=np.fmax(active_rule3,Init_level_hi)
active_rule7=np.fmax(active_rule5,bwd_level_hi)
```

Listing 4. Start of the accumulation procedure of the truncated functions

4. The final step is a defuzzification procedure. That is, at this stage, fuzzy procedures were brought to crisp sets in order to obtain a crisp classification of traffic according to one of the indicators contained in the term set. The centroid method and the following fragment of the code shown in Listing 5 were used for defuzzification:

```
aggregated = np.fmax(tip_activation_lo,
                     np.fmax(tip_activation_md, tip_activation_hi))
tip = fuzz.defuzz(x_tip, aggregated, 'centroid')
tip_activation = fuzz.interp_membership(x_tip, aggregated, tip)
```

Listing 5. Start of the defuzzification procedure

After the completed stages, the system was tested for recognition of the legitimacy of traffic, potential attack, zero-day attack and the actual state of the system during the penetration.

Thus, when the values of the attributes selected by the machine-learning algorithm are like presented in the figure below the operation of the algorithm is tested.

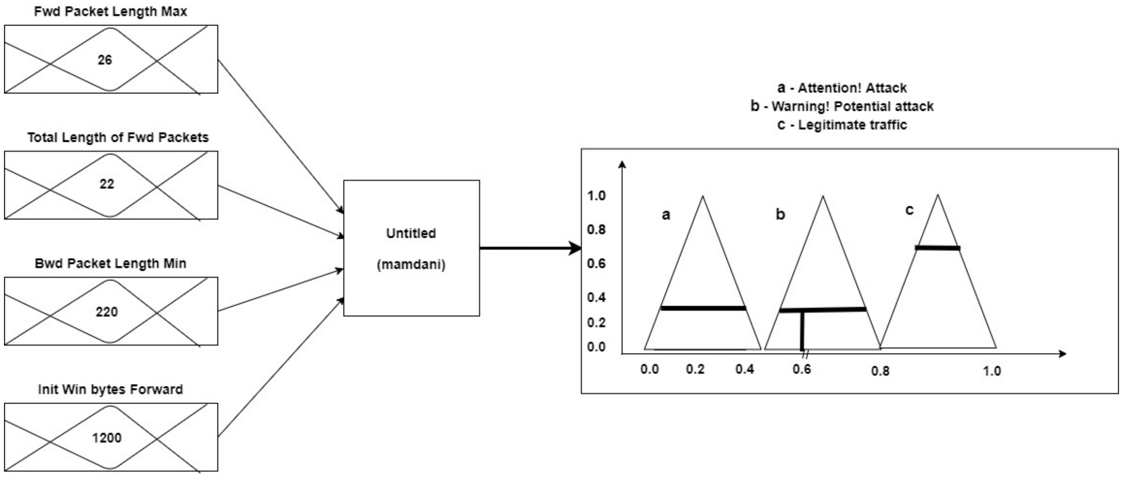

Fig. 4. Recognition testing on the potential penetration into the network infrastructure

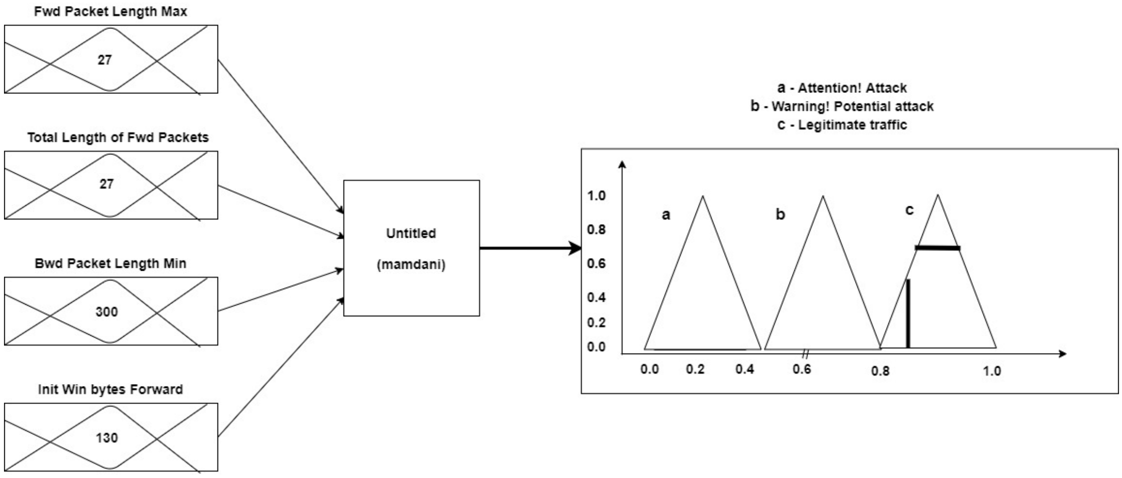

Fig. 5. System testing to classify network legitimate traffic

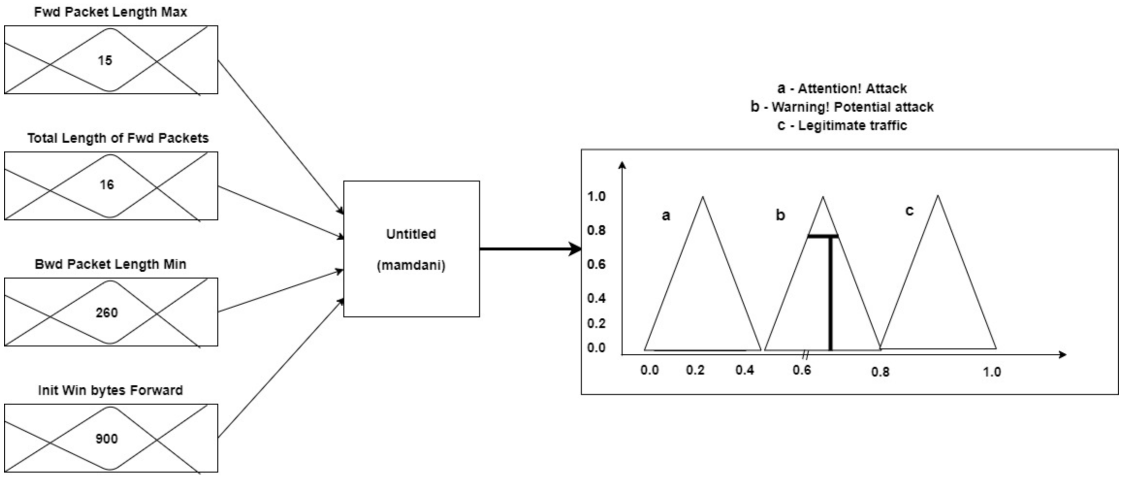

Fig. 6. Recognition testing on zero-day vulnerability

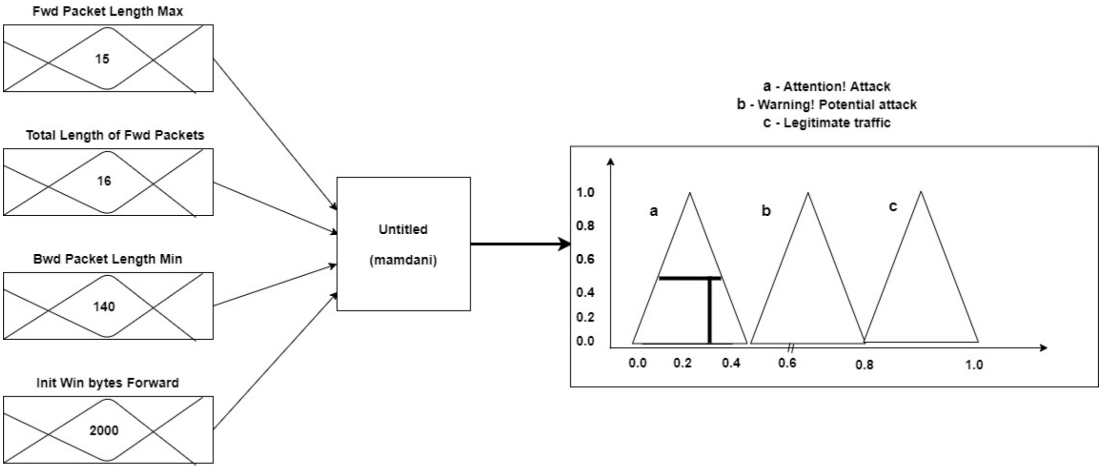

Fig. 7. System testing for current attack recognition

After a series of experiments, it can be concluded that the system performs its task and classifies network traffic as a potential attack (Fig. 4), legitimate traffic (Fig. 5), a zero-day attack (Fig. 6) or a current attack (Fig.7).

Conclusion

In conclusion we can say that the developed technique for hybridization of intelligent methods based on the preprocessing of network traffic, through the machine-learning algorithm and subsystem operation of fuzzy logic for recognition of malicious traffic, enables a reduction of a number of false responses and improves the efficiency of detecting network anomalies by an average of 15-17 % compared to the standard methods in the field under consideration.

The advantages of the developed technique include the possibility to reduce the rule base for fuzzy logic subsystem by 16 % compared to the existing IDS developments based on fuzzy logic, due to the preprocessing of raw data and reducing key parameters by a several-fold factor, on the basis of which the network traffic classification is carried out. As a result of system testing for 215000 connections after data preprocessing, only 4 parameters have been selected and the rule base has only 6 rules.

Thus, a technique for combined searching of attacks based on the detecting of abuse and network anomalies has been developed during the study. A new approach to network traffic processing is presented, which consists in predicting the target variable value on the basis of several variables at the input rather than on the use of known signature bases. The advantages of the proposed anomaly detection system architecture are shown and the results of the testing on weekly network traffic are given.

It can be concluded that the developed approach completely fulfils the given tasks and can be used both to detect the known, previously encountered attacks and to detect the new ones. The algorithm makes it possible to reduce the number of questionable and controversial responses and can also be used in the development of new solutions for detecting network anomalies and malicious network traffic.

REFERENCES

1. **Le C.M., Fang H.A., Nguyen A.C., Nguyen C.T.** Integrated IDS/IPS Open-Source Model with Improved Machine Learning. *Results of Applied and Research Studies in Natural History and Technology: Compendium of Scientific Papers on the Proceedings of the International Scientific and Practical Conference on 27 Dec. 2019.* Belgorod: LLC Advanced Scientific Research Agency (APNI), 2019. Pp. 81–87. Available: https://apni.ru/article/152-integrirovannaya-sipidsips-model-mezh-duotkr

2. **Chumakov V.E.** Analysis of Modern Methods of Network Infrastructure Security. International Journal of Applied Sciences and Technology. Collection 4, 2019. Available: *https:///e-integral.ru/rubriki/tehnichesk-iekienauki/d0-b8-0-0-bd-d1-82-d0-b5-d0-b3--d1-80-d0b-0---d0-b0--d0-b0-Bbie-4---20192-42* (Accessed: 29.08.2020).

3. **Shanmugavadivu R., Nagarajan Dr.N.** Network Intrusion Detection System using Fuzzy Logic. Indian Journal of Computer Science and Engineering. 2. Available: *https:///www.researchgate.net/publication/50417996_Network_Intrusion_Detection_System_using_Fuzzy_Logic* (Accessed: 01.09.2020).

4. **Seo H.S., Cho T.H.** Application of Fuzzy Logic for Distributed Intrusion Detection. Computational Intelligence and Security. Lecture Notes in Computer Science. Vol. 3802. Springer, Berlin, Heidelberg. Available: *https:///doi.org/10.1007/11596981_51* (Accessed: 02. 09. 2020).

5. **Shanmugam B., Idris N.B.** Improved Intrusion Detection System Using Fuzzy Logic for Detecting Anamoly and Misuse Type of Attacks. *International Conference of Soft Computing and Pattern Recognition*, Malacca, Pp. 212–217. DOI: 10.1109/Soc.2009.51

6. **Kesavulu Reddy Ekambaram.** Neural Networks for Intrusion Detection and its Applications. Lecture Notes in Engineering and Computer Science. 2. 1210–1214. Available: *https:///www.researchgate.net/publication/286697952_Neural_Nworkets_for_Intrusion_Detection_and_Its_Applications* (Accessed: 04.09.2020).

7. **Vishnu Balan E., Priyan M.K., Gokulnath C., Usha Devi G.** Fuzzy Based Intrusion Detection Systems in MANET. Procedia Computer Science, Vol. 50, Pp. 109–114. Available: *https:///doi.org/10.1016/j.procs.2015.04.071.* (Accessed: 04.09.2020).

8. Network Protocols of the OSI Model. Full articles about networks and computer security. Available: *http://blogsisadmina.ru/seti/setevye-protokoly-modeli-osi.html* (Accessed: 04.09.2020).

9. The Archive Data Set. The Archive to Test Machine Learning Algorithms. Available: *http://archive.ics.uci.edu/ml/machine-learning-databases/* (Accessed: 05.09.2020).

10. **Olivas E., Martín-Guerrero J., Camps-Valls G., Serrano-López A., Calpe J., Gómez-Chova L.** A Low-complexity Fuzzy Activation Function for Artificial Neural Networks. IEEE Transactions on Neural Networks. 14. 1576–1579. 10.1109/TNN.2003.820444. Available: *https://www.researchgate.net/publication/220279588_A_low-complexity_fuzzy_activation_function_for_artificial_neural_networks* (Accessed: 06.09.2020).

11. **García-Teodoro P., Díaz-Verdejo J., Maciá-Fernández G., Vázquez E.** Anomaly-based network intrusion detection: Techniques, systems and challenges. Computers & Security, 2009, Vol. 28, Iss. 1–2, Pp. 18–28. Available: *http://www.sciencedirect.com/science/article/pii/S0167404808000692* (Accessed: 29.08.2020).

12. **Zhang J., Zulkernine M.** Anomaly Based Network Intrusion Detection with Unsupervised Outlier Detection. *2006 IEEE International Conference on Communications*, Istanbul, 2006, Pp. 2388–2393. DOI: 10.1109/ICC.2006.255127

13. **Samrin R., Vasumathi D.** Review on Anomaly. Based Network Intrusion Detection System. *2017 International Conference on Electrical, Electronics, Communication, Computer, and Optimization Techniques (ICEECCOT)*, Mysuru, 2017, Pp. 141–147. DOI: 10.1109/ICEECCOT.2017.8284655

14. **Schindler T.** Anomaly Detection in Log Data using Graph Databases and Machine Learning to Defend Advanced Persistent Threats. Informatik e.V. (Hrsg.): Informatik 2017. Available: *https://arxiv.org/pdf/1802.00259.pdf* (Accessed: 01.09.2020).

15. **Bahlali A.R.** Anomaly-Based Network Intrusion Detection System: A Machine Learning Approach. 2019. DOI: 10.13140/RG.2.2.29553.84325

Received 14.07.2020.

СПИСОК ЛИТЕРАТУРЫ

1. **Le C.M., Fang H.A., Nguyen A.C., Nguyen C.T.** Integrated IDS/IPS open-source model with improved machine learning // Results of Applied and Research Studies in Natural History and Technology: Com-

pendium of Scientific Papers on the Proc. of the Internat. Scientific and Practical Conf. on 27 Dec. 2019. Belgorod: LLC Advanced Scientific Research Agency (APNI), 2019. Pp. 81–87 // URL: https:///apni.ru/article/152-integrirovannaya-sipidsips-model-mezh-duotkr

2. **Chumakov V.E.** Analysis of modern methods of network infrastructure security // Internat. J. of Applied Sciences and Technology. Collection. 2019. No. 4 // URL: https:///e-integral.ru/rubriki/tehnicheskiekienauki/d0-b8-0-0-bd-d1-82-d0-b5-d0-b3--d1-80-d0b-0---d0-b0--d0-b0-Bbie-4---20192-42 (Дата обращения: 29.08.2020).

3. **Shanmugavadivu R., Nagarajan Dr.N.** Network intrusion detection system using fuzzy logic // Indian Journal of Computer Science and Engineering. 2 // URL: https:///www.researchgate.net/publication/50417996_Network_Intrusion_Detection_System_using_Fuzzy_Logic (Дата обращения: 01.09.2020).

4. **Seo H.S., Cho T.H.** Application of fuzzy logic for distributed intrusion detection // Computational Intelligence and Security. Lecture Notes in Computer Science, Vol. 3802. Springer, Berlin, Heidelberg // URL: https:///doi.org/10.1007/11596981_51 (Дата обращения: 02.09.2020).

5. **Shanmugam B., Idris N.B.** Improved intrusion detection system using fuzzy logic for detecting anomaly and misuse type of attacks // Internat. Conf. of Soft Computing and Pattern Recognition. Malacca. Pp. 212–217. DOI: 10.1109/Soc.2009.51.

6. **Kesavulu Reddy Ekambaram.** Neural networks for intrusion detection and its applications // Lecture Notes in Engineering and Computer Science. 2. 1210–1214 // URL: https:///www.researchgate.net/publication/286697952_Neural_Nworkets_for_Intrusion_Detection_and_Its_Applications (Дата обращения: 04.09.2020).

7. **Vishnu Balan E., Priyan M.K., Gokulnath C., Usha Devi G.** Fuzzy based intrusion detection systems in MANET // Procedia Computer Science. Vol. 50. Pp. 109–114 // URL: https:///doi.org/10.1016/j.procs.2015.04.071. (Дата обращения: 04.09.2020).

8. Network protocols of the OSI model // Full articles about networks and computer security. URL: http://blogsisadmina.ru/seti/setevye-protokoly-modeli-osi.html (Дата обращения: 04.09.2020).

9. The archive Data Set // The archive to test machine learning algorithms // URL: http://archive.ics.uci.edu/ml/machine-learning-databases/ (Дата обращения: 05.09.2020).

10. **Olivas E., Martín-Guerrero J., Camps-Valls G., Serrano-López A., Calpe J., Gómez-Chova L.** A low-complexity fuzzy activation function for artificial neural networks // IEEE Transactions on Neural Networks. No. 14. Pp. 1576–1579. DOI: 10.1109/TNN.2003.820444 // URL: https://www.researchgate.net/publication/220279588_A_low-complexity_fuzzy_activation_function_for_artificial_neural_networks (Дата обращения: 06.09.2020).

11. **García-Teodoro P., Díaz-Verdejo J., Maciá-Fernández G., Vázquez E.** Anomaly-based network intrusion detection: Techniques, systems and challenges // Computers & Security. 2009. No. 28. Iss. 1–2. Pp. 18–28 // URL: http://www.sciencedirect.com/science/article/pii/S0167404808000692 (Дата обращения: 29.08.2020).

12. **Zhang J., Zulkernine M.** Anomaly based network intrusion detection with unsupervised outlier detection // 2006 IEEE Internat. Conf. on Communications. Istanbul, 2006. Pp. 2388–2393. DOI: 10.1109/ICC.2006.255127

13. **Samrin R., Vasumathi D.** Review on anomaly based network intrusion detection system // 2017 Internat. Conf. on Electrical, Electronics, Communication, Computer, and Optimization Techniques. Mysuru, 2017. Pp. 141–147. DOI: 10.1109/ICEECCOT.2017.8284655

14. **Schindler T.** Anomaly Detection in Log Data using Graph Databases and Machine Learning to Defend Advanced Persistent Threats. Informatik e.V. (Hrsg.): Informatik 2017 // URL: https://arxiv.org/pdf/1802.00259.pdf (Дата обращения: 01.09.2020).

15. **Bahlali Ahmed Ramzi.** Anomaly-based network intrusion detection system: A machine learning approach. 2019. DOI: 10.13140/RG.2.2.29553.84325. (Дата обращения: 03.09.2020)

Статья поступила в редакцию 14.07.2020.

THE AUTHOR / СВЕДЕНИЯ ОБ АВТОРЕ

Chumakov Vladislav E.
Чумаков Владислав Евгеньевич
E-mail: chumakov.dssa@mail.ru

DOI: 10.18721/JCSTCS.13304
УДК 681.518

APPLICATION OF CLASSIFIER SEQUENCES IN THE TASK OF STATE ANALYSIS OF INTERNET OF THINGS DEVICES

M.E. Sukhoparov[1], *I.S. Lebedev*[1], *A.V. Garanin*[2]

[1] St. Petersburg Institute for Informatics and Automation of RAS,
St. Petersburg, Russian Federation;

[2] New technologies LLC,
St. Petersburg, Russian Federation

Development of the industrial Internet concept dictates the need for identification and improvement of approaches, models, and methods for analyzing the state of the Internet of Things. Implementation of modern industrial, social, and household systems is impossible without the use of artificial intelligence methods in the machine-to-machine communication of individual elements, automatic data collection, analysis, and storage. The paper presents an approach to identifying the state of devices based on the application of classification technology, which implements compositions of independently trained algorithms processing time series, reflecting the functioning of elements during the implementation of processes. The application of the proposed solution allows parallel processing of information received from the device, which enables scaling. The developed approach was tested on time series sequences, obtained experimentally in different operating conditions, and processed by a sequence of classifiers. The paper presents the results of the probability estimate of erroneously classified states. The main advantages of the proposed solution are relatively small requirements to computational resources, simplicity of implementation, and the ability to scale by adding new classification algorithms.

Keywords: state analysis, Internet of Things, discriminant analysis, state monitoring, classification algorithm, Bayesian classifier, decision trees.

Citation: Sukhoparov M.E., Lebedev I.S., Garanin A.V. Application of classifier sequences in the task of state analysis of Internet of Things devices. Computing, Telecommunications and Control, 2020, Vol. 13, No. 3, Pp. 44–54. DOI: 10.18721/JCSTCS.13304

ПРИМЕНЕНИЕ ПОСЛЕДОВАТЕЛЬНОСТЕЙ КЛАССИФИКАТОРОВ В ЗАДАЧЕ АНАЛИЗА СОСТОЯНИЯ УСТРОЙСТВ ИНТЕРНЕТА ВЕЩЕЙ

М.Е. Сухопаров[1], *И.С. Лебедев*[1], *А.В. Гаранин*[2]

[1] Санкт-Петербургский институт информатики и автоматизации РАН,
Санкт-Петербург, Российская Федерация;

[2] ООО "Новые технологии",
Санкт-Петербург, Российская Федерация

Развитие концепции промышленного Интернета обусловливает необходимость поиска и совершенствования подходов, моделей и методов анализа состояния элементов Интернета Вещей. Реализация современных индустриальных, промышленных, социальных и бытовых систем невозможна без применения методов искусственного интеллекта межмашинного обмена отдельных элементов, автоматического сбора, анализа, хранения данных. В статье представлен подход к идентификации состояния устройств, основанный на использовании технологии классификации, реализующей композиции независимо обученных алгоритмов, обрабатывающих временные ряды, отражающих функционирование элементов во время выполнения процессов. Применение предлагаемого решения позволяет осуществлять параллельную обработку поступающей от устройства информации, что дает возможность масштабирования. Разработанный подход протестирован на последовательностях временных рядов, полученных экспериментальным путем в различных условиях функционирования, обработанных последовательностью классификаторов. Приведены результаты оценки вероятности ошибочно классифицированных состояний. Основными достоинствами предложенного решения являются относительно небольшие требования к вычислительным ресурсам, простота реализации, возможности по масштабированию путем добавления новых классифицирующих алгоритмов.

Ключевые слова: анализ состояния, Интернет Вещей, дискриминантный анализ, мониторинг состояния, алгоритм классификации, байесовский классификатор, деревья решений.

Ссылка при цитировании: Сухопаров М.Е., Лебедев И.С., Гаранин А.В. Применение последовательностей классификаторов в задаче анализа состояния устройств Интернета Вещей // Computing, Telecommunications and Control. 2020. Vol. 13. No. 3. Pp. 44–54. DOI: 10.18721/JCSTCS.13304

Introduction

Rapid development of the Internet of Things (IoT) concept based on wireless technologies, cloud computing, and distributed systems is a fundamental trend for information and cyber-physical systems. Implementation of modern industrial, social, and household systems is impossible without the use of artificial intelligence methods in the machine-to-machine communication of individual elements, automatic data collection, analysis, and storage. The common usage of various sensing elements and networks is focused on the solution of a large number of industrial and household tasks as well as social needs with minimum human participation. It brings undeniable advantages, on one hand, and determines the necessity to solve problems of state analysis and reveal functioning anomalies connected with failures, malfunctions, and incorrect process execution, on the other hand.

Interaction of IoT components with each other through the external environment predetermines the need to create various condition monitoring systems, which provide secure machine-to-machine communication, network access, data transfer, routing, intelligent data processing, etc. At the same time, it is necessary to take into account the dynamic development of information systems, assuming simultaneous use of both “old” and “new” devices of various developers, a large number of exchange protocols, and data processing in conditions of constant addition of new segments.

Production processes of typification and unification of separate computing elements, lack of proper physical security of the IoT elements that results from being outside the controlled zone of devices, the possibility of situations related to firmware upgrades, software updates, information collection, and access to standard devices allow the use of reverse engineering methods to improve condition monitoring in various operating modes.

Thus, the task of the condition monitoring system development for IoT devices appears where one of the directions presents the development of algorithms, models, methods of processing and analysis of the side channels data containing information about the ongoing process, as is proven in papers [5–8].

Execution of instructions and predefined sequences of actions is put in correspondence with the permissible values of functioning parameters that are registered through various channels. Detectable values form time series on the basis of which, with the use of methods of machine learning and statistical analysis, templates are determined, and normal and abnormal states are calculated.

Available approaches

During the operation of IoT devices, collisions may arise both at the level of the information system and a stand-alone device. For example, the introduction of software and hardware firmware upgrades, containing errors in the manufacture of household devices, such as routers, printers, and webcams, was associated with a number of situations that resulted in the loading of channels. Such loading limited the processes of receiving and transmitting information, as demonstrated in works [10–12].

To prevent such incidents, improvement and adaptation of models and methods of condition monitoring aimed at evaluating functionality and performance take place. These are based on the principles of statistical analysis, cause-effect analysis, transitions, and formation of precedent and event models, as described in papers [5–9].

Models based on statistics accumulate information about the functioning parameters in different modes and states, and later, with the purpose of the abnormal situation detection with the help of methods of neural networks, Markov models, machine learning, and others, tuples of features are processed, according to monograph [13] and paper [14].

For the detection of internal failures and malfunctions of functioning devices, monitoring programs are used that monitor execution of code segments and destabilizing situations such as buffer overflow, as demonstrated in works [8, 12–16].

Another direction is the processing of side channels, where the state is analyzed using time series of parameters reflecting changes in CPU utilization, internal memory usage, and intensity of message exchange, according to monograph [17] and papers [18–20].

The variety of IoT elements, a large number of objects, interaction protocols, data processing technologies, heterogeneity of formats, constantly changing architecture, and configuration changes may lead to various failures and malfunctions affecting the functioning parameters. Analysis of values of side channels (for example, electromagnetic and acoustic radiations, voltage, and power consumption) during the execution of various operations and instructions by the device makes it possible to implement external, relatively independent, not consuming computing resources of the IoT devices for the condition monitoring system [21–23].

Research objective

The development of IoT devices, software, and hardware is carried out using standard microchips and standard libraries of different manufacturers and developers. Methods of rapid development of software and hardware parts, which make it possible to use ready-made components of different manufacturers, lead to the devices starting to represent a “black box”.

IoT devices do not have vast computational resources and have a limited set of executable instructions, which permits consideration and identification of a relatively small number of states and their transitions.

During operation, the processes of IoT devices run in the dynamics, while many parameters are changed simultaneously.

The state of the external environment $u(t)$, caused by the receipt of control instructions to the device, reception and transmission of messages, and the element functioning, determined by the internal situations of data processing and implementation of computational algorithms, characterized by the transient characteristics $h(t)$, makes it possible to consider the device as a dynamic system. There are q inputs and d outputs, according to manual [11]; a control instruction and the values of the environment variables are supplied to the input. Then signals $S(t)$ (for example, indicating the resource load) appear at the output.

These signals are recorded by different sensors. The values of signals received through external channels contain the values of the noise component $\nu(t)$, determined by the properties of the measuring device, characteristics of the received signal, etc.

The state model of the IoT device is determined by the ratio presented in paper [12]:

$$\sum_{i=1}^{q}\sum_{j=1}^{d}\int_0^t u_i(t)h_{ij}(t-\tau)d\tau = \sum_{j=1}^{d}\int_0^t f(s_j(t-\tau),\nu_j(t-\tau))d\tau, \tag{1}$$

where q is the number of source channels; h are transient responses of the i-th channel for the j-th channel, registering sensor values received through the channel; f is the function of measured values.

At discrete instants of time of device operation $t_0, t_1, ..., t_n$, registration of vectors of numerical sequences takes place. Values $X(t)$ reflect data received from the sensors, containing a mixture of wanted signal $S(t)$ and the noise expressed by the parameter $\nu(t)$:

$$X(t) = \mathrm{F}\left[S(t), v(t)\right], \tag{2}$$

where vector X represents the result of mixed, mutually independent signals $S(t)$ with distortion of the noise component $\nu(t)$. Vector X represents a time series of values received from recording devices.

Vectors $X_1, X_2, ..., X_n$ reflect the process behavior in multidimensional coordinate space and define a set of states Z. The states are separated by a set of classes C, where the subsets are divided into dangerous C_1 and safe C_2 states.

Thus, there is a labeled finite training set:

$$X = \left\{(x_{11},\ ...,\ x_{n1}),\ (x_{12},\ ...,\ x_{n2}),\ ...,\ (x_{1m},\ ...,\ x_{nm})\right\}. \tag{3}$$

It is necessary to build a classification algorithm a of an input vector X_i for the representation $Z \rightarrow C$.

Proposed approach

The labeled training set contains values of time series from recording devices in predefined states and modes of operation. The known states $\{z_1, ..., z_l\} \in Z$ are defined only for the objects of the observed sequences $\{(x_{11}, ..., x_{n1}),(x_{12}, ..., x_{n2}), ..., (x_{1m}, ..., x_{nm})\}$.

From the investigated IoT device, a random vector function $X(t) = f(S(t), v(t))$ is observed in the interval $t_0 \leq t \leq T$, where time series $x_i = X(t_i)$ is registered at discrete instants of time $t_0, t_1, ..., t_k$.

A set of state classes $C = \{c_0, c_1, ..., c_n\}$ has been determined, in one of which at the discrete instant of time t_j the system can be located.

There are k classifiers a_i, $I = 1, ..., k$ trained independently of each other; X – a variety of feature sets; $a_i(x_i) \rightarrow c_j \in C$ – response of the i-th classifier; $\{P_i(c_j \mid x_i)\}_{j=0}^{n}$ – a posteriori probability for the i-th classifier after training; $w_i = \dfrac{1}{k}$ – weighting factors; $a(x) = \arg\max\limits_{j=0,\dots,n}\sum\limits_{i=0}^{k} w_i P_i(c_j \mid x_i)$ – the general classifier.

Such models can be trained independently of each other, which makes it possible to parallelize processes. The proposed approach to state identification distinguishes itself by the use of the classification technology, which implements compositions of independently trained algorithms. These algorithms process time series and reflect the functioning of the device during the process execution. It makes it possible to determine the device state without increasing the volume of the stored information.

Experiment

The analysis of the above approach was carried out based on the experiment, during which the state determined by the data processing algorithm of the computational node was identified. Time series reflecting computational resource load recorded by the monitoring program were used as input data. The schematic course of the experiment is presented in Fig. 1.

Various algorithms were run on the computing device. Only background processes were functioning in the state Z_1. In the second case, node C acted as a transit node, transmitting the incoming information without processing (state Z_2). In the third situation (state Z_3), besides the processes of receiving and transmitting, processes of searching for predetermined information were additionally carried out (Fig. 2–5).

In the course of the experiment, the classification algorithms a_j of the input vector X_i for the representation $Z \to C$ were considered. Operating classifiers $\{a_1, a_2, ..., a_k\} \in k = 4$ (Naive Bayes classifier, decision trees, discriminant mining, and k-nearest neighbor algorithm), trained independently of each other, produced sequences of results $Z = \{(z_{a_1}^{c_0}, z_{a_1}^{c_1}, ..., z_{a_1}^{c_n}), (z_{a_2}^{c_0}, z_{a_2}^{c_1}, ..., z_{a_2}^{c_n}), ..., (z_{a_j}^{c_0}, z_{a_j}^{c_1}, ..., z_{a_j}^{c_n}), ..., (z_{a_k}^{c_0}, z_{a_k}^{c_1}, ..., z_{a_k}^{c_n})\}$.

The resulting class c_i of the state z_i predicted by each model is determined by averaging the values of the calculated probabilities:

$$a_{c_i} = \frac{1}{K} \sum_{k=1}^{K} w_k a_k(x_i).$$

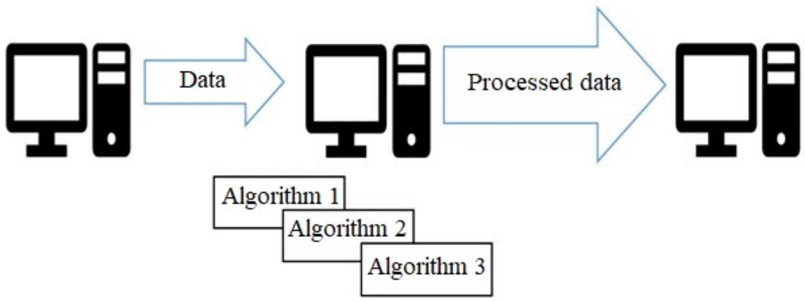

Fig. 1. Schematic course of the experiment

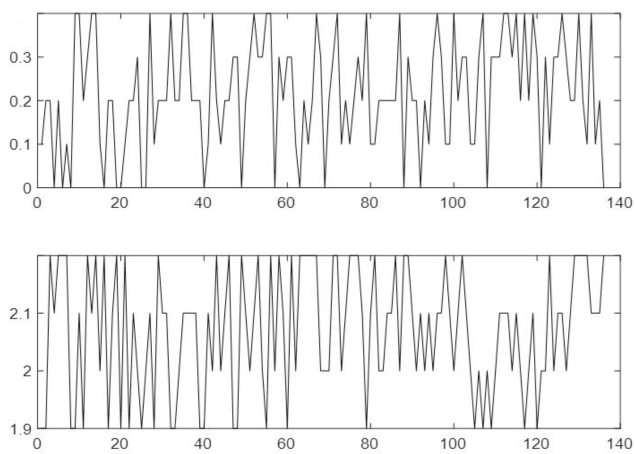

Fig. 2. Example of a sample of resource loading, expressed in percent (from top to bottom – network and processor, respectively), from time samples (time reports from 0 to 140) for the state Z_1

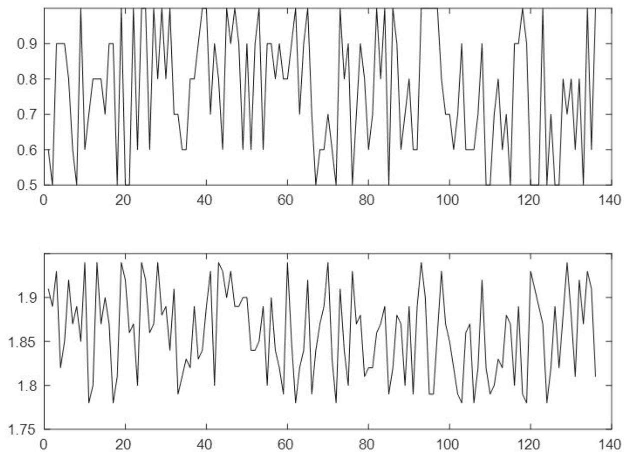

Fig. 3. Example of a sample of resource loading, expressed in percent (from top to bottom – network and processor, respectively), from time samples (time reports from 0 to 140) for the state Z_2

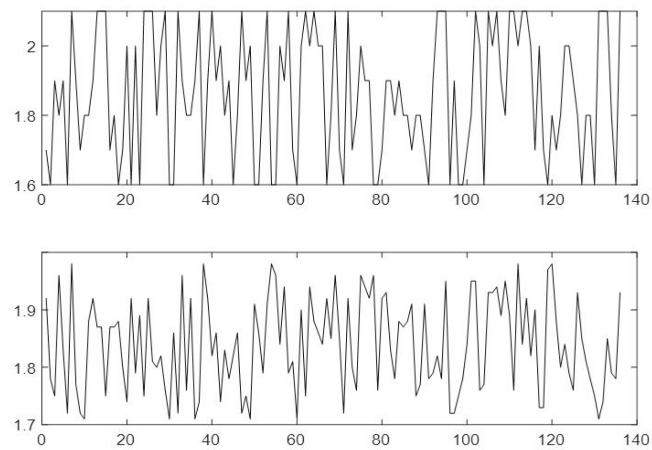

Fig. 4. Example of a sample of resource loading, expressed in percent (from top to bottom – network and processor, respectively), from time samples (time reports from 0 to 140) for the state Z_3

Table 1 presents the probabilities of erroneous classification obtained as the result of applying several "weak" classifiers trained in advance on the labeled sample of classifiers a_{c_i}: the Naive Bayes classifier, decision trees, discriminant mining, and k-nearest neighbor algorithm.

Table 1

Probability of erroneously classified sample values

Classifiers	Cluster 1	Cluster 2	Cluster 3	Total for sample
Naive Bayes classifier	0.18	0.02	0.02	0.07
Discriminant mining	0.16	0.02	0.02	0.07
Decision tree	0.08	0.04	0.04	0.05
k-nearest neighbor algorithm	0.2	0.08	0.06	0.11

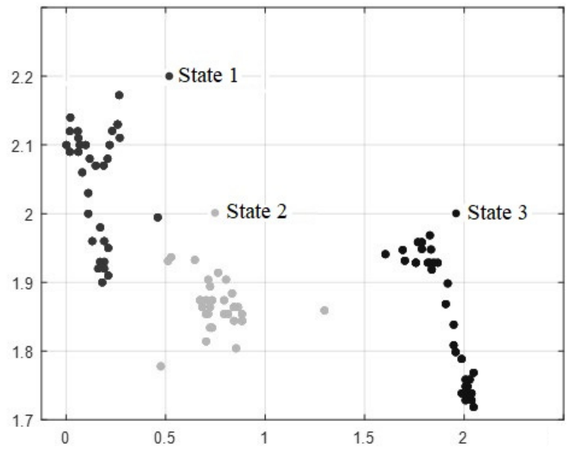

Fig. 5. Results of states on two-dimensional coordinate axes

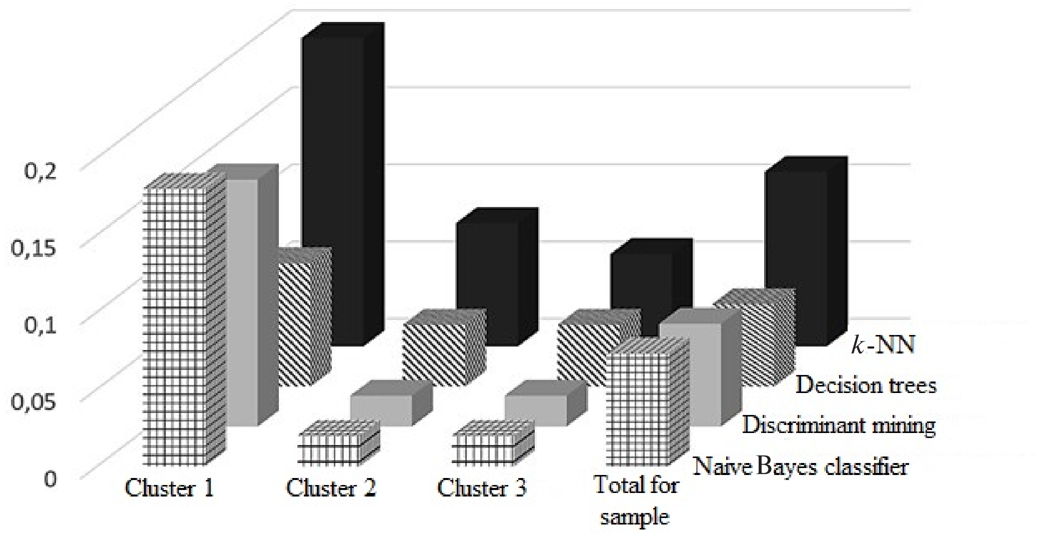

Fig. 6. Probabilities of erroneous classification

Fig. 6 presents a visualization of the probability estimate of erroneous classification.

The overall accuracy of the approach on the obtained experimental data for the case of full classification amounted to 0.93. At the same time, it should be noted that the data were not pre-processed or cleaned from noise, and the sampling rate of the obtained values was relatively low.

Thus, the proposed approach allows us to determine the class of the current state. The presented solution can be used as a theoretical basis for the integration of machine learning methods in the state analysis of the information security of IoT devices.

Conclusions

Analysis of a large number of different dynamically changing indicators in order to determine the states of IoT devices represents a time-consuming process that requires automation.

The heterogeneous characteristics of sequences received from recording devices in different modes of operation are unbalanced, and they have “emissions” that cannot always be separately identified by different classifiers in a correct manner. Application of a sequence of different classifiers has an impact on the results of the method and makes it possible to avoid detailed analysis of possible hidden patterns, deregulation, and correlation of sequences.

The proposed approach is focused on using several classifiers, which produce a response independently from each other and average the error by “collective voting”.

The use of classifiers in a parallel mode of processing of incoming sequences allows to reduce the processing time when determining the current state class.

The main limitation of the proposed approach is the necessity to select synchronized time series from recording devices, and in case of averaging – the lengths of the considered intervals.

The main advantages of the proposed approach are relatively small requirements to computational resources, simplicity of its implementation, and the possibility of scaling by adding new classifiers.

REFERENCES

1. **Farwell J.P., Rohozinski R.** Stuxnet and the Future of Cyber War. *Survival*, 2011, Vol. 53, No. 9, Pp. 23–40. DOI: 10.1080/00396338.2011.555586

2. **Yeung D.Y., Ding Y.** Host-based intrusion detection using dynamic and static behavioral models. *Pattern Recognition*, 2003, Vol. 36, Pp. 229–243. DOI: 10.1016/S0031-3203(02)00026-2

3. **Igure V., Laughter S., Williams R.** Security issues in SCADA networks. *Computers & Security*, 2006, Vol. 25, No. 7, Pp. 498–506. DOI: 10.1016/j.cose.2006.03.001

4. **Semenov V.V., Lebedev I.S., Sukhoparov M.Ye.** Identifikatsiya sostoyaniya informatsionnoy bezopasnosti bespilotnykh transportnykh sredstv s ispolzovaniyem iskusstvennykh neyronnykh setey [State identification of information security of unmanned vehicles using artificial neural networks]. *Metody i tekhnicheskiye sredstva obespecheniya bezopasnosti informatsii: Materialy XXVIII nauchno-tekhnicheskoy konferentsii* [*Proc. of the 28th Scientific and Technical Conf. on Methods and Information Security Engineering*], 2019, No. 28, Pp. 46–47. (rus)

5. **Zikratov I.A., Zikratova T.V., Lebedev I.S.** Doveritelnaya model informatsionnoy bezopasnosti multiagentnykh robototekhnicheskikh sistem s detsentralizovannym upravleniyem [Trusted model of information security of multi-agent robotics systems with decentralized control]. *Nauchno-Tekhnicheskiy Vestnik Informatsionnykh Tekhnologiy, Mekhaniki i Optiki* [*Scientific and Technical Journal of Information Technologies. Mechanics and Optics*], 2014, No. 2 (90), Pp. 47–52. (rus)

6. **Gao D., Reiter M., Song D.** Beyond output voting: Detecting compromised replicas using HMM-based behavioral distance. *IEEE Transactions on Dependable and Secure Computing*. 2009, Vol. 6, No. 2, Pp. 96–110. DOI: 10.1109/TDSC.2008.39

7. **Devesh M., Kant A.K., Suchit Y.R., Tanuja P., Kumar S.N.** Fruition of CPS and IoT in context of Industry 4.0. *Intelligent Communication, Control and Devices. Advances in Intelligent Systems and Computing*, 2020, Vol. 989, Pp. 367–375.

8. **Bevir M.K., O'Sullivan V.T., Wyatt D.G.** Computation of electromagnetic flowmeter characteristics from magnetic field data. *Journal of Physics D Applied Physics*, 1981, Vol. 14, No. 3, Pp. 373–388. DOI: 10.1088/0022-3727/14/3/007

9. **Semenov V.V., Lebedev I.S., Sukhoparov M.E., Salakhutdinova K.I.** Application of an autonomous object behavior model to classify the cybersecurity state. *Internet of Things, Smart Spaces, and Next Generation Networks and Systems*, 2019, Pp. 104–112. DOI: 10.1007/978-3-030-30859-9_9

10. **Semenov V.V., Lebedev I.S., Sukhoparov M.Ye.** Podkhod k klassifikatsii sostoyaniya informatsionnoy bezopasnosti elementov kiberfizicheskikh sistem s ispolzovaniyem pobochnogo elektromagnitnogo izlucheniya [Approach to classification of the information security state of elements of cyber physical systems by applying side electromagnetic radiation]. *Nauchno-Tekhnicheskiy Vestnik Informatsionnykh Tekhnologiy, Mekhaniki i Optiki* [*Scientific and Technical Journal of Information Technologies, Mechanics and Optics*], 2018, No. 1, Pp. 98–105. (rus)

11. **Soshnikova L.A, Tamashevich V.N., Ushbe G., Shefer M.** *Mnogomernyj statisticheskij analiz v ekonomike* [*Multivariate statistical analysis in economics*]. Moscow: UNITI – Dana Publ., 1999, 598 p. (rus)

12. **Sukhoparov M.Ye., Semenov V.V., Salakhutdinova K.I., Lebedev I.S.** Vyyavleniye anomalnogo funktsionirovaniya ustroystv «Industrii 4.0» na osnove povedencheskikh patternov [Detection of abnormal functioning of Industry 4.0 devices based on behavioral patterns]. *Problemy Informatsionnoy Bezopasnosti. Kompyuternyye Sistemy* [*Information Security Problems. Computer Systems*], 2020, No. 1 (41), Pp. 96–102. (rus)

13. **Bendat D., Pirsol A.** *Primeneniye korrelyatsionnogo i spektralnogo analiza* [*Application of correlation and spectral analysis*]. Moscow: Mir Publ., 1983. 312 p. (rus)

14. **Zasov V.A., Tarabardin M.A., Nikonorov Ye.N.** Algoritmy i ustroystva dlya identifikatsii vkhodnykh signalov v zadachakh kontrolya i diagnostiki dinamicheskikh obyektov [Algorithms and devices for identification of input signals in tasks of control and diagnostics of dynamic objects]. *Vestnik Samarskogo Gosudarstvennogo Aerokosmicheskogo Universiteta* [*Journal of Samara University. Aerospace and Mechanical Engineering*], 2009, No. 2, Pp. 115–123. (rus)

15. **Lockhart D.J.** Expression monitoring by hybridization to high-density oligonucleotide arrays. *Natural Biotechnol*, 1996, Vol. 14, Pp. 1675–1680. DOI: 10.1038/nbt1296-1675

16. **Golub T.R.** Molecular classification of cancer: Class discovery and class prediction by gene expression monitoring. *Science*, 1999, Vol. 286, Pp. 531–537. DOI: 10.1126/science.286.5439.531

17. **Anderberg M.R.** *Cluster analysis for applications*. New York: Academic Press, 1976. 376 p.

18. **Dembele D., Kastner P.** Fuzzy C-means method for clustering microarray data. *Bioinformatics*, 2003, Vol. 19, No. 8, Pp. 973–980. DOI: 10.1093/bioinformatics/btg119

19. **Rousseeuw J.P.** Silhouettes: A graphical aid to the interpretation and validation of cluster analysis. *Journal of Computational and Applied Mathematics*, 1987, Vol. 20, Pp. 53–65. DOI: 10.1016/0377-0427(87)90125-7

20. **Whitfield M.L.** Identification of genes periodically expressed in the human cell cycle and their expression in tumors. *Molecular Biology of the Cell*, 2002, Vol, 13, No. 6, Pp. 1977–2000. DOI: 10.1091/MBC.02-02-0030

21. **Wyglinski A.M., Huang X., Padir T., Lai L., Eisenbarth T.R., Venkatasubramanian K.** Security of autonomous systems employing embedded computing and sensors. *IEEE Micro*, 2013, Vol. 33 (1), Art. No. 6504448, Pp. 80–86. DOI: 10.1109/MM.2013.18

22. **Nikolaevskiy I., Lukyanenko A., Polishchuk T., Polishchuk V.M., Gurtov A.V.** isBF: scalable in-packet bloom filter based multicast. *Computer Communications*, 2015, Vol. 70, Pp. 79–85. DOI: 10.1145/2480362.2480484

23. **Gupta H., Sural S., Atluri V., Vaidya J.** A side-channel attack on smartphones: deciphering key taps using built-in microphones. *Journal of Computer Security*, 2018, Vol. 26 (2), Pp. 255–281. DOI: 10.3233/JCS-17975

Received 28.08.2020.

СПИСОК ЛИТЕРАТУРЫ

1. **Farwell J.P., Rohozinski R.** Stuxnet and the Future of Cyber War // Survival. 2011. Vol. 53. No. 9. Pp. 23–40. DOI: 10.1080/00396338.2011.555586

2. **Yeung D.Y., Ding Y.** Host-based intrusion detection using dynamic and static behavioral models // Pattern Recognition. 2003. Vol. 36. Pp. 229–243. DOI: 10.1016/S0031-3203(02)00026-2

3. **Igure V., Laughter S., Williams R.** Security issues in SCADA networks // Computers & Security. 2006. Vol. 25. No. 7. Pp. 498–506. DOI: 10.1016/j.cose.2006.03.001

4. **Семенов В.В., Лебедев И.С., Сухопаров М.Е.** Идентификация состояния информационной безопасности беспилотных транспортных средств с использованием искусственных нейронных сетей // Методы и технические средства обеспечения безопасности информации: Матер. XXVIII науч.-техн. конф. 2019. № 28. С. 46–47

5. **Зикратов И.А., Зикратова Т.В., Лебедев И.С.** Доверительная модель информационной безопасности мультиагентных робототехнических систем с децентрализованным управлением // Научно-технический вестник информационных технологий, механики и оптики. 2014. № 2 (90). С. 47–52.

6. **Gao D., Reiter M., Song D.** Beyond output voting: Detecting compromised replicas using HMM-based behavioral distance // IEEE Transactions on Dependable and Secure Computing. 2009. Vol. 6. No. 2. Pp. 96–110. DOI: 10.1109/TDSC.2008.39

7. **Devesh M., Kant A.K., Suchit Y.R., Tanuja P., Kumar S.N.** Fruition of CPS and IoT in context of Industry 4.0. // Intelligent Communication, Control and Devices. Advances in Intelligent Systems and Computing. 2020. Vol. 989. Pp. 367–375.

8. **Bevir M.K., O'Sullivan V.T., Wyatt D.G.** Computation of electromagnetic flowmeter characteristics from magnetic field data // J. of Physics D Applied Physics. 1981. Vol. 14. No. 3. Pp. 373–388. DOI: 10.1088/0022-3727/14/3/007

9. **Semenov V.V., Lebedev I.S., Sukhoparov M.E., Salakhutdinova K.I.** Application of an autonomous object behavior model to classify the cybersecurity state // Internet of Things, Smart Spaces, and Next Generation Networks and Systems. 2019. Pp. 104–112. DOI: 10.1007/978-3-030-30859-9_9

10. **Семенов В.В., Лебедев И.С., Сухопаров М.Е.** Подход к классификации состояния информационной безопасности элементов киберфизических систем с использованием побочного электромагнитного излучения // Научно-технический вестник информационных технологий, механики и оптики. 2018. № 1. С. 98–105.

11. **Сошникова Л.А., Тамашевич В.Н., Усбе Г., Шефер М.** Многомерный статистический анализ в экономике. М.: ЮНИТИ – Дана, 1999. 598 с.

12. **Сухопаров М.Е., Семенов В.В., Салахутдинова К.И., Лебедев И.С.** Выявление аномального функционирования устройств «Индустрии 4.0» на основе поведенческих паттернов // Проблемы информационной безопасности. Компьютерные системы. 2020. № 1 (41). С. 96–102.

13. **Бендат Д., Пирсол А.** Применение корреляционного и спектрального анализа. М.: Мир, 1983. 312 с.

14. **Засов В.А., Тарабардин М.А., Никоноров Е.Н.** Алгоритмы и устройства для идентификации входных сигналов в задачах контроля и диагностики динамических объектов // Вестник Самарского государственного аэрокосмического университета. 2009. № 2. С. 115–123.

15. **Lockhart D.J.** Expression monitoring by hybridization to high-density oligonucleotide arrays // Natural Biotechnol. 1996. Vol. 14. Pp. 1675–1680. DOI: 10.1038/nbt1296-1675

16. **Golub T.R.** Molecular classification of cancer: Class discovery and class prediction by gene expression monitoring // Science. 1999. Vol. 286. Pp. 531–537. DOI: 10.1126/science.286.5439.531

17. **Anderberg M.R.** Cluster analysis for applications. New York: Academic Press, 1976. 376 p.

18. **Dembele D., Kastner P.** Fuzzy C-means method for clustering microarray data // Bioinformatics. 2003. Vol. 19. No. 8. Pp. 973–980. DOI: 10.1093/bioinformatics/btg119

19. **Rousseeuw J.P.** Silhouettes: A graphical aid to the interpretation and validation of cluster analysis // J. of Computational and Applied Mathematics. 1987. Vol. 20. Pp. 53–65. DOI: 10.1016/0377-0427(87)90125-7

20. **Whitfield M.L.** Identification of genes periodically expressed in the human cell cycle and their expression in tumors // Molecular Biology of the Cell. 2002. Vol. 13. No. 6. Pp. 1977–2000. DOI: 10.1091/MBC.02-02-0030

21. **Wyglinski A.M., Huang X., Padir T., Lai L., Eisenbarth T.R., Venkatasubramanian K.** Security of autonomous systems employing embedded computing and sensors // IEEE Micro. 2013. Vol. 33 (1). Art. No. 6504448. Pp. 80–86. DOI: 10.1109/MM.2013.18

22. **Nikolaevskiy I., Lukyanenko A., Polishchuk T., Polishchuk V.M., Gurtov A.V.** isBF: scalable in-packet bloom filter based multicast // Computer Communications. 2015. Vol. 70. Pp. 79–85. DOI: 10.1145/2480362.2480484

23. **Gupta H., Sural S., Atluri V., Vaidya J.** A side-channel attack on smartphones: deciphering key taps using built-in microphones // J. of Computer Security. 2018. Vol. 26 (2). Pp. 255–281. DOI: 10.3233/JCS-17975

Статья поступила в редакцию 28.08.2020.

THE AUTHORS / СВЕДЕНИЯ ОБ АВТОРАХ

Sukhoparov Mikhail E.
Сухопаров Михаил Евгеньевич
E-mail: sukhoparovm@gmail.com

Lebedev Ilya S.
Лебедев Илья Сергеевич
E-mail: isl_box@mail.ru

Garanin Anton V.
Гаранин Антон Владимирович
E-mail: anton.v.garanin@yandex.ru

DOI: 10.18721/JCSTCS.13305
УДК 621.3.049.77

MODELING THE IMPACT OF TECHNOLOGICAL PROCESS VARIATIONS ON R-2R DAC STATIC CHARACTERISTICS

E.A. Salonina[1], *Ya.V. Belyaev*[2], *I.M. Piatak*[1]

[1] Peter the Great St. Petersburg Polytechnic University, St. Petersburg, Russian Federation;

[2] Concern CSRI Elektropribor, JSC, St. Petersburg, Russian Federation

Digital-to-analog converter (DAC) is widely used in modern integrated electronics, converting digital signals into analog ones. This paper considers an R-2R structure DAC, its operation principle and static characteristics: integral non-linearity (INL) and differential non-linearity (DNL). For the accuracy of this DAC conversion, it is important that the element resistance ratio is maintained for the entire circuit. The authors considered the influence of random and systematic errors of DAC elements resistances on the transfer function and static characteristics of DAC, as well as the use of special DAC element placements to compensate for systematic errors. Systematic errors are presented as three types of gradients: linear, quadratic and central quadratic. These gradients were modeled in MATLAB. Using the MATLAB script, the authors calculated the static characteristics of the R-2R DAC for two resistor placements: regular and common centroid, taking into account the impact of three different gradients. These placements were compared based on the modeling and calculation results.

Keywords: digital-analog conversion, R-2R, linear gradient, quadratic gradient, resistor mismatch, MATLAB, common centroid.

Citation: Salonina E.A., Belyaev Ya.V., Piatak I.M. Modeling the impact of technological process variations on R-2R DAC static characteristics. Computing, Telecommunications and Control, 2020, Vol. 13, No. 3, Pp. 55–62. DOI: 10.18721/JCSTCS.13305

МОДЕЛИРОВАНИЕ ВОЗДЕЙСТВИЯ ТЕХНОЛОГИЧЕСКОГО РАЗБРОСА НОМИНАЛОВ ЭЛЕМЕНТОВ НА СТАТИЧЕСКИЕ ХАРАКТЕРИСТИКИ ЦАП ТИПА R-2R

Е.А. Салонина[1], *Я.В. Беляев*[2], *И.М. Пятак*[1]

[1] Санкт-Петербургский политехнический университет Петра Великого, Санкт-Петербург, Российская Федерация;

[2] ЦНИИ «ЭЛЕКТРОПРИБОР», Санкт-Петербург, Российская Федерация

ЦАП широко используются в современной интегральной электронике, осуществляя преобразование цифрового сигнала в аналоговый. В статье рассматривается ЦАП структуры R-2R, его принцип работы и статические характеристики: интегральная нелинейность (INL) и дифференциальная нелинейность (DNL). Для точности преобразования данного ЦАП важно, чтобы соотношение сопротивлений элементов сохранялось для всей схемы. Изучено влияние случайных и систематических погрешностей номиналов резисторов на выходную и статические характеристики ЦАП, а также использование специальных расстановок элементов ЦАП для компенсации систематических погрешностей. Систематические ошибки представлены в виде трех типов градиентов: линейного, квадратичного и центрального квадратичного. Выполнено моделирование данных градиентов в MATLAB. С помощью скрипта MATLAB сделан расчет статических характеристик ЦАП R-2R с учетом воздействия трех различных градиентов при двух расстановках резисторов: «обычная» и «с общим центром». По результатам моделирования и расчета выполнено сравнение данных расстановок.

Ключевые слова: цифро-аналоговый преобразователь, R-2R, линейный градиент, квадратичный градиент, MATLAB, расстановка с общим центром.

Ссылка при цитировании: Салонина Е.А., Беляев Я.В., Пятак И.М. Моделирование воздействия технологического разброса номиналов элементов на статические характеристики ЦАП типа R-2R // Computing, Telecommunications and Control. 2020. Vol. 13. No. 3. Pp. 55–62. DOI: 10.18721/JCSTCS.13305

Introduction

Digital-to-analog converters (DAC) are widely used in modern complex mixed-signal integrated circuits, performing a conversion of a digital signal into an analog one. There are various types of DACs, which convert input signals with different resolutions into the output analog voltage or current. All digital-to-analog converters can be divided into the two main groups: serial and parallel DACs [1].

A DAC based on resistive matrix R-2R belongs to the parallel DACs of the binary architecture, since the output signal is formed by summing the voltages from the switched weighting elements [2]. In general, the weighting elements are resistances and, according to the weighting method, they are formed as a resistive ladder [1]. The schematic of an ideal 8-bit R-2R DAC is shown in Fig. 1.

As a rule, DAC converts an input signal from the digital binary code to the output continuous voltage. The output analog signal formed as a sum of the voltages at the DAC inputs is multiplied by the appropriate weighting coefficients. In the ideal case, when manufacturing DACs, there is no weight element ratio error, so the resistor ratios from the R-2R ladder are precisely matched and the DAC weights can be $2^{(-(N-i+1))}$, where “N” is the DAC resolution, “i” is the bit number [3]. In reality, there are always random and systematic errors due to imperfectly matched resistors from the R-2R ladder [4]. To minimize DAC conversion error, it is necessary to maintain a certain ratio between R and 2R resistances [5–6].

Random errors are the component (e.g. weighting components – resistors) errors that occur during chip production. They can be calculated within the normal distribution with the manufacturer’s specified variation. Systematic errors are the errors caused by external factors affecting all weighting elements simultaneously and depending on the placement of each element on the chip [7].

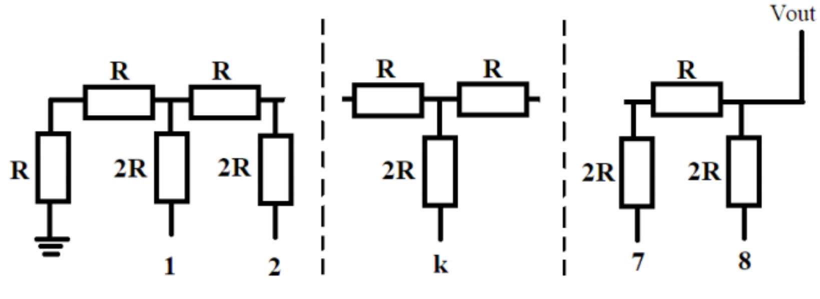

Fig. 1. Schematic of an ideal R-2R DAC based on a resistive ladder

The problem of systematic errors

In this paper, we will consider systematic errors affecting R-2R resistances. To reduce random errors, geometric dimensions of the weighting components can be increased [8–10]. Therefore, random errors become insignificant and the impact of systematic errors increases. Thus, the impact of a systematic error typically prevails over that of a random error.

Under certain assumptions, systematic errors can be represented with some accuracy in the form of a linear or quadratic gradient [11–13] describing the deviation of the weight elements (resistances) placed on a chip. In order to solve the problem of the negative impact of these gradients, which leads to increased DAC integral and differential non-linearities, designers widely use gradient-compensated placement for the weighting elements where gradient is compensated and the matched resistance ratio for all elements is preserved [14].

On the one hand, the optimal placement of DAC array elements in terms of minimizing the area occupied on the chip and the absence of parasitic capacitances implies simplification of the connection and reduction of parasitic capacitances [1]. However, this placement can be susceptible to various systematic errors which have a negative impact on DAC characteristics [15].

Simulation by MATLAB script

In order to find a compromise between gradient compensation and connection simplification, it is necessary to evaluate DAC characteristics (in particular, integral and differential non-linearity) for the given placement of the weighting elements (resistors). The MATLAB script used in this paper can simulate horizontal and vertical gradients on the weighting elements placed on the chip. The script allows to model three types of the gradient: linear, quadratic and central quadratic (Fig. 2).

The script also calculates the actual weighting coefficients and the DAC transfer characteristic taking into account the non-idealities of the resistance values. The R-2R array element placement is formed as a number matrix with the element numeration strictly ordered as shown in Fig. 3. The proposed script is

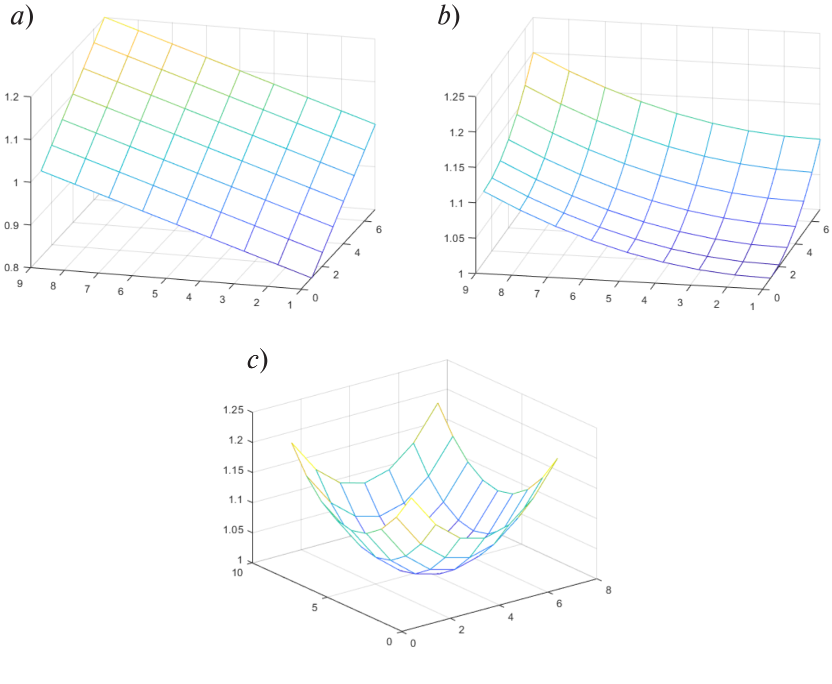

Fig. 2. The gradient map simulation: *a* – linear; *b* – quadratic; *c* – central quadratic

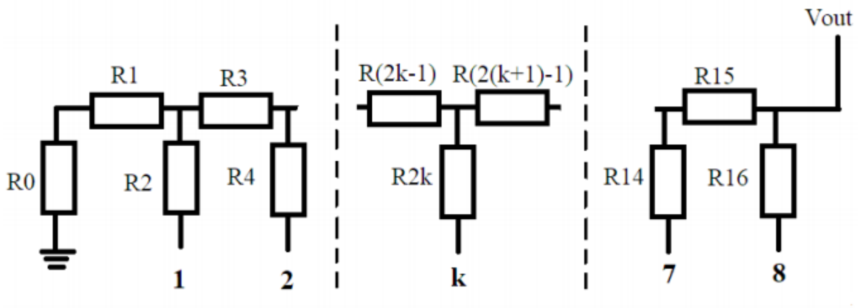

Fig. 3. R-2R weighting elements

suitable for any number of the weighting elements on a chip, as well as for any DAC resolution; the calculation of integral nonlinearity (INL) and differential nonlinearity (DNL) is also included in the MATLAB script.

Comparison of the various ways of placing R-2R array elements on a chip is studied and static DAC characteristics are evaluated (in particular, INL and DNL) for a given type of gradient and the placement of DAC weighting elements on the chip. The script produces the following graphs:

1. Transfer characteristic – relationship between the value of the output voltage V_{out} and the given DAC input code.
2. DNL – deviation of an output step from the ideal analog LSB value scaled to the value of conversion step (LSB).
3. INL – deviation of the actual transfer characteristic from the ideal transfer curve for each output level scaled to the value of conversion step (LSB) [16].

Comparison of two placements

In this paper, we consider two choices for the placement of the 8-bit DAC weighting elements: with a common center ("common-centroid") and without compensation for distortion ("regular"). The first one was designed to achieve full compensation of the linear gradient and the second one was chosen as the simplest in terms of connections and the area on the chip.

The "common centroid" placement is an example of a linear gradient compensation layout, but it occupies a large area on a chip and it is difficult to connect the elements with each other due to the significant distance between them and possible connection crossings [17]. The "regular" layout without gradient compensation was chosen as the smallest placement area with the simplest connection of elements. Script examples with these placements are shown in Fig. 4. Numbers from 0 to 16 in the matrix denote R-2R

a)

```
Rmatrix =
[16 4 6 8 10 12 16 ;
14 5 7 9 11 13 14 ;
15 4 6 8 10 12 -1 ;
-1 2 3 2 1 0 -1 ;
-1 -1 -1 -1 -1 -1 -1 ;
-1 0 1 2 3 2 -1 ;
-1 12 10 8 6 4 15 ;
14 13 11 9 7 5 14 ;
16 12 10 8 6 4 16 ;] ;
```

b)

```
Rmatrix =
[0 1 3 5 7 9 11 13 15 ;
-1 2 4 6 8 10 12 14 16 ;
-1 2 4 6 8 10 12 14 16 ; ] ;
```

Fig. 4. Code example of the weighting elements matrix:
a – "common centroid" placement; *b* – "regular" placement

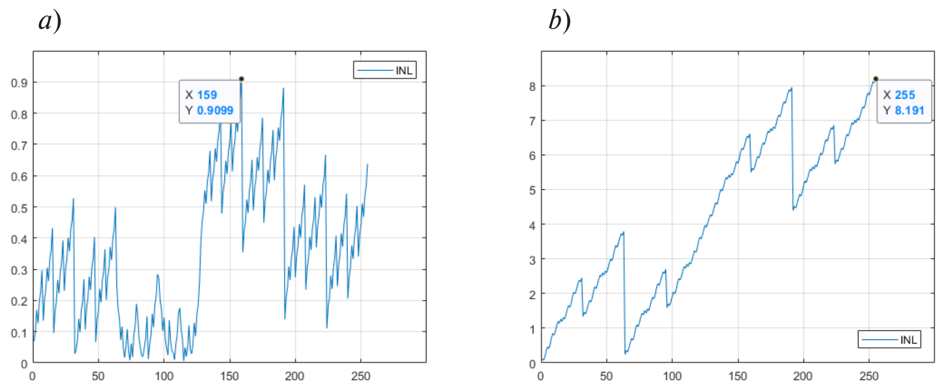

Fig. 5. INL plots for the central quadratic gradient simulation:
a – "common centroid" placement; *b* – "regular" placement

matrix elements according to the numeration in Fig. 3, which includes the resistance of the given weighting element. The number "–1" denotes an empty cell.

Three types of gradients were simulated separately: linear, quadratic and central quadratic. The maximum gradients value was limited to 20 %. Each gradient was set on both axes. Taking the gradients into account, DAC output characteristics were calculated for two placements ("common centroid" and "regular"), as well as DNL and INL, scaled to the value of the minimum step of the transfer characteristic, which is LSB (least significant bit). The results of the modeling are given in Table 1.

Table 1

Simulation results

Gradient type	Maximum value of DNL, LSB		Maximum value of INL, LSB	
	"regular" layout	"common centroid" layout	"regular" layout	"common centroid" layout
Linear	–6.894	$\sim 10^{-14}$	13.590	$\sim 10^{-14}$
Quadratic	–3.027	–0.901	6.234	2.174
Central quadratic	0.742	–3.553	0.910	8.191

For the linear gradient, the best placement was of the "common centroid" type. According to the modeling result, it allows INL of the order of 10^{-14} LSB, which is comparable to the accuracy of MATLAB calculations.

For the quadratic gradient, the "common centroid" placement is less suitable than for a linear gradient, as INL in this case reaches 2.174 LSB. This value is higher than acceptable (INL can be considered acceptable if not higher than ±1 LSB, acceptable DNL does not exceed ±0.5 LSB). However, compared to the "regular" placement, the "common centroid" placement result was better.

For the central quadratic gradient, the best placement was the "regular" one. It gives the maximum DNL = 0.742 LSB and INL = 0.910 LSB, while in the "common centroid" arrangement these values are –3.553 LSB and 8.191 LSB, respectively. INL plots for this gradient are shown in Fig. 5.

Conclusion

This paper considered the non-linearities in the R-2R DAC static characteristics caused by systematic errors of the weighting elements (resistances). A MATLAB script was developed to simulate these errors in the form of matrix gradients and to calculate the static DAC characteristics taking into account these gradients for different weighting elements placement. INL and DNL were estimated for three types of gradients (linear, quadratic, central quadratic) and for two types of placements ("regular" and "common centroid"). The result shows that the "common centroid" placement is better for both linear and quadratic gradients. On the other hand, the "regular" placement is better for the central quadratic gradient. In addition, the MATLAB script written in the process of the research can be further used to model gradient impact on various R-2R DAC weighting element placements and DAC static characteristics.

REFERENCES

1. **Kuznetsov K.P.** Issledovaniye metodik razmeshcheniya vzveshivayushchikh elementov TsAP s binarnoy strukturoy. Available: *https://elib.spbstu.ru/dl/3/2020/vr/vr20-4137.pdf*. (Accessed: October 2020). (rus)

2. **Rabal A., Otin A., Urriza I., Gines A.J., Leger G., Rueda A.** A compact R-2R DAC for BIST applications. *Proceedings of the 2016 IEEE 21st International Mixed-Signal Testing Workshop*, 2016. DOI: 10.1109/IMS3TW.2016.7524224

3. **Hirai M., Yamamoto S., Arai H., Kuwana A., Tanimoto H., Gendai Y., Kobayashi H.** Systematic construction of resistor ladder network for N-ary DACs. *Proceedings of the 2019 IEEE 13th International Conference on ASIC (ASICON)*, 2019, Pp. 1–4. DOI: 10.1109/ASICON47005.2019.8983583

4. **Chen C., Lu N.** Nonlinearity analysis of R-2R ladder-based current-steering digital to analog converter. *Proceedings of the 2013 IEEE International Symposium on Circuits and Systems*, 2013, Pp. 833–836. DOI: 10.1109/ISCAS.2013.6571976

5. **Xu W., Zhang R., Shi C.** Research of segmented 8bit voltage-mode R-2R Ladder DAC. *Proceedings of the 2015 IEEE 11th International Conference on ASIC*, 2016. DOI: 10.1109/ASICON.2015.7517105

6. **Lin Y., Geiger R.** Resistors layout for enhancing yield of R-2R DACs. *Proceedings of the 2002 IEEE International Symposium on Circuits and Systems*, 2002, Pp. 97–100. DOI: 10.1109/ISCAS.2002.1010649

7. **Yu T., Fang S., Chen C., Sun Y., Chen P.** Device array layout synthesis with nonlinear gradient compensation for a high-accuracy current-steering DAC. *IEEE Transactions on Computer-Aided Design of Integrated Circuits and Systems*, 2018, Vol. 37, No. 4, Pp. 717–728. DOI: 10.1109/TCAD.2017.2729402

8. **Khorami A., Sharifkhani M.** Elimination of the effect of bottom-plate capacitors in C-2C DAC using a layout technique. *Microelectronics Journal*, 2015, Vol. 46, No. 12, Pp. 1275–1282.

9. **Zhang W., Qu R., Zhu M.** Non-ideality analysis of current steering DAC. *Proceedings of the 2020 IEEE International Conference on Artificial Intelligence and Information Systems*, 2020, Pp. 278–282. DOI: 10.1109/ICAIIS49377.2020.9194898

10. **van der Wagt J.P.A., Chu G.G., Conrad C.L.** A layout structure for matching many integrated resistors. *IEEE Transactions on Circuits and Systems I: Regular Papers*, 2004, Vol. 51, No. 1, Pp. 186–190. DOI: 10.1109/TCSI.2003.821303

11. **Yao D., Sun Y., Higashino M., Mohyar S.N., Yanagida T., Arafune T., Tsukiji N., Kobayashi H.** DAC linearity improvement with layout technique using magic and latin squares. *Proceedings of the 2017 International Symposium on Intelligent Signal Processing and Communication Systems*, 2017, Pp. 616–621. DOI: 10.1109/ISPACS.2017.8266552

12. **Srivastava R.K., Vellathu A., Kaipu S.V.R., Jattana H.S., Rampal A.** A systematic method to find an optimized quad-quadrant random walk sequence for reducing the mismatch effect in current steering DAC. *Proceedings of the 2017 International Conference on Microelectronic Devices, Circuits and Systems*, 2017, Pp. 1–6. DOI: 10.1109/TCAD.2017.2729402

13. **Yenuchenko M.S., Korotkov A.S., Morozov D.V., Pilipko M.M.** A switching sequence for unary digital-to-analog converters based on a knight's tour. *IEEE Transactions on Circuits and Systems I: Regular Papers*, 2019, Vol. 66, No. 6, Pp. 2230–2239. DOI: 10.1109/TCSI.2018.2890412

14. **Konstantinov A.I., Yenuchenko M.S., Korotkov A.S.** Efficiency analysis of techniques for weighting elements arrangement on the chip of unary digital-to-analog converter. *Radioelectronics and Communications Systems*, 2017, Vol. 60, No 5, Pp. 225–232. (rus) DOI: 10.20535/S0021347017050041

15. **Tong X., Wang C., Wang F.** Linearity optimization of current steering DAC based on improved layout topology. *Proceedings of the 2019 IEEE International Conference on Electron Devices and Solid-State Circuits*, 2019, Pp. 1–3. DOI: 10.1109/EDSSC.2019.8754219

16. **Parmar S.S., Gharge A.P.** R-2R ladder circuit design for 32-bit digital-to-analog converter (DAC) with noise analysis and performance parameters. *Proceedings of the 2016 International Conference on Communication and Signal Processing*, 2016, Pp. 467–468. DOI: 10.1109/ICCSP.2016.7754180

17. **Lin M.P., Chang Y., Hung C.** Recent research development and new challenges in analog layout synthesis. *Proceedings of the 2016 21st Asia and South Pacific Design Automation Conference (ASP-DAC)*, 2016, Pp. 617–622. DOI: 10.1109/ASPDAC.2016.7428080

Received 05.07.2020.

СПИСОК ЛИТЕРАТУРЫ

1. **Кузнецов К.П.** Исследование методик размещения взвешивающих элементов ЦАП с бинарной структурой // URL: https://elib.spbstu.ru/dl/3/2020/vr/vr20-4137.pdf. (Дата обращения: октябрь 2020). (rus)

2. **Rabal A., Otin A., Urriza I., Gines A.J., Leger G., Rueda A.** A compact R-2R DAC for BIST applications // Proc. of the 2016 IEEE 21st Internat. Mixed-Signal Testing Workshop (IMSTW 2016). 2016. DOI: 10.1109/IMS3TW.2016.7524224

3. **Hirai M., Yamamoto S., Arai H., Kuwana A., Tanimoto H., Gendai Y., Kobayashi H.** Systematic construction of resistor ladder network for N-ary DACs // Proc. of the 2019 IEEE 13th Internat. Conf. on ASIC. 2019. Pp. 1–4. DOI: 10.1109/ASICON47005.2019.8983583

4. **Chen C., Lu N.** Nonlinearity analysis of R-2R ladder-based current-steering digital to analog converter // Proc. of the 2013 IEEE Internat. Symp. on Circuits and Systems. 2013. Pp. 833–836. DOI: 10.1109/ISCAS.2013.6571976

5. **Xu W., Zhang R., Shi C.** Research of segmented 8bit voltage-mode R-2R ladder DAC // Proc. of the 2015 IEEE 11th Internat. Conf. on ASIC. 2016. DOI: 10.1109/ASICON.2015.7517105

6. **Lin Y., Geiger R.** Resistors layout for enhancing yield of R-2R DACs // Proc. of the 2002 IEEE Internat. Symp. on Circuits and Systems. 2002. Pp. 97–100. DOI: 10.1109/ISCAS.2002.1010649

7. **Yu T., Fang S., Chen C., Sun Y., Chen P.** Device array layout synthesis with nonlinear gradient compensation for a high-accuracy current-steering DAC // IEEE Transactions on Computer-Aided Design of Integrated Circuits and Systems. 2018. Vol. 37. No. 4. Pp. 717–728. DOI: 10.1109/TCAD.2017.2729402

8. **Khorami A., Sharifkhani M.** Elimination of the effect of bottom-plate capacitors in C-2C DAC using a layout technique // Microelectronics J. 2015. Vol. 46. No. 12. Pp. 1275–1282.

9. **Zhang W., Qu R., Zhu M.** Non-ideality analysis of current steering DAC // Proc. of the 2020 IEEE Internat. Conf. on Artificial Intelligence and Information Systems. 2020. Pp. 278–282. DOI: 10.1109/ICAIIS49377.2020.9194898

10. **van der Wagt J.P.A., Chu G.G., Conrad C.L.** A layout structure for matching many integrated resistors // IEEE Transactions on Circuits and Systems I: Regular Papers. 2004. Vol. 51. No. 1. Pp. 186–190. DOI: 10.1109/TCSI.2003.821303

11. **Yao D., Sun Y., Higashino M., Mohyar S.N., Yanagida T., Arafune T., Tsukiji N., Kobayashi H.** DAC linearity improvement with layout technique using magic and latin squares // Proc. of the 2017 Internat. Symp. on Intelligent Signal Processing and Communication Systems. 2017. Pp. 616–621. DOI: 10.1109/ISPACS.2017.8266552

12. **Srivastava R.K., Vellathu A., Kaipu S.V.R., Jattana H.S., Rampal A.** A systematic method to find an optimized quad-quadrant random walk sequence for reducing the mismatch effect in current steering DAC // Proc. of the 2017 Internat. Conf. on Microelectronic Devices, Circuits and Systems. 2017. Pp. 1–6. DOI: 10.1109/TCAD.2017.2729402

13. **Yenuchenko M.S., Korotkov A.S., Morozov D.V., Pilipko M.M.** A switching sequence for unary digital-to-analog converters based on a knight's tour // IEEE Transactions on Circuits and Systems I: Regular Papers. 2019. Vol. 66. No. 6. Pp. 2230–2239. DOI: 10.1109/TCSI.2018.2890412

14. **Константинов А.И., Енученко М.С., Коротков А.С.** Анализ эффективности методик расстановки взвешивающих элементов на кристалле унарного цифро-аналогового преобразователя // Известия вузов. Радиоэлектроника, 2017. Т. 60. № 5. С. 225–232. DOI: 10.20535/S0021347017050041

15. **Tong X., Wang C., Wang F.** Linearity optimization of current steering DAC based on improved layout topology // Proc. of the 2019 IEEE Internat. Conf. on Electron Devices and Solid-State Circuits. 2019. Pp. 1–3. DOI: 10.1109/EDSSC.2019.8754219

16. **Parmar S.S., Gharge A.P.** R-2R ladder circuit design for 32-bit digital-to-analog converter (DAC) with noise analysis and performance parameters // Proc. of the 2016 Internat. Conf. on Communication and Signal Processing. 2016. Pp. 467–468. DOI: 10.1109/ICCSP.2016.7754180

17. **Lin M.P., Chang Y., Hung C.** Recent research development and new challenges in analog layout synthesis // Proc. of the 2016 21st Asia and South Pacific Design Automation Conf. (ASP-DAC). 2016. Pp. 617–622. DOI: 10.1109/ASPDAC.2016.7428080

Статья поступила в редакцию 05.07.2020.

THE AUTHORS / СВЕДЕНИЯ ОБ АВТОРАХ

Salonina Ekaterina A.
Салонина Екатерина Александровна
E-mail: salonina.ea@gmail.com

Belyaev Yakov V.
Беляев Яков Валерьевич
E-mail: designcenter.spb@mail.ru

Piatak Ivan M.
Пятак Иван Михайлович
E-mail: i.m.piatak@gmail.com

DOI: 10.18721/JCSTCS.13306
УДК 621.317.311, 621.317.321, 621.317.335.2, 621.317.39

TELEMETRY DEVICE FOR CONTROL OF TECHNICAL STATE OF CHEMICAL CURRENT SOURCES

I.G. Balaban, A.L. Balaban, A.A. Khovpachev, E.V. Shilin

Southern-Russian State Polytechnical University,
Novocherkassk, Russian Federation

The article describes the device for telemetry and control of the technical state of chemical current sources. The controlled parameters are the residual capacity, voltage, discharge current, temperature of current sources. The article presents a functional scheme of the device, its feature being galvanic isolation of the current source circuit and the monitoring device. To provide galvanic isolation, the authors propose a circuit solution for non-contact current measurement in order to reduce the error in measuring currents of various magnitudes. An asynchronous parallel-serial data transfer interface is used for the exchange with the upper-level system. The article describes the algorithm of telemetry device operation, which is implemented for the 1887VE4U microcontroller. When developing the device, the main difficulty was the need to ensure the minimum weight and dimensions and use only domestic-made electronic components to comply with the import substitution strategy in the Russian economy.

Keywords: telemetry, noncontact measurement, discharging current, current sensor, capacity, voltage, chemical current source.

Citation: Balaban I.G., Balaban A.L., Khovpachev A.A., Shilin E.V. Telemetry device for control of technical state of chemical current sources. Computing, Telecommunications and Control, 2020, Vol. 13, No. 3, Pp. 63–74. DOI: 10.18721/JCSTCS.13306

УСТРОЙСТВО ТЕЛЕМЕТРИИ И КОНТРОЛЯ ТЕХНИЧЕСКОГО СОСТОЯНИЯ ХИМИЧЕСКИХ ИСТОЧНИКОВ ТОКА

И.Г. Балабан, А.Л. Балабан, А.А. Ховпачев, Е.В. Шилин

Южно-Российский государственный политехнический университет
(НПИ) им. М.И. Платова, г. Новочеркасск, Российская Федерация

Описано устройство телеметрии и контроля технического состояния химических источников тока. Контролируемыми параметрами являются остаточная ёмкость, напряжение, разрядный ток, температура источников тока. Приведена функциональная схема устройства, особенностью которой является обеспечение гальванической развязки цепи источника тока и устройства контроля. Для обеспечения гальванической развязки предложено использовать схемотехническое решение для бесконтактного измерения тока с целью снижения погрешности при измерении токов различной величины. Для обмена с системой верхнего уровня использован асинхронный параллельно-последовательный интерфейс передачи данных. Описан алгоритм работы устройства телеметрии, который реализован для микроконтроллера 1887ВЕ4У. При разработке устройства основная трудность заключалась в необходимости обеспечить минимальные массогабаритные параметры и использовать электронные компоненты только отечественного производства в рамках реализации стратегии импортозамещения в экономике России.

Ключевые слова: телеметрия, бесконтактное измерение, разрядный ток, датчик тока, ёмкость, напряжение, химический источник тока.

Ссылка при цитировании: Балабан И.Г., Балабан А.Л., Ховпачев А.А., Шилин Е.В. Устройство телеметрии и контроля технического состояния химических источников тока // Computing, Telecommunications and Control. 2020. Т. 13. № 3. С. 63–74. DOI: 10.18721/JCSTCS.13306

Introduction

Chemical current sources (CCS) are widely used in everyday human life (uninterruptible power supplies, cars, household appliances, etc.) and in various industries (for autonomous power supply of civilian, military, space and other specialized equipment).

When supplying power to industrial facilities, two types of CCS are used: primary batteries and secondary batteries. The most common batteries are saline, alkaline, lithium. Lithium cells and batteries from the listed are the most energy-intensive and capable of delivering powerful current pulses.

The problem of diagnosing the state of CCS and the possibility of predicting their performance is one of the central problems of the production and operation of current sources [1]. According to the requirements for the operation of lithium CCS for long-term and high-quality operation, as well as their timely replacement, it is necessary to ensure control of the main parameters – residual capacity, voltage and discharge current.

There is a term “smart” CCS [2]. It is a current source, which contains a parameter monitoring device and sends information about the current state of the battery, discharge current, voltage, capacity and temperature of the battery to the monitoring system in real time. Such control devices must have minimum weight and dimensions.

Reducing the influence of the human factor, labor intensity of maintenance and the need for remote diagnostics during battery operation is an important task and requires introducing monitoring and diagnostics devices into the electric power facilities [3–10]. In addition, one of the problems arising during the operation of lithium batteries is the absence or insufficient number of effective methods and devices for non-destructive and continuous monitoring of parameters in all operating modes, including during operation [11].

There are many methods for determining capacity. These can be methods based on measurements of the open circuit voltage [12], discharge voltage [13–19], internal resistance of a CCS [20–23], as well as density, optical refractive index, dielectric constant of the electrolyte, intensity of infrared radiation emitted by the outer surface of the CCS [24, 25].

For lithium power sources, the number of successfully tested methods is limited due to the peculiarities of such power sources. These methods include: impedance measurement, fluctuation of the discharge voltage, assessment of the discharge current at constant and pulse current, microcalorimetry [1].

The method of potentiostatic diagnostics of the capacity of an active electrode of a nickel-cadmium battery, which is based on the relationship between the current arising during potentiostatic polarization of a nickel oxide electrode, and the residual capacity is given in [26]. However, this method for determining capacity is only intended for a nickel-cadmium battery.

Devices for monitoring the state of CCS are proposed in [27–32]. A device for measuring direct current with galvanic isolation was proposed in [33]. The disadvantage of these devices is that they do not simultaneously measure the voltage, discharge current, residual capacity and temperature of the CCS. In addition, the overall dimensions of the devices are not indicated.

A computer system for monitoring the parameters of power supplies consisting of CCS is proposed in [34]. The monitored parameters include voltage, current and discharge time. However, the system does not take into account the residual capacity of the CCS, and also has large weight and size characteristics.

The known devices for monitoring the parameters of the CCS do not meet all the necessary requirements for the quantity and quality of the monitored parameters, permissible weight and dimensions, and the possibility of information communication with upper-level systems.

The authors have developed a device that allows continuous monitoring of the CCS parameters. The introduction of a telemetry and parameter control device into the CCS makes it possible to create a "smart" battery and to simplify obtaining objective information about the current state of the battery. The information obtained will make it possible to analyze the operation of batteries in order to increase their reliability, determine ways to improve equipment and establish the causes of its failures.

Within the framework of the implementation of the import substitution strategy in the Russian economy, only domestic-made electronic components were used in the development of the device.

Functional scheme of the device

The developed device consists of the following functional units: non-contact current measurement unit, voltage measurement unit, temperature measurement unit, microcontroller (MC), power supply.

The functional scheme of the current measurement unit is shown in Fig. 1.

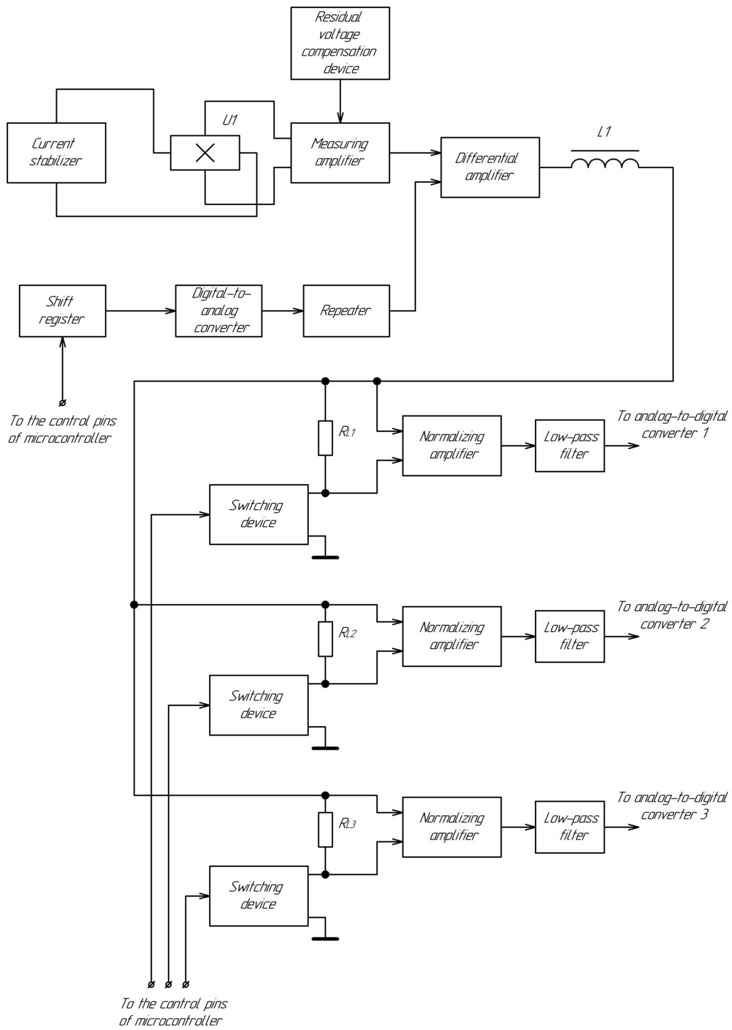

Fig. 1. Functional scheme of the current measurement unit

The non-contact current measurement unit implements the circuit design developed by the authors for the contactless current measurement, in which three current measurement subranges are used in order to reduce the error. Contactless measurement is implemented using a compensation current sensor of our own production, since the existing current sensors either cannot be used in terms of design, weight or dimensions, or are not produced in the Russian Federation (for example, manufactured by LEM [35]).

The current sensor consists of a toroidal ferromagnetic core, a compensation coil $L1$, consisting of 10,000 turns, and a Hall sensor $U1$ PKHE61A1 [36], which is installed in the gap of the core with a wound compensation winding.

The proposed circuitry principles of non-contact current measurement make it possible to galvanically isolate the battery circuits and control circuits in order to prevent the destruction of the controlled battery in the event of the control device malfunction.

The amplified voltage from the Hall sensor is used in the compensation type sensors to generate a compensation current I_c in the secondary winding. As a result, a magnetic flux is created, which compensates for the magnetic flux created by the primary current I_d. If the magnetic flux is fully compensated (equal to zero), then the magnetic potential of the two windings is identical [37].

The Hall sensor is powered by a current stabilizer. One of the parameters of the Hall sensor is the residual voltage, so the device is included in the circuit to compensate for the residual voltage.

The measured current creates a magnetic flux in the magnetic circuit, which induces an electromotive force (EMF) in the Hall sensor, proportional to the discharge current. The EMF signal from the terminals of the converter is amplified by the measuring amplifier (MA) and fed to one of the inputs of the differential amplifier.

A signal from a digital-to-analog converter (DAC) is fed to the second input of the differential amplifier through a repeater. The digital-to-analog converter is controlled through a shift register to save discrete pins of the microcontroller.

This is necessary to compensate for the offset voltage at the output of the instrumentation amplifier and the possible uncompensated residual voltage of the Hall sensor at the input of the measuring amplifier.

The signal goes to the compensation winding $L1$ from the output of the measuring amplifier and, then, goes to the load resistors (shunts) R_{L1}, R_{L2} or R_{L3}, which are earthed by means of switching devices controlled by the MC. The current flowing through the winding and one of the load resistors creates a magnetic flux in the opposite direction in the magnetic circuit.

Thus, a negative feedback magnetic system is created. In this case, the following equality must be satisfied

$$I_d \cdot W_d = I_c \cdot W_c,$$

where I_d is a discharge current; W_d is the number of conductors through which current flows I_d ($W_d = 1$); I_c is a compensation current flowing through the coil; W_c is the number of turns of the compensation coil.

The sensor operates at almost zero magnetic flux, which eliminates the temperature drift of the sensor's conversion factor. Thus, the resulting compensation current I_c flowing through the coil accurately represents the discharge current I_d to be measured. A voltage proportional to the primary current I_d can be obtained by a series connection with the secondary winding of the load resistor-shunt.

The use of three different size load resistors-shunts allows changing the range of current measurement and allows you to reduce the error when measuring currents of different magnitude. The voltage drop across resistors R_{L1}, R_{L2} or R_{L3}, created by the compensation current, is converted by the normalizing amplifiers into a normalized signal, which passes through a low-pass filter (LPF) and then is transmitted to the input of an analog-to-digital converter (ADC) built into the microcontroller.

The voltage measuring unit must be galvanically isolated from the rest of the circuit of the parameter monitoring device in order to exclude the failure of the developed device in the event of a malfunction of the controlled object. In this regard, a *DC/DC* converter is used to power the voltage measuring unit, which is controlled from the MC through a galvanic isolation and a switching device. In addition, the controlled voltage of the CCS is also supplied through the switching device not to constantly load and discharge the battery.

Since the value of the monitored voltage can reach +40 V, there is a voltage divider at the input helping to adjust the input resistance of the voltage measuring unit and reduce the voltage to be applied to the input of the measuring amplifier. The MA amplifies the voltage and transmits it to the input of the low-pass filter, from the output of which, through the repeater, the voltage signal is fed to the input of the ADC unit with a built-in Serial Peripheral Interface (SPI). The ADC unit is exchanged through galvanic isolation with the microcontroller and digitally transmits the measured voltage value using the SPI interface.

The temperature measuring unit contains a resistive temperature sensor built into one of the arms of the bridge measuring circuit. The bridge is powered by a voltage stabilizer connected to one of the diagonals of the measuring bridge. The voltage signal from the other diagonal of the bridge is fed to the input of the measuring amplifier, amplified and fed to the input of the low-pass filter and transmitted to the ADC built into the microcontroller.

The microcontroller is one of the central blocks of the device. It is designed to collect and process information about the magnitude of current, voltage, solve computational problems, including the problem of calculating the residual capacity of the battery, communication and data exchange with the upper-level system and the control panel.

The data on the discharge current, capacity of the monitored battery and voltage will be transmitted via the asynchronous parallel-serial data interface. The array returned by the device will consist of 48 bits and 6 eight-bit words (8 digits for markers of discharge current, voltage and temperature, and 16 digits for capacity). The first word is a marker for the beginning of the information transfer. The second word contains information about the current of discharge. The third and fourth words contain information about the capacity of the monitored battery. The fifth word contains voltage information. The sixth word contains information about the temperature of the battery.

Algorithm

The operation algorithm of the telemetry device and control of the technical state of chemical current sources is shown in Fig. 2.

At the first stage, the MC modules are initialized (interrupt controller, analog-to-digital converter, watchdog timer, input-output ports, interfaces and others). After that, the device proceeds to the cyclic measurement of the monitored parameters: discharge current I_d, voltage and residual capacity of the CCS.

The discharge current measurement subroutine is responsible for current measurement (Fig. 3), the voltage measurement subroutine is responsible for voltage measurement.

If the value of the discharge current I_d is in the range from 40 to 120 A then the discharge current I_{d1} is assumed equal to I_d and the subroutine ends.

In the opposite case, a more accurate determination of the current is required. For this, the load R_{L1} is disconnected and it is determined whether the measured value of the discharge current I_d belongs to the range from 5 to 40 A. If it does, then the R_{L2} load is switched with the control signal from the MC and the voltage is measured at the ADC2 input. After that, the value of the discharge current I_{d2} is determined and the subroutine ends. The magnitude of the current corresponds to the voltage signal fed to the ADC2.

If the measured value of the discharge current I_d does not belong to the range from 5 to 40 A then the readings are in the range from 0 to 5 A. Similar to the previous steps: the load R_{L3} is switched, the voltage is measured at the input of ADC3 and the value of the discharge current I_{d3} is determined, which corresponds to the voltage signal received by the ADC3. Then the subroutine ends.

The residual capacity of the CCS is calculated at the next stage by the measured value of the discharge current as the difference between the nominal value of the capacity Q_{nom} and the capacity of the discharge Q_d.

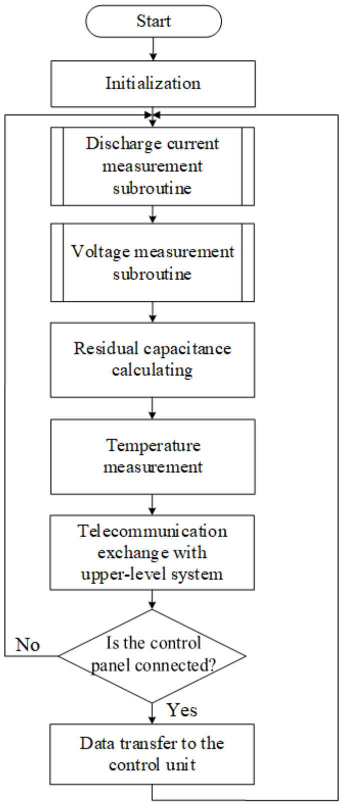

Fig. 2. Algorithm of the telemetry device and control of the technical state of chemical current sources

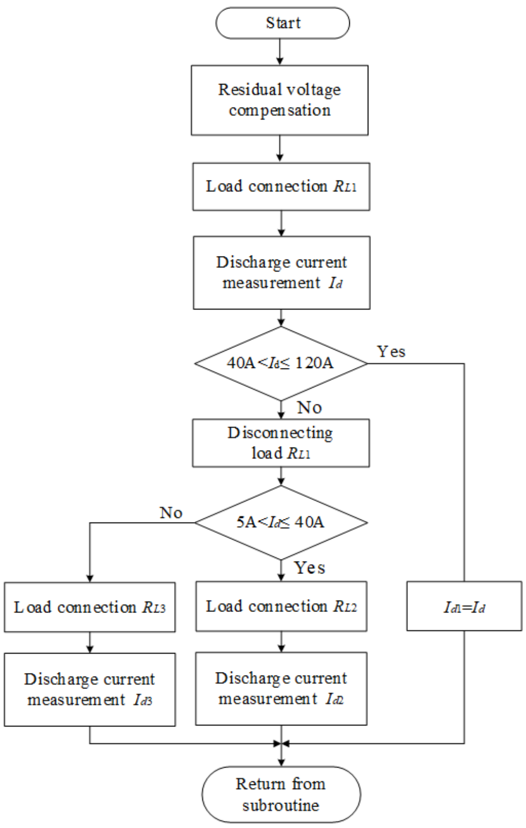

Fig. 3. Algorithm of the current discharge measurement subroutine

$$Q_{SC} = Q_{nom} - Q_d = Q_{nom} - \int_0^t I_d dt = Q_{nom} - \sum_{i=1}^{n} I_d \Delta t_i,$$

where Q_{nom} is the nominal value of the controlled CCS capacity (technical datasheet value); Q_d is the value of the capacity for which the CCS was discharged; I_c is the current value of discharge current; Δt_i is the time elapsed since the last measurement of the discharge current.

The device exchanges data (discharge current I_d, voltage, residual capacity and temperature of the CCS) with the upper-level system by means of telemetry after each measurement cycle. When a control panel is connected, the measured values are transmitted to it. It can be used to configure the device.

The algorithm is implemented in software using the 1887VE4U microcontroller [38]. The program is written in a high-level language C (ISO/IEC 9899:1999) in a software development environment Keil µVision. It consists of a head module and subroutines [39].

Conclusion

The device for telemetry and control of the technical state of chemical current sources developed by the authors allows analyzing the operation of both batteries and autonomous devices in order to increase their reliability, determine ways to improve equipment and establish the causes of its failures.

A three-dimensional model of the developed device for telemetry and control of the technical state of chemical current sources is shown in Fig. 4.

Device characteristics: voltage measurement range from 0 to +40 V, current from 0 to 120 A, capacity from 0 to 511 A/h and temperatures from 0 to +100 ºC.

The error in measuring current and capacity does not exceed 5 %, in voltage and temperature is not more than 1 %. The values of the discharge current, voltage and capacity are transmitted to the upper-level system via an asynchronous parallel-serial interface; it is possible to connect a control panel. Operating temperature range varies from 0 to +50 ºC, relative humidity 60 % at a temperature of +25 ºC.

It should be noted that in connection with the state policy of import substitution and the development of the production of a domestic electronic component base, the device includes domestic components only.

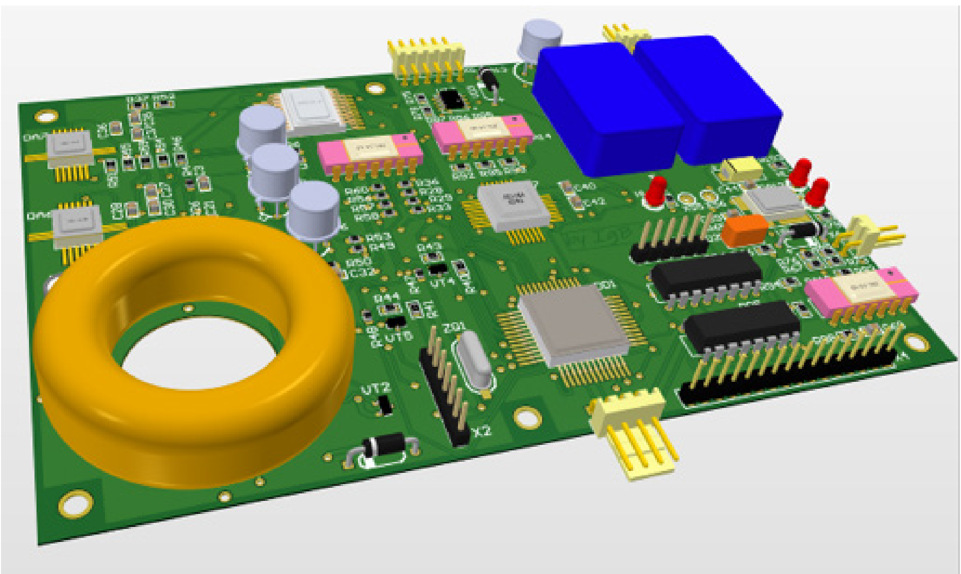

Fig. 4. Three-dimensional model of the device for telemetry and control of the technical state of chemical current sources

REFERENCES

1. **Fedotov D.B., Yalyushev N.I., Maftey A.N., Makovetskiy D.V.** Diagnostic of lithium-thionyl chloride cells self-discharge. *Elektrokhimicheskaya Energetika* [*Electrochemical Energetics*], 2017, Vol. 17, No. 1, Pp. 9–18. (rus) DOI: 10.18500/1608-4039-2017-17-1-9-18

2. **Pleshakov M.S., Korokhov V.V., Asfatsaduryan M.Yu., Maftey A.N.** The batteries for versatile space tug "Fregat" power supply system. *Vestnik NPO im. S.A. Lavochkina*, 2014, No. 1, Pp. 84–88. (rus)

3. **Lachin V.I., Solomentsev K.Yu.** *Metody i ustroystva kontrolya sostoyaniya elektroenergeticheskikh obyektov s diskretno-raspredelennymi parametrami: Monografiya* [*Methods and devices for monitoring the state of electric power facilities with discretely distributed parameters: Monograph*]. Novocherkassk: YuRGTU (NPI) Publ., 2012, 342 p. (rus)

4. IEEE guide for selection and use of battery monitoring equipment in stationary applications. *IEEE Std 1491-2012 (Revision of IEEE Std 1491-2005)*, 25 June 2012, Pp. 1–50. DOI: 10.1109/IEEESTD.2012.6226325

5. **Godbole R.M., Chaudhari P., Rane M.** Estimating real time lifespan of nonrechargable coin cells by parameter measurements. *2019 IEEE 5th International Conference for Convergence in Technology (I2CT)*, 2019, Pp. 1–6. DOI: 10.1109/I2CT45611.2019.9033647

6. **Dineva A., Ferkó K., Székely M., Gyökér G., Vajda I.** High precision test system for the investigation of the condition of lithium-ion batteries. *2018 International Symposium on Fundamentals of Electrical Engineering*, 2018, Pp. 1–6. DOI: 10.1109/ISFEE.2018.8742422

7. **Yang Zhenji, Fu Yongjie.** Design of the battery resistance measurement system. *IEEE 2011 10th International Conference on Electronic Measurement & Instruments*, 2011, Pp. 240–243. DOI: 10.1109/ICEMI.2011.6037806

8. **Yeqin Wang, Yixing Liu.** Electronic control system design and test of pure electric vehicle battery management system. *2011 Second International Conference on Mechanic Automation and Control Engineering*, 2011, Pp. 1289–1292. DOI: 10.1109/MACE.2011.5987178

9. **Zenati A., Desprez P., Razik H., Rael S.** A methodology to assess the State of Health of lithium-ion batteries based on the battery's parameters and a Fuzzy Logic System. *2012 IEEE International Electric Vehicle Conference*, 2012, Pp. 1–6. DOI: 10.1109/IEVC.2012.6183268

10. **Cox D.C., Perez-Kite R.** Battery state of health monitoring, combining conductance technology with other measurement parameters for real-time battery performance analysis. *INTELEC. 22nd International Telecommunications Energy Conference (Cat. No.00CH37131)*, 2000, Pp. 342–347. DOI: 10.1109/INTLEC.2000.884272

11. **Fedotov D.B., Yalyushev N.I., Maftey A.N.** Experience of application of sources of the current of system lithium-tionilhlorid in the space-rocket technics. *Elektrokhimicheskaya Energetika* [*Electrochemical Energetics*], 2013, Vol. 13, No. 2, Pp. 90–95. (rus)

12. **Smith Leonard S.** Device indicating the time remaining of the useful of battery. *US patent 4625175*. 1983.

13. **Makhija Surender K.** Electronic battery testing device and method for testing batteries. *US Patent 6037778*. 1997.

14. **Anbuku Adnan, Pascoe Philip.** Battery capacity measurement. *UK patent 2350686*. 2000.

15. **Eguchi Yasuhito.** Battery pack, battery remaining capacity detection method and application device driven with battery pack as power source. *US Patent 6064182*. 1998.

16. **Sandifer J.R.** Slate-of-charge measurement of the litium-carbon monofluoride battery by chronopo-tentiometry. *J. Appl. Electrochem*, 1986, Vol. 16, No. 2, Pp. 307–308.

17. **Solovyev V.M.** Sposob opredeleniya yemkosti khimicheskogo istochnika toka [Method for determining the capacity of a chemical current source]. *SU Patent 997143*. 1983. (rus)

18. **Tuphorn Hans.** Measurement method for determining the quality of a battery. *DE patent 3516498*. 1986.

19. **Maslov M.D.** Sposob opredeleniya ostatochnoy yemkosti svintsovogo akkumulyatora [Method for determining the residual capacity of a lead-acid battery]. *RU Patent 2182388*. 2002. (rus)

20. **Fischer D., Carkner S.** Automatic battery detection system and method for detecting a rechargeable battery with low remaining charge. *EP patent 1065774*. 2000.

21. **Bertness Kevin I.** Electronic battery tester. *US patent 5914605*. 2002.

22. **Vetter Mike, Miels Torsten.** Determining state of charge of battery connected to charger involves forming ratio of battery voltage and load current differences for two different charger output voltages at same temperature. *DE patent 19903239*. 1999.

23. **Joseph Patino, Russell L. Simpson.** Optimized method for determining remaining life cycles in a rechargeable battery. *US patent 6023150*. 1998.

24. **Russell D. Moulton, Benjamin Chaloner-Gill.** Use of IR (thermal) imaging for determining cell diagnostic. *US Patent 5483068*. 1994.

25. **Nizhnikovskiy Ye.A.** Nerazrushayushchiy kontrol kachestva khimicheskogo istochnika toka s ispolzovaniyem metoda mikrokalometrii [Non-destructive quality control of a chemical power source using the microcalometry method]. *Elektrokhimicheskaya energetika*, 2003, Vol. 3, No. 2, Pp. 80–85. (rus)

26. **Breslavets V.P., Lipkin M.S., Barsukov S.G., Sukhoverkhov D.A., Lipkin S.M.** Diagnostika nikel-kadmiyevykh akkumulyatorov potentsiostaticheskim impulsnym metodom [Diagnostics of nickel-cadmium batteries by potentiostatic pulse method]. *Izv. vuzov. Elektromekhanika*, 2007, Pp. 55–56. (rus)

27. **Kholodkov V.P., Lachin V.I., Malina A.K., Gorbatenko N.I., Demidov B.A., Gitis M.Ya., Zverev A.A.** Ustroystvo kontrolya napryazheniya galvanicheski svyazannykh khimicheskikh istochnikov toka [Voltage monitoring device for galvanically coupled chemical current sources]. *SU patent 1125672*. 1983. (rus)

28. **Lachin V.I., Malina A.K., Solomentsev K.Yu.** Avtonomnaya informatsionno-izmeritelnaya sistema kontrolya parametrov akkumulyatornykh batarey. *Puti uluchsheniya ekspluatatsionnykh kharakteristik sudovogo elektrooborudovaniya*, 1990, No. 500, Pp. 13–16. (rus)

29. **Lachin V.I., Kholodkov V.P., Malina A.K., Samchenko V.Ye., Solomentsev K.Yu.** *Izmeritelno-vychislitelnaya sistema kontrolya parametrov mnogoelementnykh system* [*Autonomous information-measuring system for monitoring battery parameters*]. Informatsionnyy listok. Rostov. TsNTI, 1990. P. 558. (rus)

30. **Dzenzerskiy V.A., Plaksin S.V., Zhitnik N.Ye., Shirman O.I.** Control of the energy state of chemical current source by impulse method. *Electrotechnic and computer systems*, 2014, No. 14, Pp. 131–139. (rus)

31. **Pimenov Yu.Ye, Belskiy V.P., Kostin Ye.A.** Avtomaticheskoye ustroystvo dlya kontrolya napryazheniya na khimicheskom istochnike toka pri razryade [Automatic device for monitoring the voltage on a chemical current source during discharge]. *SU Patent 1376136*. 1986. (rus)

32. **Kukoz F.I., Lyubiyev O.N., Chernov V.G., Zatolokina T.Yu.** Sposob kontrolya sostoyaniya khimicheskogo istochnika toka [Method for monitoring the state of a chemical current source]. *SU Patent 1024996*. 1983. (rus)

33. **Malina A.K., Lachin V.I., Kholodkov V.P., Demidov B.A., Poyedintsev I.F., Oleynikova L.V.** Ustroystvo dlya izmereniya postoyannogo toka [DC current measuring device]. *SU Patent 1265634*. 1984. (rus)

34. **Klyuchnikov A.V., Kuznetsov A.V., Kuzminykh N.A., Lysykh A.V.** Computer-aided system development for control the parameters of composite power supply devices. *Nauchno-Tekhnicheskiy Vestnik Povolzhya. Tekhnicheskiye Nauki* [*Scientific and Technical Volga Region Bulletin*], 2014, No. 1, Pp. 93–95. (rus)

35. Life Energy Motion. Available: *https://www.lem.com/en* (Accessed: 03.09.2020).

36. Preobrazovateli Kholla. Available: *https://sensorspb.wixsite.com/hallsensor* (Accessed: 31.08.2020).

37. **Volovich G.** Integralnyye datchiki Kholla [Integral Hall Sensors]. *Sovremennaya Elektronika* [*Modern Electronics*], 2004, Pp. 26–31. (rus)

38. Mikrokontroller 1887VE4U. Available: *https://niiet.ru/product/id5* (Accessed: 31.08.2020). (rus)

39. **Balaban I.G., Balaban A.L., Yufanova Yu.V.** Software development for microcontroller of accumulator batteries telemetry device. *Mathematical Modeling of Processes and Systems: papers of the IX International Youth Scientific-Practical Conference*, 2019, Pp. 68–72.

Received 15.08.2020.

СПИСОК ЛИТЕРАТУРЫ

1. **Федотов Д.Б., Ялюшев Н.И., Мафтей А.Н., Маковецкий Д.В.** Диагностика саморазряда литий-тионилхлоридных источников тока // Электрохимическая энергетика. 2017. Т. 17. № 1. С. 9–18.

2. **Плешаков М.С., Корохов В.В., Асфацадурьян М.Ю., Мафтей А.Н.** Батареи системы электроснабжения межорбитального космического буксира «Фрегат» // Вестник НПО им. С.А. Лавочкина. 2014. № 1. С. 84–88.

3. **Лачин В.И., Соломенцев К.Ю.** Методы и устройства контроля состояния электроэнергетических объектов с дискретно-распределенными параметрами: Монография. Новочеркасск: ЮРГТУ(НПИ), 2012. 342 с.

4. IEEE guide for selection and use of battery monitoring equipment in stationary applications // IEEE Std 1491-2012 (Revision of IEEE Std 1491-2005). 25 June 2012. Pp. 1–50. DOI: 10.1109/IEEESTD.2012.6226325

5. **Godbole R.M., Chaudhari P., Rane M.** Estimating real time lifespan of nonrechargable coin cells by parameter measurements // 2019 IEEE 5th Internat. Conf. for Convergence in Technology (I2CT). 2019. Pp. 1–6. DOI: 10.1109/I2CT45611.2019.9033647

6. **Dineva A., Ferkó K., Székely M., Gyökér G., Vajda I.** High precision test system for the investigation of the condition of lithium-ion batteries // 2018 Internat. Symp. on Fundamentals of Electrical Engineering. 2018. Pp. 1–6. DOI: 10.1109/ISFEE.2018.8742422

7. **Yang Zhenji, Fu Yongjie.** Design of the battery resistance measurement system // IEEE 2011 10th Internat. Conf. on Electronic Measurement & Instruments. 2011. Pp. 240–243. DOI: 10.1109/ICEMI.2011.6037806

8. **Yeqin Wang, Yixing Liu.** Electronic control system design and test of pure electric vehicle battery management system // 2011 2nd Internat. Conf. on Mechanic Automation and Control Engineering. 2011. Pp. 1289–1292. DOI: 10.1109/MACE.2011.5987178

9. **Zenati A., Desprez P., Razik H., Rael S.** A methodology to assess the State of Health of lithium-ion batteries based on the battery's parameters and a Fuzzy Logic System // 2012 IEEE International Electric Vehicle Conf. 2012. Pp. 1–6. DOI: 10.1109/IEVC.2012.6183268

10. **Cox D.C., Perez-Kite R.** Battery state of health monitoring, combining conductance technology with other measurement parameters for real-time battery performance analysis // 22nd Internat. Telecommunications Energy Conf. (Cat. No.00CH37131). 2000. Pp. 342–347. DOI: 10.1109/INTLEC.2000.884272

11. **Федотов Д.Б., Ялюшев Н.И., Мафтей А.Н.** Опыт применения литий-тионилхлоридных источников тока в ракетно-космической технике // Электрохимическая энергетика. 2013. Т. 13. № 2. С. 90–95.

12. **Smith Leonard S.** Device indicating the time remaining of the useful of battery // US patent 4625175. 1983.

13. **Makhija Surender K.** Electronic battery testing device and method for testing batteries // US Patent 6037778. 1997.

14. **Anbuku Adnan, Pascoe Philip.** Battery capacity measurement // UK patent 2350686. 2000.

15. **Eguchi Yasuhito.** Battery pack, battery remaining capacity detection method and application device driven with battery pack as power source // US Patent 6064182. 1998.

16. **Sandifer J.R.** Slate-of-charge measurement of the litium-carbon monofluoride battery by chronopo-tentiometry // J. Appl. Electrochem. 1986. Vol. 16. No. 2. Pp. 307–308.

17. **Соловьев В.М.** Способ определения ёмкости химического источника тока // Патент СССР 997143. 1983.

18. **Tuphorn Hans.** Measurement method for determining the quality of a battery // DE patent 3516498. 1986.

19. **Маслов М.Д.** Способ определения остаточной ёмкости свинцового аккумулятора // Патент РФ 2182388. 2002.

20. **Fischer D., Carkner S.** Automatic battery detection system and method for detecting a rechargeable battery with low remaining charge // EP patent 1065774. 2000.

21. **Bertness Kevin I.** Electronic battery tester // US patent 5914605. 2002.

22. **Vetter Mike, Miels Torsten.** Determining state of charge of battery connected to charger involves forming ratio of battery voltage and load current differences for two different charger output voltages at same temperature // DE patent 19903239. 1999.

23. **Joseph Patino, Russell L. Simpson.** Optimized method for determining remaining life cycles in a rechargeable battery // US patent 6023150. 1998.

24. **Russell D. Moulton, Benjamin Chaloner-Gill.** Use of IR (thermal) imaging for determining cell diagnostic // US Patent 5483068. 1994.

25. **Нижниковский Е.А.** Неразрушающий контроль качества химического источника тока с использованием метода микрокалометрии // Электрохимическая энергетика. 2003. Т. 3. № 2. С. 80–85.

26. **Бреславец В.П., Липкин М.С., Барсуков С.Г., Суховерхов Д.А., Липкин С.М.** Диагностика никель-кадмиевых аккумуляторов потенциостатическим импульсным методом // Изв. вузов. Электромеханика. 2007. С. 55–56.

27. **Холодков В.П., Лачин В.И., Малина А.К., Горбатенко Н.И., Демидов Б.А., Гитис М.Я., Зверев А.А.** Устройство контроля напряжения гальванически связанных химических источников тока // Патент СССР 1125672. 1983.

28. **Лачин В.И., Малина А.К., Соломенцев К.Ю.** Автономная информационно-измерительная система контроля параметров аккумуляторных батарей // Пути улучшения эксплуатационных характеристик судового электрооборудования. 1990. Вып. 500. С. 13–16.

29. **Лачин В.И., Холодков В.П., Малина А.К., Самченко В.Е., Соломенцев К.Ю.** Измерительно-вычислительная система контроля параметров многоэлементных систем: Информационный листок. Ростов: ЦНТИ, 1990. С. 558.

30. **Дзензерский В.А., Плаксин С.В., Житник Н.Е., Ширман О.И.** Контроль энергетического состояния химического источника тока импульсным методом // Электротехнические и компьютерные системы. 2014. № 14. С. 131–139.

31. **Пименов Ю.Е., Бельский В.П., Костин Е.А.** Автоматическое устройство для контроля напряжения на химическом источнике тока при разряде // Патент SU 1376136 A1. 1986.

32. **Кукоз Ф.И., Любиев О.Н., Чернов В.Г., Затолокина Т.Ю.** Способ контроля состояния химического источника тока // Патент SU 1024996 A1. 1983.

33. **Малина А.К., Лачин В.И., Холодков В.П., Демидов Б.А., Поединцев И.Ф., Олейникова Л.В.** Устройство для измерения постоянного тока // Патент СССР 1265634. 1984.

34. **Ключников А.В., Кузнецов А.В., Кузьминых Н.А., Лысых А.В.** Создание компьютерной системы контроля параметров составных блоков питания // Научно-технический вестник Поволжья. Технические науки. 2014. № 1. С. 93–95.

35. Life Energy Motion // URL: https://www.lem.com/en (Дата обращения: 03.09.2020).

36. Преобразователи Холла // URL: https://sensorspb.wixsite.com/hallsensor (Дата обращения: 31.08.2020).

37. **Волович Г.** Интегральные датчики Холла // Современная электроника. 2004. С. 26–31.

38. Микроконтроллер 1887ВЕ4У // URL: https://niiet.ru/product/id5 (Дата обращения: 31.08.2020).

39. **Balaban I.G., Balaban A.L., Yufanova Yu.V.** Software development for microcontroller of accumulator batteries telemetry device // Mathematical modeling of processes and systems: papers of the IX Internat. Youth Scientific-Practical Conf., 2019. Pp. 68–72.

Статья поступила в редакцию 15.08.2020.

THE AUTHORS / СВЕДЕНИЯ ОБ АВТОРАХ

Balaban Igor G.
Балабан Игорь Геннадиевич
E-mail: i.balaban@inbox.ru

Balaban Anna L.
Балабан Анна Леонидовна
E-mail: ulapm20@mail.ru

Khovpachev Anatolii A.
Ховпачев Анатолий Андреевич
E-mail: hov-aa@yandex.ru

Shilin Evgenii V.
Шилин Евгений Валерьевич
E-mail: shilineugene@yandex.ru

DOI: 10.18721/JCSTCS.13307
УДК 658.012.011.56:658.312:681.586

DYNAMIC DESIGN OF HIGH-PRECISION GAS FLOWMETERS

A.I. Nagorny, V.N. Tisenko

Peter the Great St. Petersburg Polytechnic University,
St. Petersburg, Russian Federation

Electrohydrodynamic phenomena are effective in various applications of electric fields when controlling volumes, jets and flows of dielectric liquid. Nowadays, one of the most important issues in this area is the implementation of gas saving technologies as well as incensement of their efficiency. It is possible to raise the accuracy of current flowmeters of variable pressure drop on narrowing devices (ND) (which occupy around 70-80 % of the whole world market) by applying innovative compensatory flowmeters with electrohydrodynamic (EH) pressure compensation. At the same time negative inverse connection covers all the signal conversion chain, which makes it possible to exclude an error of each link inside the conversion chain after ND. This article describes the stages of development of an innovative electrohydrodynamic pressure compensation gas flowmeters with electrohydrodynamic inverters (EHI-2F) by using dynamic design and computer methods. They are competitive on the market in terms of accuracy, speed and sensitivity to pressure drop on the ND.

Keywords: gas flowmeters, accuracy, compensation charts, pressure compensation, electrohydrodynamic inverters, dynamic design.

Citation: Nagorny A.I., Tisenko V.N. Dynamic design of high-precision gas flowmeters. Computing, Telecommunications and Control, 2020, Vol. 13, No. 3, Pp. 75–87. DOI: 10.18721/JCSTCS.13307

ДИНАМИЧЕСКОЕ КОНСТРУИРОВАНИЕ ВЫСОКОТОЧНЫХ РАСХОДОМЕРОВ ГАЗА

А.И. Нагорный, В.Н. Тисенко

Санкт-Петербургский политехнический университет Петра Великого,
Санкт-Петербург, Российская Федерация

Электрогидродинамические явления эффективны в различных приложениях электрических полей при управлении объёмами, струями и потоками диэлектрических жидкостей. Повысить точность наиболее распространенных в мире расходомеров переменного перепада давлений можно в разработанных принципиально новых компенсационных расходомерах с электрогидродинамической (ЭГД) компенсацией по давлению с использованием электрогидродинамических обратных преобразователей с двухфазным диэлектриком – ЭГОП-2Ф. При этом отрицательной обратной связью охватывается вся прямая цепь преобразования сигналов после сужающего устройства (СУ), что позволяет исключить погрешность всех звеньев после СУ расходомера. В статье рассмотрены (с использованием методов динамического конструирования и применением электро-вычислительных машин) этапы разработки инновационных компенсационных по давлению ЭГД расходомеров газа с ЭГОП-2Ф, конкурентоспособных на рынке по показателям точности, быстродействия и чувствительности к перепаду давлений на СУ.

Ключевые слова: расходомеры газа, точность, компенсационные схемы, компенсация по давлению, электрогидродинамические обратные преобразователи, динамическое конструирование.

Ссылка при цитировании: Нагорный А.И., Тисенко В.Н. Динамическое конструирование высокоточных расходомеров газа // Computing, Telecommunications and Control. 2020. Vol. 13. No. 3. Pp. 75–87. DOI: 10.18721/JCSTCS.13307

Introduction

Papers [1–17, 20, 21] show effective use of electrohydrodynamic phenomena in various applications of electric fields when controlling volumes, jets and flows of dielectric fields.

Nowadays, one of the most important issues in this area is the implementation of gas saving technologies as well as incensement of their efficiency [1, 18, 19]. It is possible to raise the accuracy of current flowmeters of variable pressure drop on narrowing devices (ND) (which have around 70-80 % of the whole worldwide market) by applying innovative compensatory flowmeters with electrohydrodynamic (EH) [1, 2, 20] pressure compensation. At the same time negative inverse connection covers all the signal conversion chain, which makes it possible to exclude an error of each link inside the conversion chain after ND.

The fact is that at the moment, there are compensating flowmeters of variable pressure differential developed and implemented, in which the error of the "displacement-electrical signal" conversion (displacement compensation schemes) and the "force-displacement" conversion (force compensation schemes) is eliminated, while the "pressure-force" conversion remains not covered by the reverse compensation connection. The principles of pressure compensation are described in [22, pp. 13–17], and the principles of force compensation are described in [23, pp. 28–42]. The principle of pressure compensation, that is, as mentioned earlier, the coverage of the entire signal transformation chain by compensatory respond, has not yet been implemented and studied.

This article describes the stages of development of fundamentally new electrohydrodynamic pressure compensation gas flowmeters with electrohydrodynamic inverters (EHI-2F) by using dynamic design (design of the controlled equipment and selection parameters of the control system to ensure the required dynamic indicators) and computer methods [7, 12]. They are competitive on the market in terms of accuracy, speed and sensitivity to pressure drop on the ND.

Further we will consider only the signal conversion chain after the narrowing device of the electrohydrodynamic gas flowmeter in more detail. Fig. 1 shows the following symbols:

W_1 (s) is the transfer function of the link "differential pressure change on the narrowing device (ND) and on the the EH inventer with a two-phase dielectric (EHI-2F) – movement of the working dielectric fluid between the coverings of the capacitive undercompensation sensor (CUS)"

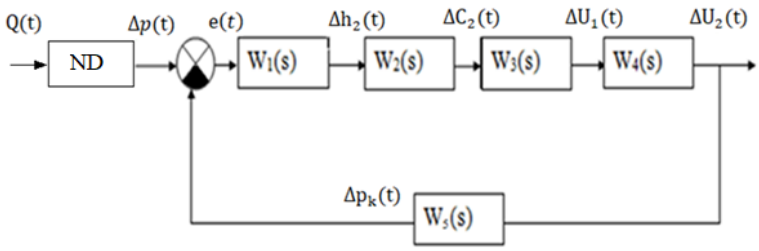

Fig. 1. Structural diagram of the compensation electrohydrodynamic flowmeter with EHI-2F (electrohydrodynamic inverter-2F)

$$W_1(s) = \frac{\Delta h2(s)}{e(s)} = \frac{k_1}{T_1^2 s^2 + 2\varepsilon T_1 s + 1}; \tag{1}$$

$W_2(s)$ is the transfer function of the dynamic element "movement of the working fluid between the coverings of the capacitive undercompensation sensor – change in the capacitance of the capacitive undercompensation sensor"

$$W_2(s) = \frac{\Delta C_2(s)}{\Delta h_2(s)} = k_2; \tag{2}$$

$W_3(s)$ is the transfer function of the element "change in capacitance-voltage at the output of CUS (capacitive undercompensation sensor)"

$$W_3(s) = \frac{\Delta U_1(s)}{\Delta C_2(s)} = \frac{k_3}{s}; \tag{3}$$

$W_4(s)$ is the transfer function of a high voltage amplifier

$$W_4(s) = \frac{\Delta U_2(s)}{\Delta U_1(s)} = \frac{k_4}{T_4 s + 1}; \tag{4}$$

$W_5(s)$ is the transfer function of the element "voltage on the electrodes of an EHI – pressure in a fluid at the output of an EHI"

$$W_5(s) = \frac{\Delta p_k(s)}{\Delta U_2(s)} = k_5, \tag{5}$$

here, k_i and T_j are the transfer coefficients and time constants of the corresponding dynamic elements.

Selection of design parameters of the electrohydrodynamic gas flowmeter using dynamic design and computer methods

Further increase in the accuracy and speed of compensatory EH flowmeters can be achieved by selecting transfer coefficients and time constants of elements within the framework of the dynamic formation technology [12], but with a stable compesation scheme.

Let us demonstrate this by the example of choosing the parameters of the element "differential pressure change on the narrowing device (ND) and on the the EH inventer with a two-phase dielectric (EHI-2F) – movement of the working dielectric fluid between the coverings of the capacitive undercompensation sensor (CUS)".

Determination of stability boundaries of the electrohydrodynamic compensation system in the plane of unknown parameters $T_1^2 - k_1$

We find the stability region of the compensation circuit in the plane of the variables of these parameters and the characteristic equation of the closed compensation circuit of the transducer of pressure difference on the control system into an electrical signal as the sum of the numerator and denominator of the transfer function of the open compensation system:

$$\Delta(s) = T_1^2 T_4 s^4 + \left(T_2 T_4 + T_1^2\right) s^3 + \left(T_4 + T_2\right) s^2 + s + k_1 k_2 k_3 k_4 k_5 = 0. \tag{6}$$

Taking into account [1], we have the initial data: $k_1 - ?, T_1^2 - ?, T_2 = 0{,}154\ \text{s}; k_2 = 801{,}6 \cdot 10^{-12}\,\dfrac{\varphi}{\text{m}}$; $k_3 = 0{,}2 \cdot 10^{12}\,\dfrac{\text{V}}{\varphi}; k_4 = 10^3; T_4 = 1 \cdot 10^{-3}\text{s}; k_5 = 4 \cdot 10^{-9}\,\dfrac{\text{Pa}}{\text{V}}$.

Denoting the variable $T_1^2 = \tau$, and another unknown parameter $k_1 = \mu$, we find the boundary of the oscillatory stability of the compensation converter of the pressure difference on the CS into an electric signal (see Fig. 1) in the plane of the unknown parameters of the flowmeter.

At the same time, we focus on the Mikhailov frequency stability criterion, assuming at the same time that the pressure difference on the control system of the flowmeter changes according to a harmonic law with a circular frequency ω. The choice of this stability criterion was based on the fact that it is applicable to both open and closed control systems. At the same time, the Mikhailov stability criterion does not limit the order of the differential equation describing the control system. To highlight the region of stability of the flowmeter, we are interested in the boundary of the oscillatory stability, when the Mikhailov hodograph, the real and imaginary part of the characteristic complex of the compensation scheme (Fig. 1) built in the coordinates, passes through the origin (Fig. 2).

The characteristic complex of the closed compensation circuit (Fig. 1) is obtained from the characteristic equation (1) by replacing the Laplace operator s with $j\omega$: $s = j\omega$, where $j = \sqrt{-1}$, ω is the circular frequency of the harmonic input signal of the pressure differential at the ND of the flowmeter.

Then equation (1) can be represented as

$$\tau Q(s) + \mu P(s) - R(s) = 0, \tag{7}$$

where $R(s)$ is a polynomial, in which neither τ nor μ are included.

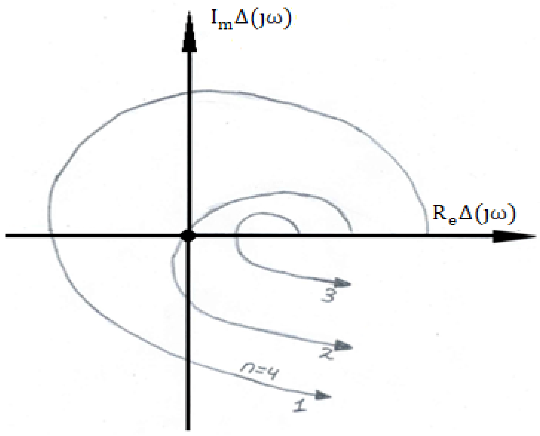

Fig. 2. Possible Nyquist hodographs from different values of unknown parameters T_1^2 and k_1 of the compensation electrohydrodynamic gas flowmeter: stability operation of the flowmeter (1); at the stability boundary (2); unstable operation of the gas flowmeter (3)

From the equations (1), (2) we can find the characteristic complex of a closed system, substituting $s = j\omega$ into the characteristic equation.

To separate the stability region of the compensation system for measuring the pressure difference on the control system (Fig. 1) for two unknown parameters τ and μ, first of all, it is necessary to find the boundary of its stability when the Mikhailov hodograph passes through the origin at some frequency, not changing its smooth spiral shape. Wherein:

$$\begin{cases} R_e\Delta(j\omega) = 0 \\ I_m\Delta(j\omega) = 0 \end{cases}. \tag{8}$$

Then, taking into account (2), (3) for the oscillation stability boundary, we have:

$$\begin{cases} \tau Q_1(\omega) + \mu P_1(\omega) = R_1(\omega) \\ \tau Q_2(\omega) + \mu P_2(\omega) = R_2(\omega) \end{cases}, \tag{9}$$

where, $Q_1(\omega)$, $P_1(\omega)$, $R_1(\omega)$ are the corresponding polynomials with τ, μ, and the constant term in (2) with even degrees ω, which corresponds to $\mathrm{Re}\Delta(j\omega) = 0$; $Q_2(\omega)$, $P_2(\omega)$, $R_2(\omega)$ are polynomials with uneven degree ω, which corresponds to $\mathrm{Im}\Delta(j\omega) = 0$.

Thus, we have two equations with two variables that are solved for τ and μ using determinants:

$$\tau = \frac{\begin{vmatrix} R_1(\omega) & P_1(\omega) \\ R_2(\omega) & P_2(\omega) \end{vmatrix}}{\begin{vmatrix} Q_1(\omega) & P_1(\omega) \\ Q_2(\omega) & P_2(\omega) \end{vmatrix}} = \frac{R_1(\omega)\cdot P_2(\omega) - P_1(\omega)\cdot R_2(\omega)}{Q_1(\omega)\cdot P_2(\omega) - P_1(\omega)\cdot Q_2(\omega)} = \frac{\Delta_1(\omega)}{\Delta(\omega)}, \tag{10}$$

$$\mu = \frac{\begin{vmatrix} Q_1(\omega) & R_1(\omega) \\ Q_2(\omega) & R_2(\omega) \end{vmatrix}}{\begin{vmatrix} Q_1(\omega) & P_1(\omega) \\ Q_2(\omega) & P_2(\omega) \end{vmatrix}} = \frac{Q_1(\omega)\cdot R_2(\omega) - R_1(\omega)\cdot Q_2(\omega)}{Q_1(\omega)\cdot P_2(\omega) - P_1(\omega)\cdot Q_2(\omega)} = \frac{\Delta_2(\omega)}{\Delta(\omega)}, \tag{11}$$

where

$$\begin{cases} \Delta(\omega) = Q_1(\omega)\cdot P_2(\omega) - P_1(\omega)\cdot Q_2(\omega); \\ \Delta_1(\omega) = R_1(\omega)\cdot P_2(\omega) - P_1(\omega)\cdot R_2(\omega); \\ \Delta_2(\omega) = Q_1(\omega)\cdot R_2(\omega) - R_1(\omega)\cdot Q_2(\omega). \end{cases}$$

Taking into account equation (1) and substituting the numerical values of the parameters, we have:

$$Q_1(\omega) = T_4\omega^4 = 10^{-3}\omega^4;\ Q_2(\omega) = -\omega^3;\ P_1(\omega) = k_2k_3k_4k_5 = 64128\cdot 10^{-8};$$

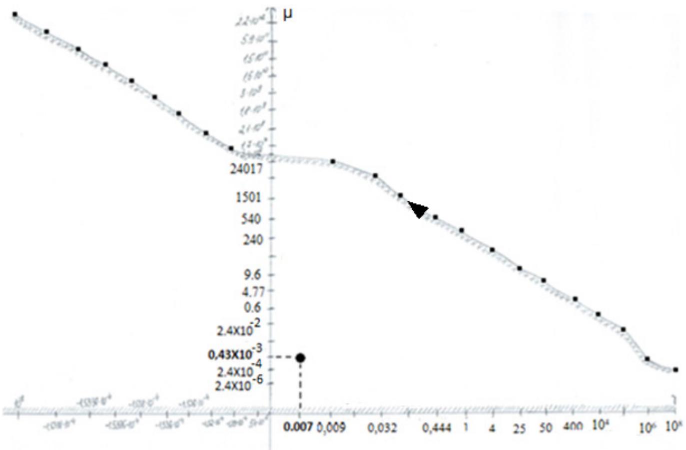

Fig. 3. Selection of unknown parameters from the range of stable operation of electrohydrodynamic flowmeter in the plane of parameters $T_1^2 = \tau$, $k_1 = \mu$

$$P_2(\omega) = 0;$$

$$R_1(\omega) = (T_4 + T_2)\omega^2 = 155 \cdot 10^{-3}\omega^2; \; R_2(\omega) = T_2 T_4 \omega^3 - \omega = 154 \cdot 10^{-6}\omega^3 - \omega.$$

We use the NAG1 program to calculate the values of τ and μ. We introduce the coefficients of polynomials with degrees ω. We consider values of frequencies of possible flowmeter operation from 10^{-4} to 10^4 1/s. A printout fragment of the PC calculation results to build a D-partition curve is shown in Appendix 1.

On the plane of the parameters τ and μ, we plot the corresponding interconnected points. Herewith frequencies are not indicated on this curve, but only the direction of the frequency increasing is indicated. Moreover, τ is plotted on the abscissa axis, and μ is on the ordinate axis. The geometrical location of these points when ω varies is the oscillatory boundary of the stability of a closed system (Fig. 1). Thus, we obtain the D curve – the plane partitions of the selected parameters τ, μ (Fig. 3).

To know which side the stability region of the system is located in the plane of the parameters τ – μ, we perform the hatching of the D-partition curve. For this, we indicate the direction of frequency increasing ω on the D-partition curve. The hatching is as follows. If one presumably stands on the D-partition curve and moves along it in the direction of frequency increasing ω, and if the main determinant $\Delta(\omega) > 0$ is positive, the curve is dashed with a double hatch to the left, which is the case here. We find special lines that are determined by equating the first and last coefficients of the characteristic equation (1) to zero. They coincide with the coordinates (Fig. 3). The special straight line along the axis does not hatch, since the sign of the determinant does not change at the intersection. The special straight line on the abscissa axis is dashed with a single hatching in the direction of the hatching of the D-partition curve, since there is an asymptotic convergence.

The area limited by shading inward is the area of stable operation of the flowmeter, which is confirmed by further calculations using the NAG2 program. From this area, select a point with coordinates (Fig. 3):

$$k_1 = \mu = 0{,}43 \cdot 10^{-3}; \; T_1^2 = \tau = 0{,}007\,\text{s}. \tag{12}$$

Selection of design parameters of a gas flowmeter based on the research results that ensure stable operation of the flowmeter

Based on the unknown parameters found in (12), we developed the design of the EHI-2F with capacitive output, which combines module transducer of the differential pressure on the flowmeter control

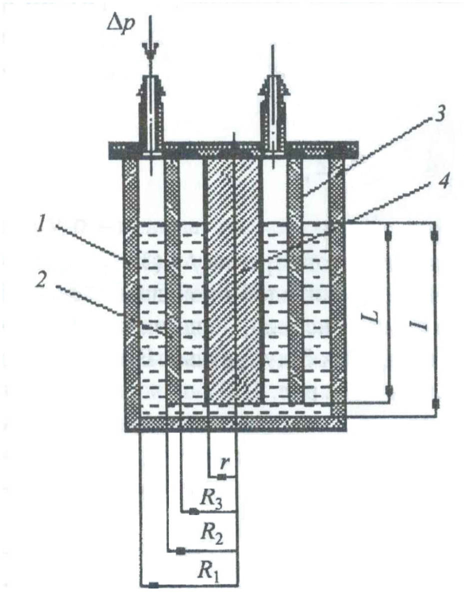

Fig. 4. Construction (based on the research results) of EHI-2F and a capacitive undercompensation sensor of an electrohydrodynamic gas flowmeter

system into the displacement of the working fluid (transformer oil), the EHI-2F as well as CUS electrodes (Fig. 4) in the single formation. Here, 1, 2 are high-voltage electrodes EHI-2F; 3,4 are lining CUS.

The design parameters in Fig. 4 are selected on the basis of (12) taking into account the following conditions [1]:

$$k_1 = \frac{R_1^2 - R_2^2}{pg\left(R_3^2 - r^2\right)}, \tag{13}$$

$$T_1 = \sqrt{\frac{\left(R_3^2 - r^2\right)}{g}\left[\frac{l_1}{R_1^2 - R_2^2} + \frac{\left(R_1 - r\right)^2}{R_1^2\left(l - l_1\right)} + \frac{l_1}{R_3^2 - r^2}\right]}. \tag{14}$$

As a result, the following rational parameters were selected to ensure the competitiveness of the developed innovative compensatory gas flowmeter on the market: R_1 = 15.75 mm; R_2 = 12.85 mm; R_3 = 11.9 mm; r = 10.95 mm; l = 60 mm; l_1 = L = 55 mm.

Conclusion

This article considered the use of compensating flowmeters of variable pressure drop with electrohydrodynamic pressure compensation to improve the accuracy and sensitivity of measuring the flow of transported liquids and gases. In addition, the article discussed the basic construction principles of the electrohydrodynamic compensation using the dynamic design methods and automatic control theory. At the initial stage, the transfer functions of all the links included in the EHI block diagram were defined. The article further identified the transfer functions in an open-loop mode and selected the settings of the two unknown parameters of the inertial link electrohydrodynamic system: transmission coefficient k_1 and time constant T_1^2. In the plane of flowmeter operability boundary, we identified the range of its stable operation.

With the selected design values of the flowmeter parameters, a point with coordinates (0.00043; 0.00725) was selected. This point is included in the stability area of the compensation scheme. This is the novelty and practical significance of the research.

Since in formulas (13, 14) we have interrelated design parameters that can be chosen in various combinations, with the abovementioned design parameters, numerous know-hows that have independent value on the market are provided in the developed innovative compensation gas flowmeter. The introduction of these flowmeters into the existing channels for the transportation of natural fuels will create a competitive advantage for the fuel suppliers by potentially reducing the product cost.

Appendix 1

Printout fragment of the PC calculation results to build a D-partition curve

Nagorny A.I.

System order 4

Coefficients of polynomials

	p1	p2	q1	q2	r1	r2
0	6.41E-0004	0.00E+0000	0.00E+0000	0.00E+0000	0.00E+0000	0.00E+0000
1	0.00E+0000	0.00E+0000	0.00E+0000	0.00E+0000	0.00E+0000	-1.00E+0000
2	0.00E+0000	0.00E+0000	0.00E+0000	0.00E+0000	1.55E-0001	0.00E+0000
3	0.00E+0000	0.00E+0000	0.00E+0000	-1.00E+0000	0.00E+0000	1.54E-0004
4	0.00E+0000	0.00E+0000	1.00E-0003	0.00E+0000	0.00E+0000	0.00E+0000

ω	τ	μ	D
1.0E-0004	1.000000E+0008	2.401447E-0006	6.412800E-0016
5.0E-0004	1.000000E+0007	2.456843E-0004	3.408876E-0014
1.0E-0003	1.000000E+0006	4.301442E-0004	1.348264E-0012
5.0E-0003	4.132412E+0004	6.143256E-0003	5.815066E-0010
1.0E-0002	1.000000E+0004	2.401345E-0002	2.484800E-0009
5.0E-0002	4.001632E+0002	6.133251E-0001	4.412800E-0008
1.0E-0001	5.000371E+0001	4.771442E+0000	2.356800E-0007
2.5E-0001	2.501130E+0001	9.600130E+0000	6.916217E-0006
5.0E-0001	3.998246E+0000	6.006021E+0001	8.020811E-0005
1.0E+0000	9.996460E-0001	2.401930E+0002	6.414724E-0004
1.5E+0000	4.442312E-0001	5.403989E+0002	2.164753E-0003
2.0E+0000	2.498210E-0001	9.606787E+0002	5.131010E-0003
2.5E+0000	1.598332E-0001	1.501034E+0003	1.002120E-0002
3.0E+0000	1.109497E-0001	2.161466E+0003	1.731629E-0002
3.5E+0000	8.147399E-0002	2.941977E+0003	2.749724E-0002
4.0E+0000	6.234288E-0002	3.842569E+0003	4.104500E-0002
4.5E+0000	4.922652E-0002	4.863245E+0003	5.844054E-0002
5.0E+0000	3.984440E-0002	6.004008E+0003	8.016481E-0002
5.5E+0000	3.290265E-0002	7.264861E+0003	1.066988E-0001
6.0E+0000	2.762285E-0002	8.645809E+0003	1.385234E-0001

6.5E+0000	2.351391E-0002	1.014685E+0004	1.761196E-0001
7.0E+0000	2.025358E-0002	1.176800E+0004	2.199685E-0001
7.5E+0000	1.762330E-0002	1.350926E+0004	2.705508E-0001
8.0E+0000	1.547061E-0002	1.537063E+0004	3.283477E-0001
8.5E+0000	1.368650E-0002	1.735212E+0004	3.938400E-0001
9.0E+0000	1.219140E-0002	1.945373E+0004	4.675087E-0001
9.5E+0000	1.092610E-0002	2.167547E+0004	5.498348E-0001
1.0E+0001	9.845800E-0003	2.401735E+0004	6.412992E-0001
1.5E+0001	7.021560E-0003	3.521780E+0004	7.316953E-0001

2.6E+0002	-1.392071E-0004	1.733120E+0007	1.127115E+0004
5.1E+0002	-1.501553E-0004	7.870795E+0007	8.506648E+0004
7.6E+0002	-1.522687E-0004	2.188252E+0008	2.815066E+0005
1.0E+0003	-1.530197E-0004	4.948673E+0008	6.607116E+0005
1.3E+0003	-1.533701E-0004	9.865324E+0008	1.282801E+0006
1.5E+0003	-1.535614E-0004	1.796032E+0009	2.207896E+0006
1.8E+0003	-1.536772E-0004	3.048092E+0009	3.496116E+0006
2.0E+0003	-1.537525E-0004	4.889949E+0009	5.207580E+0006
2.3E+0003	-1.538042E-0004	7.491358E+0009	7.402409E+0006
2.5E+0003	-1.538413E-0004	1.104458E+0010	1.014072E+0007
2.8E+0003	-1.538687E-0004	1.576440E+0010	1.348264E+0007
3.0E+0003	-1.538896E-0004	2.188812E+0010	1.748829E+0007
3.3E+0003	-1.539059E-0004	2.967552E+0010	2.221777E+0007
3.5E+0003	-1.539188E-0004	3.940894E+0010	2.773123E+0007
3.8E+0003	-1.539293E-0004	5.139321E+0010	3.408876E+0007
4.0E+0003	-1.539378E-0004	6.595568E+0010	4.135051E+0007
4.3E+0003	-1.539449E-0004	8.344621E+0010	4.957658E+0007
4.5E+0003	-1.539508E-0004	1.042372E+0011	5.882709E+0007
4.8E+0003	-1.539559E-0004	1.287234E+0011	6.916217E+0007
5.0E+0003	-1.539602E-0004	1.573224E+0011	8.064193E+0007
5.3E+0003	-1.539639E-0004	1.904741E+0011	9.332649E+0007
5.5E+0003	-1.539671E-0004	2.286408E+0011	1.072760E+0008
5.8E+0003	-1.539699E-0004	2.723075E+0011	1.225505E+0008
6.0E+0003	-1.539723E-0004	3.219817E+0011	1.392102E+0008
6.3E+0003	-1.539745E-0004	3.781933E+0011	1.573152E+0008
6.5E+0003	-1.539764E-0004	4.414948E+0011	1.769256E+0008
6.8E+0003	-1.539781E-0004	5.124612E+0011	1.981015E+0008
7.0E+0003	-1.539797E-0004	5.916901E+0011	2.209031E+0008
7.3E+0003	-1.539810E-0004	6.798014E+0011	2.453904E+0008
7.5E+0003	-1.539823E-0004	7.774377E+0011	2.716236E+0008
7.8E+0003	-1.539834E-0004	8.852640E+0011	2.996628E+0008

8.0E+0003	-1.539844E-0004	1.003968E+0012	3.295682E+0008
8.3E+0003	-1.539853E-0004	1.134259E+0012	3.613998E+0008
8.5E+0003	-1.539862E-0004	1.276871E+0012	3.952177E+0008
8.8E+0003	-1.539870E-0004	1.432559E+0012	4.310821E+0008
9.0E+0003	-1.539877E-0004	1.602099E+0012	4.690532E+0008
9.3E+0003	-1.539883E-0004	1.786292E+0012	5.091909E+0008
9.5E+0003	-1.539889E-0004	1.985961E+0012	5.515556E+0008
9.8E+0003	-1.539895E-0004	2.201951E+0012	5.962071E+0008

REFERENCES

1. **Nagornyy V.S., Nagornyy I.V.** *Converters of small pressures and pressure differences into an electric signal with electrohydrodynamic pressure compensation*. St. Petersburg: Publishing House of Polytechnic University, 2011, 224 p. (rus)

2. **Nagorniy A.I., Nagorniy V.S., Tisenko V.N.** Improved-accuracy innovative compensatory flowmeters of variable pressure differential applied in Oil & Gas Industry. IEEE Xplore Digital Library 9-16 Sept. 2018. Available: *https://ieeexplore.ieee.org/document/8501824*

3. **Nagorniy V.S., Smirnovsky A.A., Kolodyazhny D.Y., Chemyshev A.S.** Charge transfer in a sharply nonuniform electric field mediated by swirling liquid flow with minimal hydraulic resistance. *Technical Physics Letters*, 2015, No. 4, Pp. 859–862.

4. **Nagorniy V.S.** Mathematical model of the processes involved in electric charge to drops of a lubricant during the electrodrop application of lubricants to chemical fibers. *Fibre Chemistry*, 2016, Vol. 47, No. 6, Pp. 514–516.

5. **Sipatov A.M., Modorskii V.Y., Babushkina A.V., Kolodyazhnyi D.Y., Nagorniy V.S.** Computation of design parameters influence on air injector fuel atomization. *Russian Aeronautics*, 2017, Vol. 32, No. 3, Pp. 428–433.

6. **Nagorniy V.S.** Dynamic characteristics of the process for imparting an electric charge to lubricant droplets in the droplet jet electrospray method for applying lubricants to synthetic yarns. *Fibre Chemistry*, 2017, Vol. 48, No 6, Pp. 500–503.

7. **Nagorniy A.I., Tisenko V.N.** Innovative potential of a new device for measuring the flow of liquids and gases. *Computer Science and Cybernetics* (*ComCon-2017*): *Collection of Reports of the Student Scientific Conference of the Institute of Computer Science and Technology*. St. Petersburg: Publishing House of Polytechnic University, 2017, 535 p. (rus)

8. **Modorskii V.Y., Sipatov A.M., Babushkina A.V., Kolodyazhny D.Y., Nagorny V.S.** Modeling technique for the process of liquid film disintegration. *International Conference on the Methods of Aerophysical Research* (*ICMAR 2016*). *AIP Conference Proceedings*, 2016, Pp. 1–7.

9. **Nagorniy V.S., Nagorniy I.V.** Limitations of EHD control flows and jets using corona discharges in gas. *IEEE International Conference on Dielectric Liquids – ICDL 2008*, Poitiers-France, 2008, Pp. 97–99.

10. **Nagorniy V.S., Nagorniy I.V.** Electrophysical principles of electrogasdynamic conversion of electrical signals into pneumatic ones by turbulization of gas jets by unipolar ion flows. *Surface Engineering and Applied Electrochemistry*, Allerton Press, Inc. distributed exclusively by Springer Science+Business Media LLC, 2007, Vol. 43, No. 3, Pp. 187–193.

11. **Nagorny V.S., Nagorny I.V.** *Electrophysical bases of electro-gas-dynamic transformation of electric signals into pneumatic ones with turbulization of jets by unipolar ion flows*. St. Petersburg: Publishing House of Polytechnic University, 2002, 328 p. (rus)

12. **Nagornyy V.S.** *Means of automation of hydro- and pneumatic systems*. St. Petersburg: Publishing House LAN, 2014, 448 p. (rus)

13. **Nagornyy V.S.** *Electroplating recording devices. Mechanical Engineering*. Leningrad: Mashinostroyeniye Publ., 1988, 269 p. (rus)

14. **Nagornyy V.S.** *Electrofluidic converters. Shipbuilding*. Leningrad: Sudostroyeniye Publ., 1987, 251 p. (rus)

15. **Denisov A.A., Nagornyy V.S.** *Electrohydrodynamic and electrogasdynamic automation devices. Mechanical Engineering*. Leningrad: Mashinostroyeniye Publ., 1979, 288 p. (rus)

16. **Nagorniy V.S.** Parameter of EHD-Interaction and efficiency electrohydrodynamic control of flows and jets of dielectric liquids and gas. *2014 International Symposium on Electrohydrodynamics*, 2014, P. 49.

17. **Nagorniy V.S., Smirnovsky A.A., Tchernysheff A.S., Kolodyazhny D.Y.** Numerical simulation of the flow in the fuel injector in the sharply inhomogeneous electric field. *Procedia Computer Science*, 2015, Vol. 51, Pp. 1219–1228.

18. **Sysoyeva S.O.** Recommendations on the choice of pressure sensors for industry and housing. *Components and Technologies*, 2008, 120 p. (rus)

19. **Plotnikov I.V.** State of measurement of variable pressure. *Instrumentation*, 1983, 43 p. (rus)

20. **Nagornyy I.V.** Improving the accuracy of gas flow measurement using pressure-compensating electrohydrodynamic converters of pressure drop into an electrical signal. *Sat. reports VI International Scientific Conference*. St. Petersburg: Publishing House of Polytechnic University, 2000, Pp. 206–209. (rus)

21. **Nagorny V.S.** Leading scientific school of Russia electro-hydro- and electro-gas dynamic automation. *Scientific Works XXIII International Scientific and Practical Conference on System Analysis Design and Management* (*SAES-2019*). St. Petersburg: Publishing House of Polytechnic University, 2019, Pp. 495–504. (rus)

22. **Kremlevsky P.P.** *Flowmeters and counters of the amount of substances: Reference. Book 2*. St. Petersburg: Polytechnic Publ., 2004. 412 p. (rus)

23. **Khansuvarov K.I., Tseitlin V.G.** *Technique for measuring pressure, flow, quantity and level of liquid, gas and steam*. Moscow: Publishing House of Standards, 1990. 287 p. (rus)

Received 07.05.2020.

СПИСОК ЛИТЕРАТУРЫ

1. **Нагорный В.С., Нагорный И.В.** Преобразователи малых давлений и перепадов давлений в электрический сигнал с электрогидродинамической компенсацией по давлению. Санкт-Петербург : Изд-во Политехн. ун-та, 2011. 224 с.

2. **Nagorniy A.I., Nagorniy V.S., Tisenko V.N.** Improved-Accuracy Innovative Compensatory Flowmeters of Variable Pressure Differential Applied in Oil & Gas Industry. IEEE Xplore Digital Library 9-16 Sept. 2018 // URL: https://ieeexplore.ieee.org/document/8501824

3. **Nagorniy V.S., Smirnovsky A.A., Kolodyazhny D.Y., Chemyshev A.S.** Charge transfer in a sharply nonuniform electric field mediated by swirling liquid flow with minimal hydraulic resistance // Technical Physics Letters. 2015. No. 4. Pp. 859–862.

4. **Nagorniy V.S.** Mathematical model of the processes involved in electric charge to drops of a lubricant during the electrodrop application of lubricants to chemical fibers // Fibre Chemistry. 2016. Vol. 47. No. 6. Pp. 514–516.

5. **Sipatov A.M., Modorskii V.Y., Babushkina A.V., Kolodyazhnyi D.Y., Nagorniy V.S.** Computation of design parameters influence on air injector fuel atomization // Russian Aeronautics. 2017. Vol. 32. No. 3, Pp. 428–433.

6. **Nagorniy V.S.** Dynamic characteristics of the process for imparting an electric charge to lubricant droplets in the droplet jet electrospray method for applying lubricants to synthetic yarns // Fibre Chemistry. 2017. Vol. 48. No. 6. Pp. 500–503.

7. **Нагорный А.И., Тисенко В.Н.** Инновационный потенциал нового прибора для измерения расхода жидкостей и газов // Сб. матер. конф. ComCon-2017. СПб.: Изд-во Политехн. ун-та, 2017. 535 с.

8. **Modorskii V.Y., Sipatov A.M., Babushkina A.V., Kolodyazhny D.Y., Nagorny V.S.** Modeling technique for the process of liquid film disintegration // Internat. Conf. on the Methods of Aerophysical Research (ICMAR 2016). AIP Conference Proceedings. 2016. Pp. 1–7.

9. **Nagorniy V.S., Nagorniy I.V.** Limitations of EHD control flows and jets using corona discharges in gas // IEEE Internat. Conf. on Dielectric Liquids, Poitiers-France, 2008. Pp. 97–99.

10. **Nagorniy V.S., Nagorniy I.V.** Electrophysical principles of electrogasdynamic conversion of electrical signals into pneumatic ones by turbulization of gas jets by unipolar ion flows // Surface Engineering and Applied Electrochemistry. Allerton Press, Inc. distributed exclusively by Springer Science+Business Media LLC, 2007. Vol. 43. No. 3. Pp. 187–193.

11. **Нагорный В.С., Нагорный И.В.** Электрофизические основы электрогазодинамического преобразования электрических сигналов в пневматические турбулизацией струй униполярными потоками ионов. СПб.: Изд-во Политехн. ун-та, 2002. 328 с.

12. **Нагорный В.С.** Средства автоматики гидро- и пневмосистем. СПб.: Лань, 2014. 448 с.

13. **Нагорный В.С.** Электрокаплеструйные регистрирующие устройства. Л.: Машиностроение. ЛО, 1988. 268 с.

14. **Нагорный В.С.** Электрофлюидные преобразователи. Л.: Судостроение, 1987. 251 с.

15. **Денисов А.А., Нагорный В.С.** Электрогидро- и электрогазодинамические устройства автоматики. Л.: Машиностроение. ЛО, 1979. 288 с.

16. **Nagorniy V.S.** Parameter of EHD-Interaction and efficiency electrohydrodynamic control of flows and jets of dielectric liquids and gas // 2014 Internat. Symp. on Electrohydrodynamics. 2014. P. 49.

17. **Nagorniy V.S., Smirnovsky A.A., Tchernysheff A.S., Kolodyazhny D.Y.** Numerical simulation of the flow in the fuel injector in the sharply inhomogeneous electric field // Procedia Computer Science. 2015. Vol. 51. Pp. 1219–1228.

18. **Сысоева С.О.** Bd Sensors Rus — на пульсе вашего давления. Рекомендации по выбору датчиков давления для промышленности и ЖКХ // Компоненты и технологии, 2008. № 78. 60–62.

19. **Плотников И.В.** Состояние измерения переменного давления. М.: Изд-во ВНИИКИ, 1983. 44 с.

20. **Нагорный И.В.** Повышение точности измерения расхода газа с помощью компенсирующих давление электрогидродинамических преобразователей падения давления в электрический сигнал // Доклады VI Междунар. науч. конф. СПб.: Изд-во Политехн. ун-та, 2000. С. 206–209.

21. **Нагорный В.С.** Ведущая научная школа России – электрогидро- и электрогазодинамическая автоматика (электрофлюидик) // Сб. науч. трудов XXIII Междунар. науч.-практ. конф. «Системный анализ в проектировании и управлении» (SAES-2019). СПб.: Изд-во Политехн. ун-та, 2019. С. 495–504.

22. **Кремлевский П.П.** Расходомеры и счетчики количества веществ: Справочник. Кн. 2. СПб.: Политехника, 2004. 412 с.

23. **Хансуваров К.И., Цейтлин В.Г.** Техника измерения давления, расхода, количества и уровня жидкости, газа и пара. М.: Издательство стандартов, 1990. 287 с.

Статья поступила в редакцию 07.05.2020.

THE AUTHORS / СВЕДЕНИЯ ОБ АВТОРАХ

Nagorny Alexandr I.
Нагорный Александр Игоревич
E-mail: nagor234@yandex.ru

Tisenko Victor N.
Тисенко Виктор Николаевич
E-mail: v_tisenko@mail.ru

ИНФОРМАТИКА, ТЕЛЕКОММУНИКАЦИИ И УПРАВЛЕНИЕ

COMPUTING, TELECOMMUNICATIONS AND CONTROL

Том 13, № 3, 2020

Учредитель — Федеральное государственное бюджетное образовательное учреждение высшего профессионального образования «Санкт-Петербургский государственный политехнический университет»

Журнал зарегистрирован Федеральной службой по надзору в сфере информационных технологий и массовых коммуникаций (Роскомнадзор). Свидетельство о регистрации ЭЛ № ФС77-77378 от 25.12.2019 г.

Телефон редакции (812)552-62-16

E-mail: infocom@spbstu.ru

Компьютерная верстка *А.А. Кононова*

Перевод на английский язык *Д.Ю. Алексеева*

Лицензия ЛР № 020593 от 07.08.97

Дата выхода 30.09.2020. Формат 60×84 1/8

Санкт-Петербургский политехнический университет Петра Великого
Адрес университета и редакции: 195251, Санкт-Петербург, ул. Политехническая, д. 29.